e-Zine for meteor observers meteornews.net

MeteorNews

ISSN 2570-4745 VOL 6 / ISSUE 4 / MAY 2021

Stacked image of the SWEMN "Villacarrillo" fireball of 2021 March 28, 04h21m15s UT over the domes of the Calar Alto Astronomical Observatory. (Credit J.M. Madiedo)

- BRAMON new showers
- Beta Tucanids
- Zeta Pavonids
- Radio meteor work
- February alpha Corvids
- Gamma Draconids
- DLM & COM mystery
- Fireballs

Contents

Identification of new meteor showers SCP (#1042) and OSG (#1043) and their associations with the asteroids 2019 OK and 2017 NT5

Lauriston de Sousa Trindade[1], Alfredo Dal'Ava Jr[1], Cristovão Jacques Faria[1,2], Marcelo Zurita[1,3], Gabriel Gonçalves Silva[1,4]

[1] **Brazilian Meteor Observation Network, Nhandeara, Brazil**
bramon@bramonmeteor.org

[2] **SONEAR - Southern Observatory for Near Earth Asteroids Research, Oliveira, Brazil**
cjacques@gmail.com

[3] **Associação Paraibana de Astronomia, João Pessoa, Brazil**
marcelozurita@gmail.com

[4] **Instituto de Química, Universidade de São Paulo, São Paulo, Brazil**
gabrielg@iq.usp.br

The Brazilian Meteor Observation Network, BRAMON, reports the discovery of two meteor showers, observed after a search in its own database. For the meteor shower #1042 SCP, one meteor was found in 2015, six meteors in 2016, four meteors in 2017, one meteor in 2018, one meteor in 2019 and three meteors in 2020, occurring between solar longitudes of 103° and 138°. The mean radiant position is at right ascension of 312.2° and declination of –20.8°. For the meteor shower #1043 OGS, the evidence is based on one meteor in 2014, one meteor in 2015, three meteors in 2016, eight meteors in 2017, two meteors in 2018 and five meteors in 2020, occurring between solar longitudes of 100° and 126°. The mean radiant position is at right ascension of 297.3° and declination of –26.7°. The asteroids 2019 OK and 2017 NT5 were identified as the most probable parent bodies of the particles responsible for the meteor showers.

1 Introduction

BRAMON is a meteor-monitoring network that was created in 2014 to record and study meteors over Brazil. The main goals of the network are the search for new meteor showers, as well as the work to provide more detailed information about very bright bolides and meteorite-dropping meteors (Zurita et al., 2019). Taking advantage of its large latitude coverage, extending from 2ºS to 30ºS, and privileged position in the southern hemisphere (Amaral et al., 2018), BRAMON accumulated thousands of meteor orbits over 7 years of activity. The collected data has allowed the search for meteor radiants and to update the already cataloged meteor showers with new orbits. As a result of this effort, it was possible to create BRAMON's own meteor orbit database, made available along with the EDMOND's database[1] (Amaral et al., 2018).

The production of a large meteor database and the study of the meteor orbit patterns are the basis of the meteor shower studies.

For a long time, the meteor phenomenon was associated with atmospheric effects of terrestrial origin. This Aristotelian model remained in force until the beginning of the 19th century. In 1861 Schiaparelli discovered the asteroid Hesperia. Five years later he demonstrated that some meteors had orbits similar to some comets and concluded that the meteor showers are the remnants of comets. In particular, he calculated the comet 1862 III as parent body of the Perseids meteors and comet 1866 I as the source for the Leonids (Schiaparelli, 1867a; 1867b).

The relationship between comets and meteor showers was only widely accepted after the confirmation, in 1872, of the association of the intense meteor shower of the Andromedids with comet 3D/Biela, correctly predicted years before (Weiss, 1868).

Not only comets can be listed as parent bodies of a meteor shower. Many asteroids have been identified as having a similar orbit as the Taurids meteor shower (Clube and Napler, 1984). Since then, many other associations with meteor showers have emerged (Porubčan et al., 2004).

There are several examples of association between asteroids and meteor showers (Jopek and Williams, 2013): the Quadrantids (QUA) meteor shower is associated with the comet C/1490Y1 and the asteroid 2003 EH1 (Jenniskens, 2004; Williams et al., 2004; Micheli et al., 2008); the Geminids (GEM) meteor shower is associated with asteroid Phaethon (Whipple, 1983); and the Taurid complex is related with the comet P/Encke (Wipple and El-Din Hamid, 1952).

[1] https://www.meteornews.net/edmond/

The origin of the meteor showers had been solved. But the perception was that meteoroid streams were not homogeneous in space. With systematic observations over many years, the fluctuations in the rates of the occurrences of meteors could be monitored. An example of this occurred with the Leonids. In 1833 there was a real meteor storm, but in the following years the ZHR (zenithal hourly rate) remained much lower, with cyclical fluctuations increasing the rates every 33 years.

Thus, the activity of meteor showers can be classified into two groups: annual showers, which are visible every single year within a defined date range and predictable activity rate, and the outbursts, in which the occurrence of a high rate of meteors in a given year does not necessarily happen again in the following years. Eventually an established annual shower may present an outburst, characterized by a noticeable increase in its meteor rates.

The outbursts can be seen as young trails, such as the ones often observed for the Leonid radiant, associated with comet 55P/Temple-Tuttle (Yeomans and Yau, 1996). More stable dust trails may be a sign of a well-established trail, making it possible to estimate the overall age of the meteoroid stream. This is the case for the Perseids and their parent comet 109P/Swift-Tuttle (Brown and Jones, 1998).

The current meteor science admits that meteoroid streams are formed by particles detached from comets and some asteroids, many of them being dormant comets. There are several mechanisms recognized to release the dust that forms the meteoroid streams: ejection, disintegration by impact, rotational instability, electrostatic repulsion, radiation pressure, dehydration stress, thermal fracture and sublimation of ice (Jewitt et al., 2015). Thus, the fragments disperse in their own orbits, but which can maintain similarity for many years or even centuries.

Considering that asteroids and dormant comets have a low ejection of particle matter and considering that the BRAMON database still has a few thousand meteor orbits, the best way to search for new meteor showers associated with asteroids would be to use the NEA asteroid list as an initial reference.

In this study, we describe the discovery of two new meteor showers from the southern hemisphere. During this work, different dissimilarity criteria were applied combined on the orbits to assure the validity of the new showers. The identification of the most probable parent body of each meteor shower was also possible using the same comparison methodology. The shower discovery was only possible thanks to the cooperation between BRAMON and SONEAR, a southern hemisphere observatory dedicated to near-Earth asteroids research.

2 Methodology

2.1 Dissimilarity criteria

All objects in the Solar System can be characterized by their Keplerian orbital elements: a (semi-major axis), q (perihelion distance), e (eccentricity), i (inclination), ω (argument of perihelion) and Ω (longitude of the ascending node). For meteoroids that are part of the meteor showers, in addition to the Keplerian orbital elements, it is necessary to compare all these orbits using a similarity criterion. The most common way to measure similarity between orbits is by the concept of the so-called discriminant criterion or D-criterion. D-criterion methods seek to measure the distance between two N-dimensional points in space, using the orbital elements of orbits that are evaluated.

During the development of D-criteria, different authors implemented distinct mathematical expressions, using different numbers of orbital parameters. In this paper the authors used 5 orbital elements for the D-criteria as proposed by Southworth and Hawkins (1963), Drummond (1981) and Jopek (1993).

The Southworth and Hawkins D-criterion (D_{SH}) has the following mathematic expression in *Equation 1*:

$$D_{SH}^2 = (q_B - q_A)^2 + (e_B - e_A)^2 + \left(2 \sin\frac{I_{BA}}{2}\right)^2 + \left(\frac{e_B+e_A}{2} \cdot 2 \sin\frac{\pi_{BA}}{2}\right)^2 \quad (1)$$

where e_A and e_B is the eccentricity, and q_A and q_B is the perihelion distance of two orbits, I_{BA} is the angle between two orbital planes, and π_{BA} is the distance of the longitudes of perihelia measured from the intersection of the orbits.

Drummond (1981), proposed some modifications in the dissimilarity criterion of Southworth & Hawkins (1963), resulting in Drummond D-Criterion (D_D), for which the definition is shown in *Equation 2*:

$$D_D^2 = \left(\frac{e_2-e_1}{e_2+e_1}\right)^2 + \left(\frac{q_2-q_1}{q_2+q_1}\right)^2 + \left(\frac{I_{21}}{180°}\right)^2 + \left(\frac{e_2+e_1}{2}\right)^2 \left(\frac{\theta_{21}}{180°}\right)^2 \quad (2)$$

where, I_{21} is the angle between the two orbital planes and θ_{21} is the angle between the perihelion points of each orbit, defined in *Equation 3*:

$$\theta_{21} = \arccos[\sin(\beta_1)\sin(\beta_2) + \cos(\beta_1)\cos(\beta_2)\cos(\lambda_2 - \lambda_1)] \quad (3)$$

where, λ and β are respectively the longitude and ecliptic latitude of the perihelion defined in *Equations 4 and 5*:

$$\lambda = \Omega + \arctan(\cos(i)\tan(\omega)) \quad (4)$$

$$\beta = \arcsin(\sin(i)\sin(\omega)) \quad (5)$$

Jopek (1993) concluded that D_{SH} depends a lot on the perihelion distance q and that D_D depends a lot on the eccentricity e. Thus, he proposed a new method (D_H), which has the following mathematical expression in *Equation 6*:

$$D_H^2 = (e_B - e_A)^2 + \left(\frac{q_B-q_A}{q_B+q_A}\right)^2 + \left(2 \sin\frac{I_{BA}}{2}\right)^2 + \left(\frac{e_B+e_A}{2}\right)^2 \cdot \left(2 \sin\frac{\pi_{BA}}{2}\right)^2 \quad (6)$$

2.2 Meteor shower search

The search began with the selection of 32 asteroids discovered by SONEAR (Southern Observatory for Near Earth Asteroid Research) that had been classified as NEAs. We employed the orbital elements by the IAU Minor Planet Data Center, available at Epoch 2459200.5 (2020-Dec-17.0).

The orbit of each asteroid was used as input in a C++/Python calculator that tested each orbit of BRAMON's database and returned the results within the thresholds established for D_D, D_{SH} and D_H. The threshold was established as D_c (Maximum tolerated discrimination value) so that, if $D(X, Y) < D_c$, the orbits are sufficiently similar and the asteroid is a candidate to be associated with the tested meteor.

There are different methods to determine the threshold: Porubčan et al. (2006) opted for a D_{SH} of 0.3 in the case of association of NEOs with the Taurid Complex; Rudawska et al. (2012a) established a D_{SH} threshold of 0.084 and D_H of 0.077 for the association of asteroids and meteor showers. Šegon et al. (2014) used a 0.15 threshold for both D_{SH} and D_H for the association between meteor showers and asteroids. In the search for meteors associated with the asteroids discovered by SONEAR we use the following thresholds: $D_D < 0.09$, $D_{SH} < 0.15$ and $D_H < 0.15$.

2.3 Backward integration

It is not possible to find a solution to the N-body problem, in an analytical way, if there are more than three gravitational interrelated massive bodies. If there are three bodies for the calculations, it is only possible to proceed analytically if one of these bodies can have the mass despised (Bhatnagar K.B. and Saha L.M., 1993).

Currently, there are several orbital integrators that solve the N-body problem. One of the classic integrators is the MERCURY hybrid symplectic integrator (Chambers, 1999). Non-symplectic integrators can preserve the amount of area in the solution of the N-body problem (Kinoshita et al., 1991). The choice of the integrator is particularly important because, during the integration, the sizes of timestep-variations can accumulate errors if there are too many close encounters in the time range chosen in the study.

The backward integration of the orbits of the asteroids and the mean orbit of the clusters of meteors found were proceeded using the Rebound package as integrator (Rein & Liu, 2012). Unlike MERCURY, Rebound has a more agile and user-friendly interface, using Python/C++ language and implements several integration algorithms. Another advantage of Rebound is that it has a module that can access the NASA JPL Horizons database directly through Internet. This gives the possibility to start backward simulations with the most accurate ephemeris data of massive bodies (barycenter) used in the study (Sun, Mercury, Earth, Moon, Mars, Ceres, Vesta, Jupiter, Saturn, Uranus and Neptune).

The initial studies were done using the integrator algorithm WHFAST (Rein and Tamayo, 2015) because it implements fast and accurate responses of a Wisdom-Holman integrator, allowing to run planetary system integrations of longer time ranges more quickly. Thus, the integration was done for 5000 years, with an initial timestep of 0.0007 days while capturing 500000 intermediate results for analysis. The objective of this verification was to compare the fluctuation of the orbital elements of multiple objects over time.

It is important to note that it is not possible to specify the ejection dates of meteoroids that have collided with the Earth's atmosphere over the past few years simply using backwards integrations. For this, it would be necessary to associate models of non-gravitational disturbances to the orbits. Thus, there is a lot of uncertainty when comparing the evolution of semi-major axis of the orbit and the eccentricity of the candidates (Egal et al., 2017; Vida et al., 2018).

3 Results

3.1 Showers identification and validation

16 meteors in BRAMON's database were found that could be associated with the asteroid 2019 OK. The mean orbital elements of the cluster were compared with the list of all meteor showers in the IAU Meteor Data Center. The comparison was made using the discrimination criteria D_D, D_{SH} and D_H, using thresholds of 0.09, 0.15 and 0.15, respectively. No meteor showers in the catalog have been associated with the cluster and this group of meteors has been identified as a new annual meteor shower. Following the naming rules for meteor showers (Jenniskens, 2007; 2008) the shower was named 17 Capricornids, receiving from the IAU MDC the number 1042 and code SCP. The orbital data of the SCP shower, as well as the orbital data of asteroid 2019 OK can be seen in *Table 1* and *Table 2*.

During the search, 20 meteors were found in the BRAMON's database that could be associated with asteroid 2017 NT5. The same procedure was adopted for this second cluster. The mean orbital elements were compared with the list of all meteor showers of the IAU Meteor Data Center, using the same D_D, D_{SH} and D_H thresholds. No meteor showers in the catalog have been associated with the cluster, therefore it was concluded that this group of meteors is part of a new annual meteor shower. Once again, following naming rules, the group was named omega Sagittariids, receiving from the IAU MDC the number 1043 and code OSG. The orbital elements data for the shower OSG as well as the orbital data for the asteroid 2017 NT5 can be seen in *Table 3* and *Table 4*.

The asteroid 2019 OK was first detected on July 24, 2019, at distance of 0.01 AU (~1500000km) from Earth and had an apparent magnitude of 14.7, being observed in the constellation of Capricorn. With a MOID of 0.000381434 AU (NASA JPL) and an absolute magnitude (H) = 23.3

Table 1 – Orbit data for the meteors associated with the SCP (#1042) shower.

Meteor	$\lambda_\odot$ (°)	α_g (°)	δ_g (°)	v_g (km/s)	a (A.U.)	e	q (A.U.)	ω (°)	Ω (°)	i (°)	D_D
20150716_044925	113.15	305.3	–20.3	25.5	2.01	0.785	0.431	107.98	293.15	0.34	0.048
20160705_052435	103.39	293.7	–22.4	23.5	1.84	0.738	0.480	104.04	283.38	0.19	0.091
20160716_034824	113.82	302.1	–22.8	24.9	2.37	0.794	0.487	100.12	293.83	2.14	0.073
20160718_044750	115.77	308.9	–21.9	25.8	2.11	0.794	0.433	107.12	295.78	2.50	0.043
20160801_224158	129.85	318.2	–19.1	25.2	1.96	0.777	0.434	107.92	309.86	3.08	0.052
20160802_015622	129.98	323.9	–23.7	25.6	1.97	0.711	0.432	108.03	309.99	9.18	0.076
20160811_010933	138.58	328.7	–15.6	23.0	1.79	0.731	0.479	104.29	318.59	2.69	0.068
20170715_000726	112.48	300.6	–21.6	25.3	2.01	0.780	0.439	107.10	292.48	1.32	0.045
20170715_075327	112.78	310.6	–24.7	21.9	1.37	0.677	0.440	113.74	292.79	3.68	0.060
20170728_021802	124.98	315.6	–19.5	26.8	2.40	0.823	0.422	107.01	304.98	2.33	0.060
20170807_070646	134.74	328.0	–17.2	25.6	2.11	0.793	0.434	106.54	314.74	2.36	0.068
20180718_071555	115.38	307.2	–20.8	24.7	2.05	0.775	0.460	104.58	295.41	0.83	0.038
20190811_051129	138.01	329.4	–17.8	25.6	2.52	0.813	0.470	101.25	318.01	4.19	0.064
20200707_063450	105.33	298.7	–26.2	24.9	1.89	0.766	0.442	107.56	285.33	4.43	0.069
20200723_023833	120.44	307.7	–20.1	24.1	2.19	0.774	0.495	100.08	300.46	0.90	0.052
20200727_040356	124.31	315.9	–18.6	26.5	2.32	0.816	0.425	106.98	304.33	1.29	0.055
Means	120.82	312.2	–20.8	24.9	–	0.772	0.450	105.90	300.82	2.59	–
Medians	118.11	309.8	–20.6	25.21	–	0.779	0.440	106.99	298.12	2.34	–
2019 OK	–	–	–	–	1.87	0.757	0.453	106.09	302.04	2.09	–

Table 2 – Sun-centered radiants for the meteors associated with the SCP (#1042) shower.

NumCur	CatCod	MetCod	$\lambda_\odot$ (°)	$\lambda_g - \lambda_\odot$ (°)	β_g (°)	v_g (km/s)	No	Code
1	BR	20150716_044925	113.158	189.6	–0.8	25.5	1042	SCP
2	BR	20160705_052435	103.399	188.4	–0.8	23.5	1042	SCP
3	BR	20160716_034824	113.825	185.5	–2.6	24.9	1042	SCP
4	BR	20160718_044750	115.772	189.9	–3.1	25.8	1042	SCP
5	BR	20160801_224158	129.858	185.0	–2.9	25.2	1042	SCP
6	BR	20160802_015622	129.988	188.5	–8.9	25.6	1042	SCP
7	BR	20160811_010933	138.582	186.9	–2.8	23.1	1042	SCP
8	BR	20170715_000726	112.480	185.8	–1.1	25.3	1042	SCP
9	BR	20170715_075327	112.789	193.7	–6.2	21.9	1042	SCP
10	BR	20170728_021802	124.980	187.4	–2.6	26.8	1042	SCP
11	BR	20170807_070646	134.740	189.6	–4.1	25.6	1042	SCP
12	BR	20180718_071555	115.386	189.1	–1.7	24.8	1042	SCP
13	BR	20190811_051129	138.010	187.4	–5.1	25.6	1042	SCP
14	BR	20200707_063450	105.333	190.3	–5.3	24.9	1042	SCP
15	BR	20200723_023833	120.440	184.6	–1.1	24.1	1042	SCP
16	BR	20200727_040356	124.318	188.6	–1.8	26.5	1042	SCP

Table 3 – Orbit data of the meteors associated with the OSG (#1043) shower.

Meteor	$\lambda_\odot$ (°)	α_g (°)	δ_g (°)	v_g (km/s)	a (A.U.)	e	q (A.U.)	ω (°)	Ω (°)	i (°)	D_D
20140803_060048	130.64	315.8	–23.3	20.3	2.15	0.710	0.621	86.20	310.65	3.17	0.068
20150702_231514	100.54	278.0	–25.5	19.7	1.80	0.660	0.608	90.58	280.55	1.68	0.064
20160706_053735	104.36	291.9	–29.6	20.7	1.80	0.680	0.575	94.18	284.36	5.15	0.067
20160707_064949	105.36	293.1	–27.4	19.0	1.62	0.630	0.599	93.56	285.36	2.77	0.061
20160812_011335	139.54	318.2	–24.8	18.2	1.98	0.660	0.676	80.63	319.55	4.78	0.070
20170703_013859	101.10	280.0	–24.8	19.3	1.84	0.660	0.626	88.16	281.11	1.27	0.064
20170703_035627	101.19	282.2	–35.4	20.4	2.12	0.700	0.638	84.54	281.19	8.35	0.070
20170715_002439	112.49	288.1	–23.6	20.4	2.38	0.730	0.643	82.58	292.49	0.96	0.060
20170718_034313	115.49	295.8	–28.8	19.6	2.16	0.700	0.656	82.11	295.48	4.51	0.026
20170723_013538	120.17	297.9	–33.9	19.0	2.22	0.690	0.693	77.36	300.17	7.86	0.038
20170723_040407	120.27	302.6	–32.4	21.5	2.68	0.760	0.638	81.94	300.27	8.06	0.062
20170725_043636	122.21	307.8	–23.8	20.1	1.84	0.680	0.594	91.71	302.21	2.58	0.068
20170726_021756	123.07	301.0	–27.0	19.4	2.29	0.710	0.673	79.34	303.07	4.20	0.029
20180716_003506	113.21	285.8	–24.2	18.2	2.14	0.670	0.698	77.17	293.23	0.78	0.066
20180730_001439	126.56	302.2	–18.9	19.3	2.22	0.700	0.663	80.91	306.77	0.03	0.049
20200719_234531	117.46	292.4	–24.3	19.2	2.10	0.690	0.659	82.17	297.47	1.63	0.032
20200721_011019	118.47	294.7	–24.5	20.1	2.44	0.730	0.660	80.29	298.48	2.07	0.049
20200721_054110	118.65	306.4	–34.2	19.6	1.89	0.660	0.635	86.63	298.65	8.97	0.028
20200722_063521	119.64	304.4	–22.5	19.2	1.85	0.660	0.630	88.04	299.67	0.49	0.048
20200806_013302	133.78	307.8	–25.8	18.7	2.61	0.730	0.718	72.19	313.78	3.92	0.062
Means	117.21	297.3	–26.7	19.6	–	0.690	0.645	84.01	297.23	3.66	–
Medians	118.56	296.8	–25.2	19.5	–	0.690	0.641	82.37	298.57	2.97	–
2017 NT5	–	–	–	–	1.87	0.676	0.605	88.94	293.57	6.04	–

Table 4 – Sun-centered radiants for the meteors associated with the OSG (#1043) shower.

NumCur	CatCod	MetCod	$\lambda_\odot$ (°)	$\lambda_g - \lambda_\odot$ (°)	β_g (°)	v_g (km/s)	No	Code
1	BRAM	20140803_060048	130.649	180.8	–6.2	20.3	1043	OSG
2	BRAM	20150702_231514	100.541	176.7	–2.3	19.7	1043	OSG
3	BRAM	20160706_053735	104.361	184.7	–7.6	20.7	1043	OSG
4	BRAM	20160707_064949	105.363	185.1	–5.6	19.0	1043	OSG
5	BRAM	20160812_011335	139.544	173.6	–8.3	18.2	1043	OSG
6	BRAM	20170703_013859	101.102	177.9	–1.6	19.3	1043	OSG
7	BRAM	20170703_035627	101.193	178.9	–12.4	20.4	1043	OSG
8	BRAM	20170715_002439	112.491	174.0	–1.2	20.4	1043	OSG
9	BRAM	20170718_034313	115.485	177.1	–7.4	19.6	1043	OSG
10	BRAM	20170723_013538	120.174	173.3	–12.6	19.0	1043	OSG
11	BRAM	20170723_040407	120.273	177.5	–12.0	21.5	1043	OSG
12	BRAM	20170725_043636	122.205	182.1	–4.7	20.1	1043	OSG
13	BRAM	20170726_021756	123.069	174.4	–6.5	19.4	1043	OSG
14	BRAM	20180716_003506	113.212	171.2	–1.5	18.2	1043	OSG
15	BRAM	20180730_001439	126.564	173.7	+1.2	19.3	1043	OSG
16	BRAM	20200719_234531	117.461	172.9	–2.4	19.2	1043	OSG
17	BRAM	20200721_011019	118.472	173.9	–3.0	20.1	1043	OSG
18	BRAM	20200721_054110	118.651	181.8	–14.5	19.6	1043	OSG
19	BRAM	20200722_063221	119.64	181.8	–2.7	19.2	1043	OSG
20	BRAM	20200806_013302	133.782	169.9	–6.7	18.7	1043	OSG

Table 5 – Observed radiant (SCP #1042) compared to the theoretical radiant (asteroid 2019 OK).

Body	$\lambda_\odot$ (°)	α_g (°)	δ_g (°)	v_g (km/s)	a (A.U.)	e	q (A.U.)	ω (°)	Ω (°)	i (°)	*D–Dis*
2019 OK	–	–	–	–	1.87	0.757	0.453	106.09	302.04	2.09	–
SCP #1042	120.81	312.2	–20.8	24.9	2.06	0.772	0.451	105.90	300.82	2.60	–
2019 OK Fitted orbit	121.60	312.1	–20.2	24.3	1.87	0.757	0.454	106.50	301.60	2.10	0.000

Table 6 – Observed radiant (OSG #1043) compared to the theoretical radiant (asteroid 2017 NT5).

Body	$\lambda_\odot$ (°)	α_g (°)	δ_g (°)	v_g (km/s)	a (A.U.)	e	q (A.U.)	ω (°)	Ω (°)	i (°)	*D–Dis*
2017 NT5	–	–	–	–	1.87	0.676	0.605	88.94	293.57	6.04	–
OSG #1043	117.21	297.3	–26.7	19.6	1.94	0.645	0.690	84.02	297.23	3.66	–
2017 NT5 Fitted orbit	112.40	295.6	–30.4	20.2		0.676	0.605	90.20	292.40	6.00	0.002

(MPO473725), it was classified as a NEO (Near Earth Object) of the Apollo class. The asteroid was initially detected by Cristóvão Jacques, Eduardo Pimentel and João Ribeiro at the SONEAR Observatory, located in Oliveira, State of Minas Gerais, Brazil.

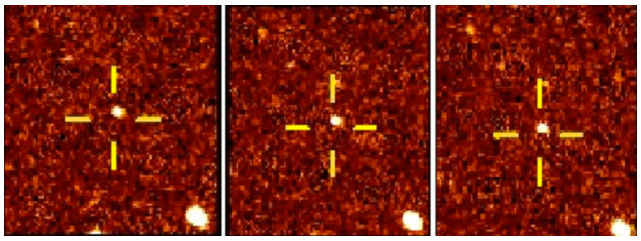

Figure 1 – First image of Asteroid 2019 OK. Courtesy SONEAR Observatory.

Figure 2 – Flyby (top view) by asteroid 2019 OK.

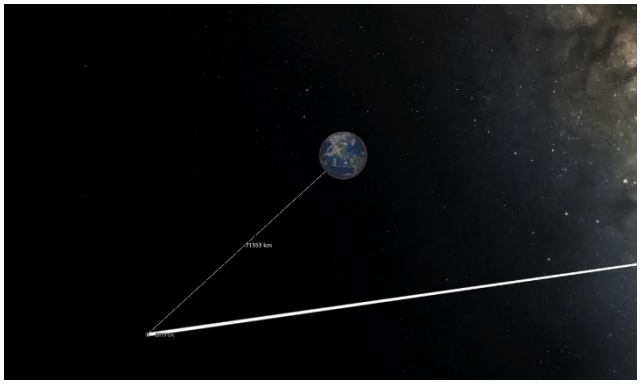

Figure 3 – Flyby (side view) by asteroid 2019 OK.

Its flyby (*Figure 1, 2 and 3*) occurred on July 25, 2019 at 01^h22^m UT, at a distance of 0.00047697 AU (NASA JPL). It has an estimated size of the 100m and an orbital period of 2.72 years (Minor Planet Center). Using the concept of asteroid families (Hirayama, 1918), the 2019 OK is member of the Flora family.

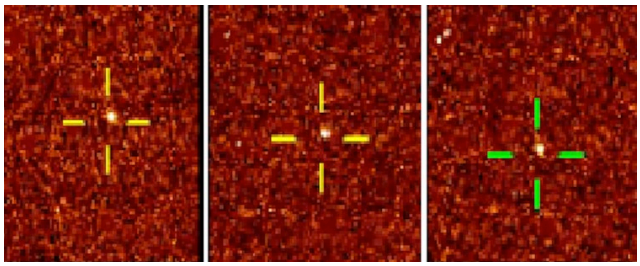

Figure 4 – First image of Asteroid 2017 NT5, Courtesy SONEAR Observatory.

The asteroid 2017 NT5 was first detected on July 12, 2017, by the SONEAR observatory. After more observations, the asteroid had its MOID calculated as 0.00257522 AU (~335381km) AU and an absolute magnitude (H) = 22.9 (MPO 416462), being classified as a NEO (Near Earth Object) of the Apollo class. Its flyby occurred on July 14, 2017 at 16^h06^mUT, when the asteroid reached a minimum distance of 0.002859082 AU (NASA JPL). It has an estimated size between 49 and 160m with an orbital period of 2.55 years (NASA JPL).

Using the orbit data from 2019 OK and 2017 NT5, the theoretical radiant (Neslušan et al., 1998) was calculated for possible meteor showers that could exist having these asteroids as parent bodies. The theoretical radiant calculated for asteroid 2019 OK was compared with the radiants observed for the meteors of SCP#1042 (*Figure 5*) listed in *Table 1* and *Table 2*. The theoretical radiant calculated for the asteroid 2017 NT5 was compared with the radiants observed for the meteors of OSG#1043 (*Figure 6*) listed in *Table 3* and *Table 4*. The results are presented in *Table 5* and *Table 6*.

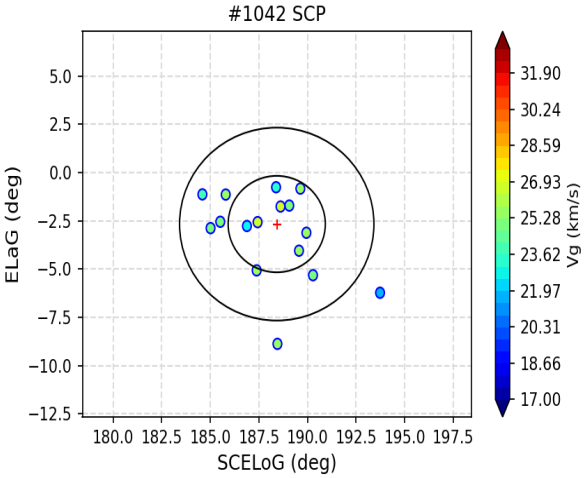

Figure 5 – The SCP radiants in Sun-centered coordinates. The concentric circles represent distances of 5° and 10° from the mean geocentric radiant.

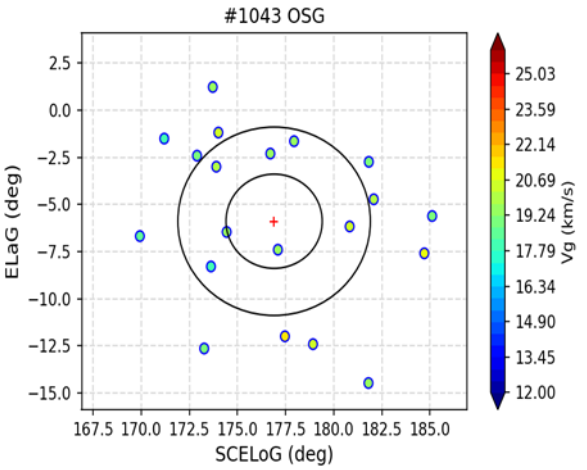

Figure 6 – The OSG radiants in Sun-centered coordinates. The concentric circles represent distances of 5° and 10° from the mean geocentric radiant.

It is often difficult to determine the limits of comparison between the original orbits of asteroids and the adjusted orbits (Neslušan et al., 1998). Depending on the method used for adjusting such orbits one can eventually discard good candidates for parent bodies. The D_{SH}-criterion appears as a parameter for measuring the uncertainty about the confirmation of a theoretical radiant (Svoren et al., 1993; 1994; Neslušan et al., 1998). The suggestion to use D_{SH} as a discriminant (Neslušan et al., 1998) is not a definitive measure, but only a form of quality assessment of the approximation between the original orbit of the tested asteroid and its adjusted orbit for an intersection with the Earth orbit. Thus, *D-Dis* and D_{SH} have the same concept: both measure dissimilarity between orbits. It is possible to accept the similarity between the mean orbit of the shower and the parent body if *D-Dis* < 0.07 and, if the distance between the two radiants does not exceed 5º, it is possible to accept a *D-Dis* value of maximum 0.1 (Neslušan et al., 1998). For the asteroid 2019 OK and the SCP meteor shower, a distance of 0.6º was found between the theoretical radiant and the observed radiant. For asteroid 2017 NT5 and the OSG meteor shower, the distance between the theoretical and observed radiant is 3.96º.

Another criterion used to associate meteors with parent bodies also includes the determination of the theoretical radiant (Neslušan et al., 1998) and has the following acceptable tolerances: $\Delta\lambda_\odot < 8º$, $\Delta\alpha < 8º$, $\Delta\delta < 8º$ and $\Delta\Omega < 6$ º (Guennoun et al., 2019). Both the SCP and OSG showers meet the criteria suggested by Guennoun et al. (2019) for their association with asteroid 2019 OK and 2017 NT5 respectively.

3.2 Backward integration

The interpretation of the charts after backward integration showed that the evolution of the mean orbital elements of the meteor clusters (Williams and Jones, 2007) and their candidate asteroidal parent bodies had similar behavior within the time interval studied. The thresholds used were: $D_{SH} = 0.15$; $D_D = 0.07$ and $D_H = 0.15$.

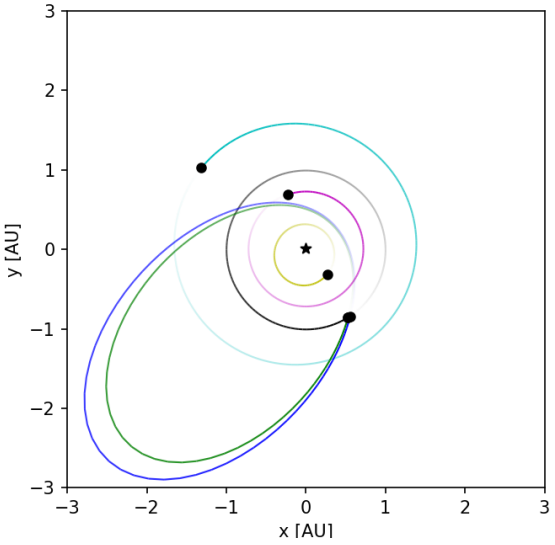

Figure 7 – The orbit (green line) and the position of the asteroid 2019 OK at the close approach in 2019 (Top view) and the mean orbit of the SCP meteor shower in blue line.

Figure 7 shows the position of the planets of the inner solar system at the time of the close approach of the asteroid 2019 OK, as well as the orbits of the asteroid itself (green line) and the mean orbit of the SCP meteors (blue line).

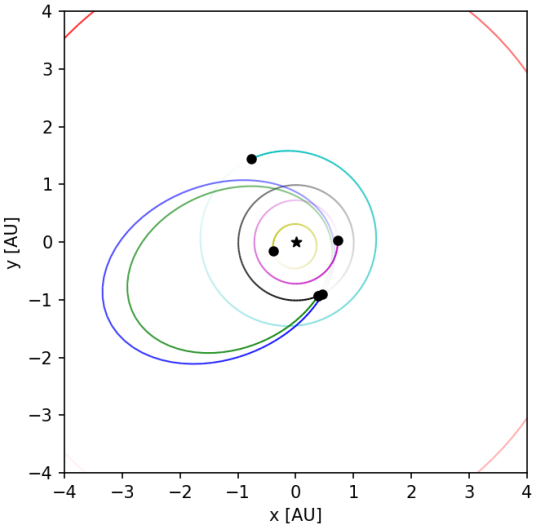

Figure 8 – The orbit (green line) and the position of asteroid 2017 NT5 at the close approach in 2017 (Top view) and the mean orbit of the OSG meteor shower in blue line.

The same workflow was applied in the research for shower #1043 OSG and its parent body candidate asteroid 2017 NT5. *Figure 8* shows the position of the planets of the inner solar system at the time of the close approach of the asteroid 2017 NT5, as well as the orbits of the asteroid itself (green line) and the mean orbit of the OSG meteors.

3.3. New meteor showers orbital elements

SCP (#1042)

The meteor shower SCP (#1042) can be found in the IAU Meteor Data Center (MDC) section "List of all showers" (Jenniskens et al., 2020). The meteors radiate from a mean geocentric radiant at RA = 312.2º and Dec.= –20. 8º, with a geocentric velocity of 24.93 km/s. The meteor shower SCP (#1042) has a peak at $\lambda_{\odot}$ = 120.82° on 2020 July 23 at 12^h UT (equinox J2000.0). The group of 16 meteors has the following mean orbital elements:

- $a \sim 2.06$ AU
- $q = 0.450$ AU
- $e = 0.772$
- $i = 2.6°$
- $\omega = 105.9°$
- $\Omega = 300.8°$

After comparing the evolution of the orbital elements of the asteroid 2019 OK and the meteor shower SCP (#1042) over past time, it appeared that they have similarity in the last 5000 years (*Figures 9 to 14*). The comparison between the theorical radiant position for the asteroid and the radiant observed for the meteor shower meets the similarity parameters (Neslušan et al., 1998; Guennoun et al., 2019). Thus, the asteroid 2019 OK is selected as the probable parent body of meteor shower SCP (#1042).

OSG (#1043)

The meteor shower OSG (#1043) can be found in the IAU Meteor Data Center (MDC) section "List of all showers" (Jenniskens et al., 2020). The meteors radiated from a mean geocentric radiant at RA = 297.3° and Dec. = –26.7º, with a geocentric velocity of 19.59 km/s. The meteor shower OSG (#1043) has a peak at $\lambda_{\odot}$ = 117.21° on 2020 July 19 at 18^h UT (equinox J2000.0). The 20 meteors give the following mean orbital elements:

- $a \sim 2.11$ AU
- $q = 0.6451$ AU
- $e = 0.69$
- $i = 3.7°$
- $\omega = 84.01°$
- $\Omega = 297.23°$

After comparing the evolution of the orbital elements of the asteroid 2017 NT5 and the meteor shower OSG (#1043), it appeared that they keep similar in the last 5000 years (*Figures 15 to 20*). Also, the comparison between the theoretical radiant position for the asteroid and the radiant observed for the meteor shower meets the similarity parameters (Neslušan et al., 1998; Guennoun et al., 2019). Thus, the asteroid 2017 NT5 is considered to be the probable parent body of the meteor shower OSG (#1043).

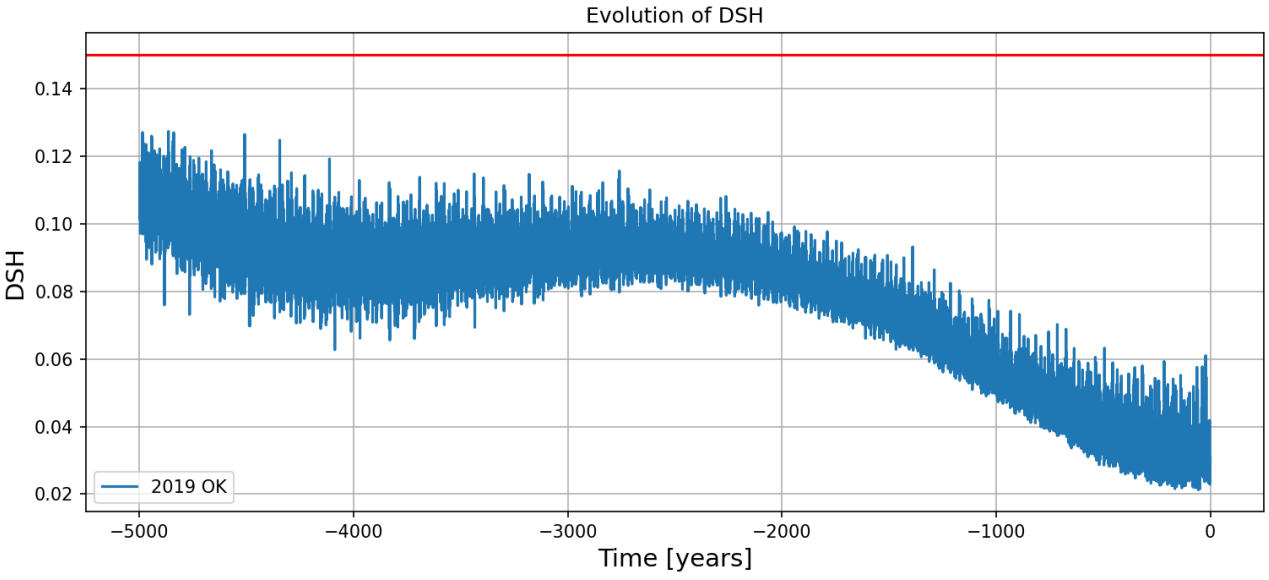

Figure 9 – D_{SH} values for the orbit of the asteroid 2019 OK compared to the mean orbit of SCP meteors in the last 5000 years.

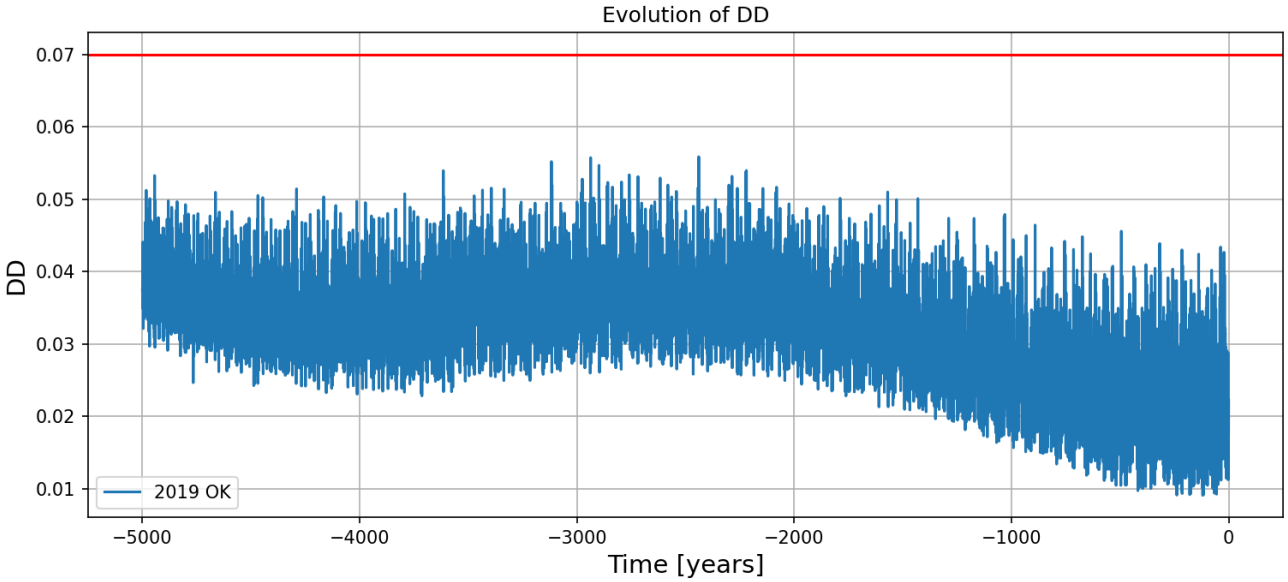

Figure 10 – D_D values for the orbit of the asteroid 2019 OK compared to the mean orbit of SCP meteors in the last 5000 years.

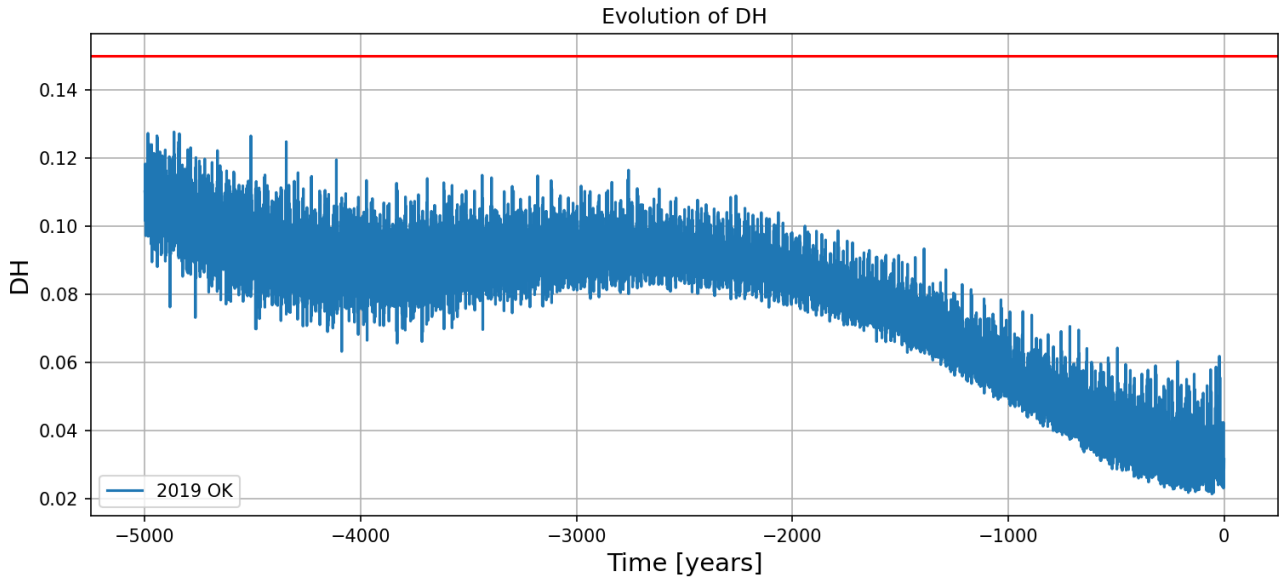

Figure 11 – D_H values for the orbit of the asteroid 2019 OK compared to the mean orbit of SCP meteors in the last 5000 years.

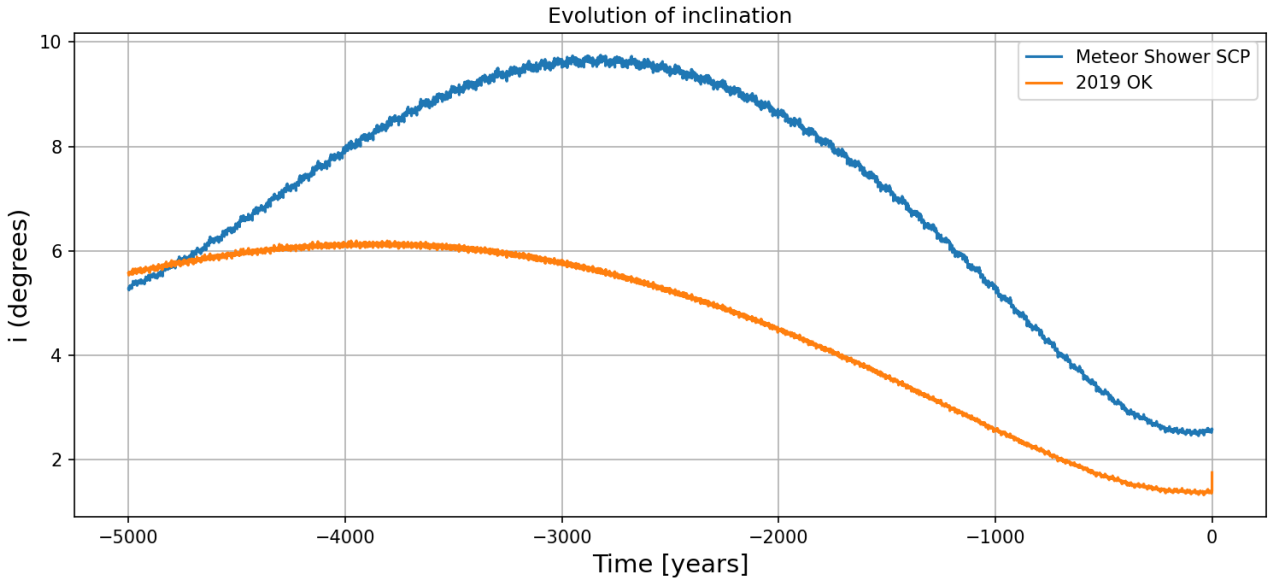

Figure 12 – Evolution of the orbit inclination *i* of asteroid 2019 OK and the median orbit of SCP meteors in the last 5000 years.

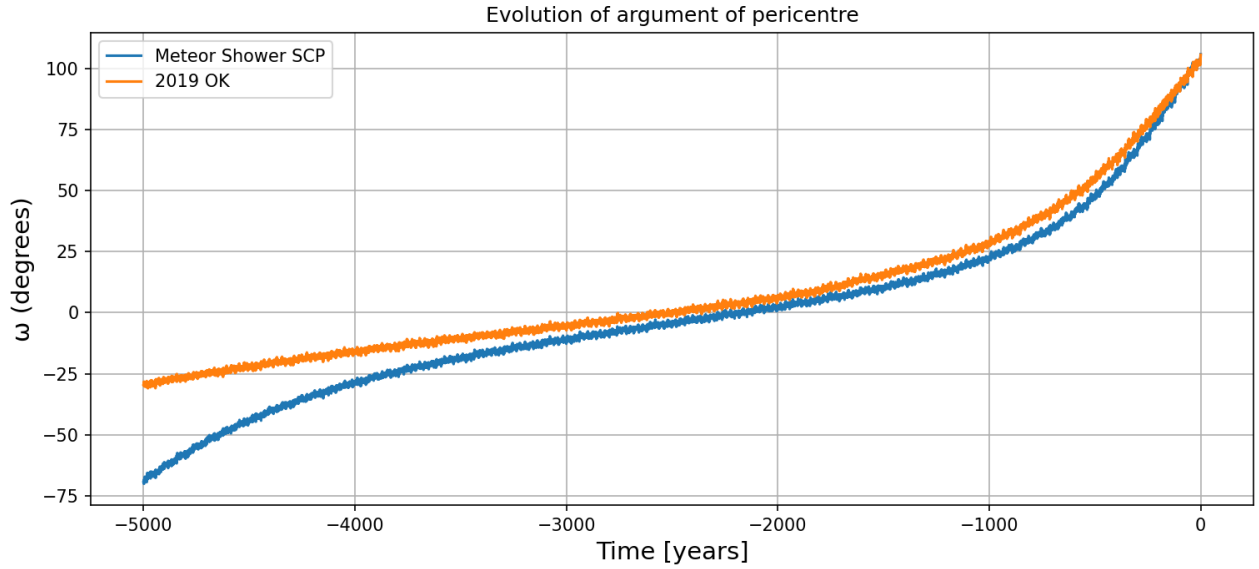

Figure 13 – Evolution of the argument of perihelion ω of asteroid 2019 OK and the mean orbit of SCP meteors in the last 5000 years.

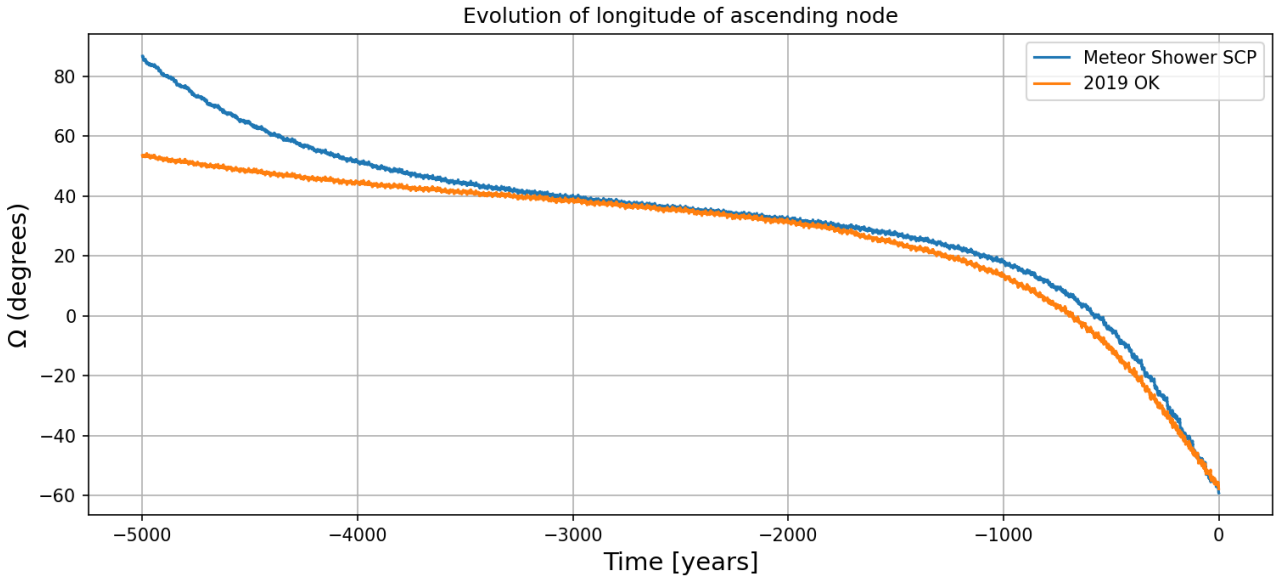

Figure 14 – Evolution of longitude of the ascending node Ω of asteroid 2019 OK and the mean orbit of SCP meteors in the last 5000 years.

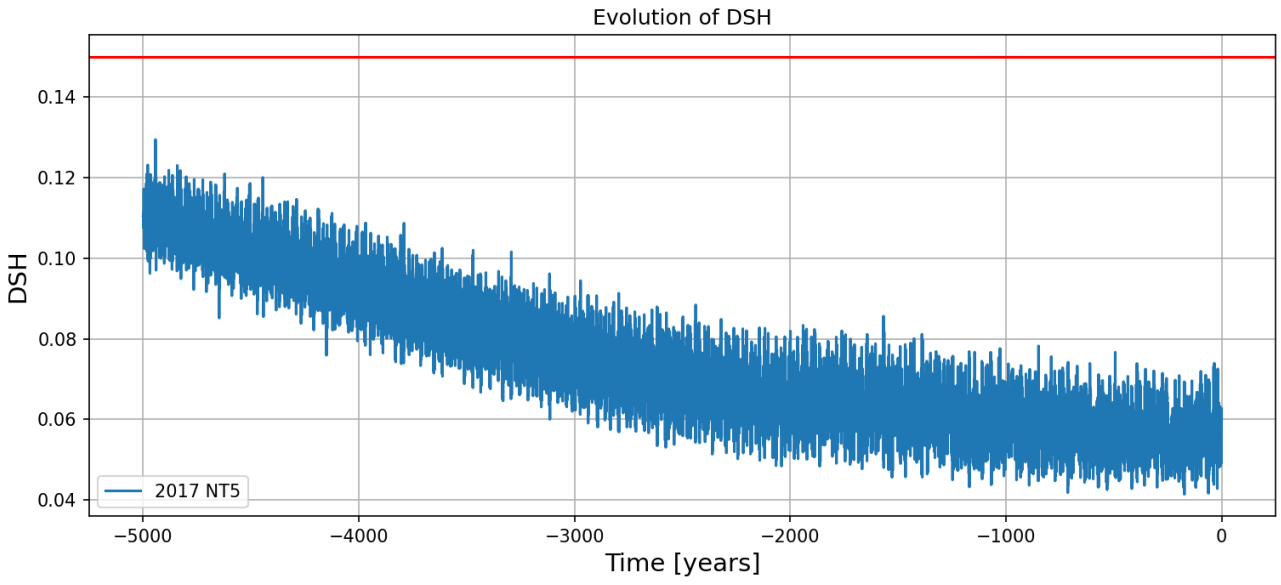

Figure 15 – D_{SH} values for the orbit of the asteroid 2017 NT5 compared to the mean orbit of OSG meteors in the last 5000 years.

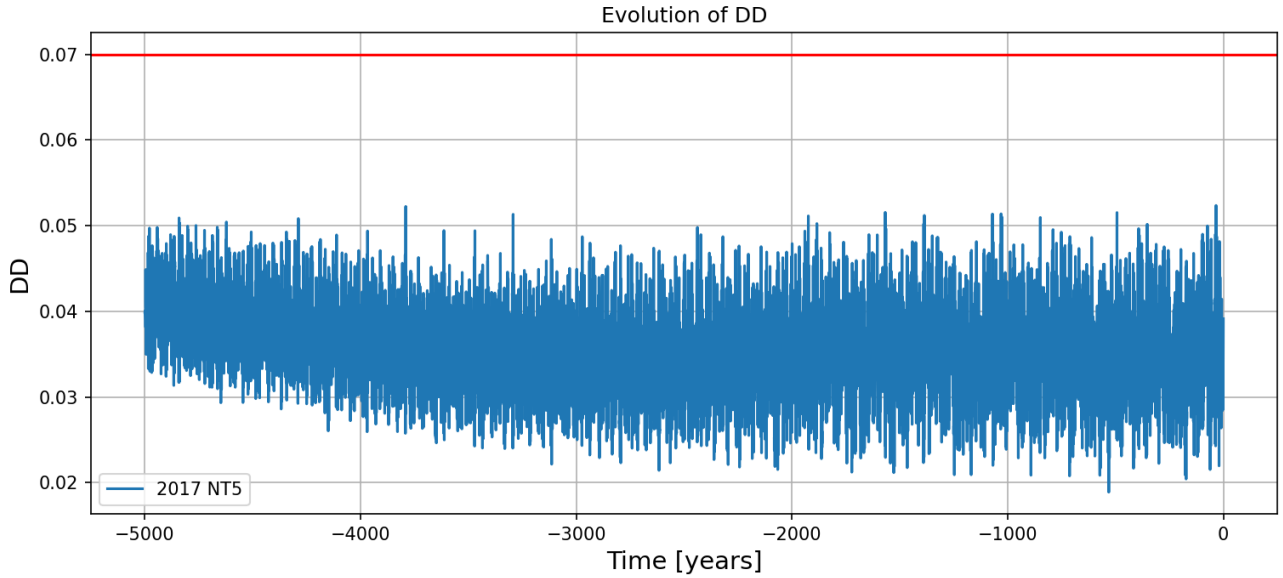

Figure 16 – D_D values for the orbit of the asteroid 2017 NT5 compared to the mean orbit of OSG meteors in the last 5000 years.

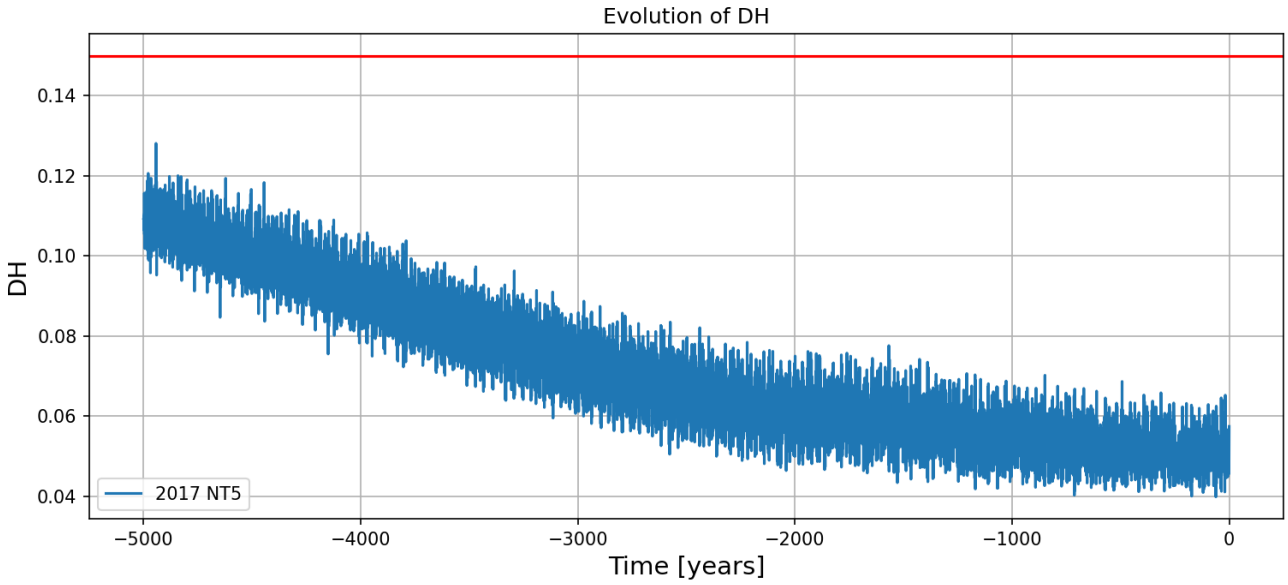

Figure 17 – D_H values for the orbit of the asteroid 2017 NT5 compared to the mean orbit of OSG meteors in the last 5000 years.

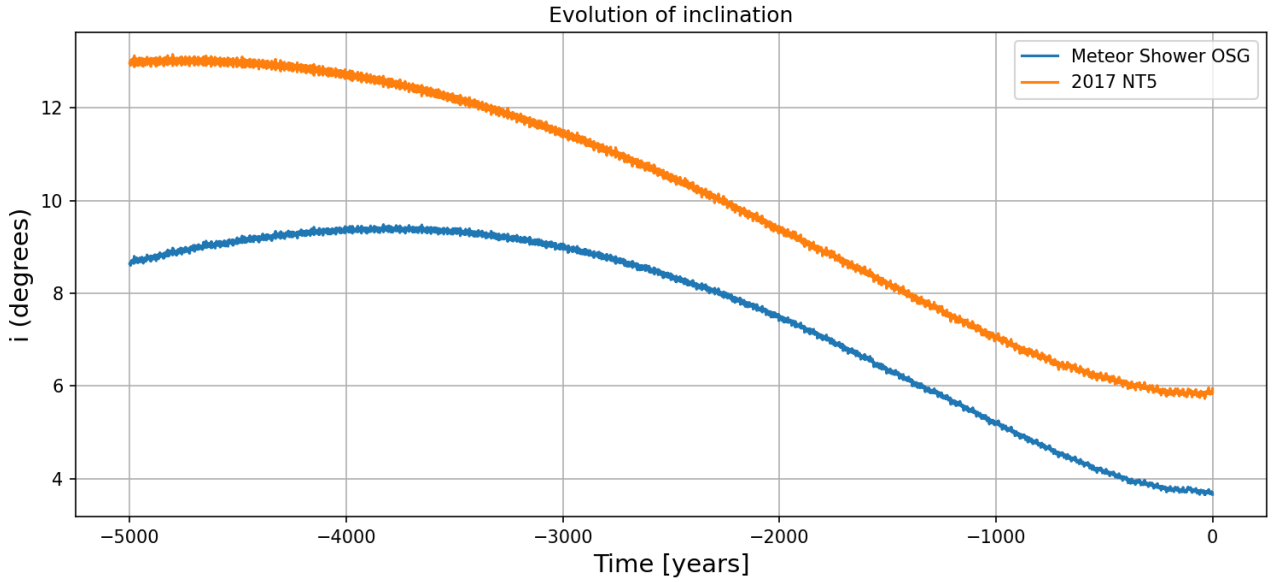

Figure 18 – Evolution of the orbit inclination *i* of asteroid 2017 NT5 and the mean orbit of OSG meteors in the last 5000 years.

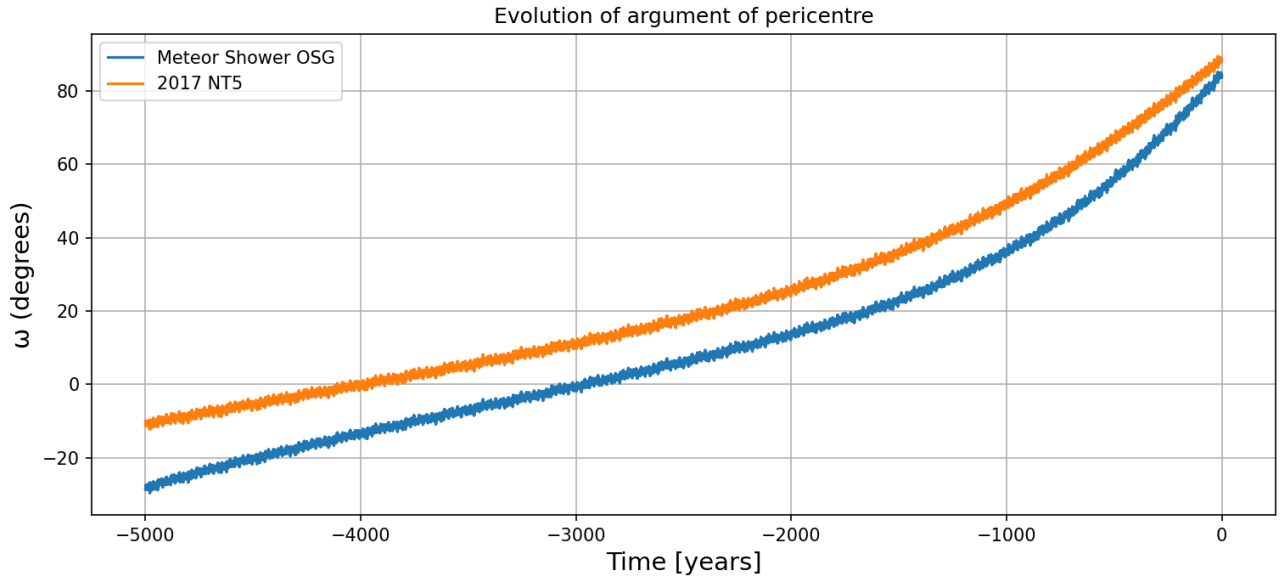

Figure 19 – Evolution of the argument of perihelion ω of the orbit of the asteroid 2017 NT5 and the mean orbit of OSG meteors in the last 5000 years.

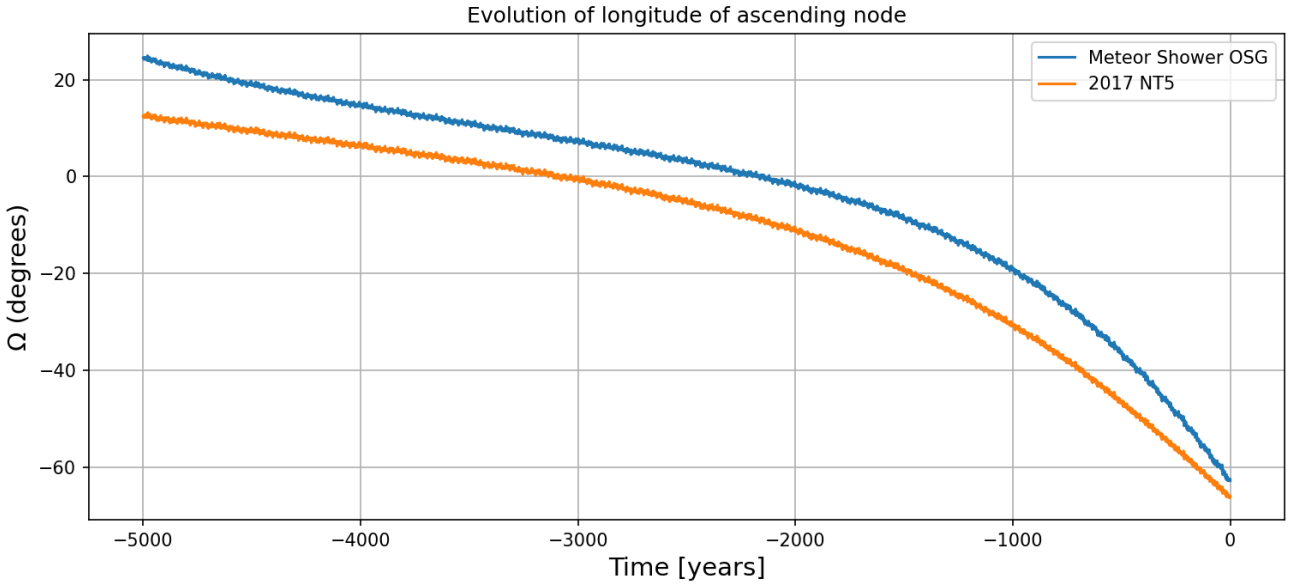

Figure 20 – Evolution of the longitude of the ascending node Ω of the orbit of the asteroid 2017 NT5 and the mean orbit of OSG meteors in the last 5000 years.

4 Conclusion

Using the different dissimilarity criteria and adopting very strict threshold values, it was possible to find in the BRAMON's database two distinct groups of meteors that correspond to two new meteor showers for the southern hemisphere: the SCP (#1042) and OSG (#1043) showers. The mean orbital elements of these showers were obtained and compared to showers already accepted to guarantee their uniqueness. Thus, these two showers became the third and fourth showers from the southern hemisphere established by BRAMON with all or almost all of the meteors being found in its database. Finally, using a strict dissimilarity criterion and the backward integration of the showers and asteroids, it was possible to pinpoint the most probable parent body of the particles responsible for the meteor showers. The asteroids 2019 OK and 2017 NT5 show great similarity with the showers and were discovered by the SONEAR observatory, showing a good interaction of the research developed by the two Brazilian institutions.

Acknowledgment

We would like to thank all station operators at BRAMON engaged in producing data for meteor studies. A special thanks to the operators who contributed with the orbits used in this study:

Stations and operators who contributed with data for the discovery of shower SCP (#1042):

- ADJ1: *Alfredo Dal'Ava Júnior*;
- ARL1, ARL 2: *Andrei Lima*;
- CFJ3, CFJ4: *Heller & Jung Observatory* (*Carlos Jung*);
- ISL: *Zaac Leite*;
- JPZ2: *Marcelo Zurita*;

- LSA1: *João Amâncio*;
- OCA3: *Leonardo Amaral*;
- RCP2: *Renato Poltronieri*;
- ROO: *Vandson Guedes*;
- SMZ4, SMZ6: *Sergio Mazzi*;
- SON: *Sonear Observatory* (*Cristovão Jacques*);
- VRG: *Wellington Albertini*;
- UNB1: *Ubiratan da Nóbrega Borges*.

Stations and operators who contributed with data for the discovery of OSG (#1043) shower:

- AAC: *Alcione Caetano*;
- ADJ1: *Alfredo Dal'Ava Júnior*;
- BFB: *Bruno Bonicontro*;
- CFJ4, CFJ6, CFJ8: *Heller & Jung Observatory* (*Carlos Jung*);
- DLM: *Daniel Leal Mateus*;
- GZT: *Gabriel Zaparolli*;
- JJS: *Jocimar Justino de Souza*;
- JZL: *Juliano Cezar Vieira Zaikievicz*;
- LSA: *João Amancio*;
- OCA3: *Leonardo Amaral*;
- RCP2: *Renato Poltronieri*;
- RSC: *Rafael Compassi*;
- SMZ4. SMZ6: *Sergio Mazzi*;
- SON: *SONEAR Observatory* (*Cristovão Jacques*);
- WSR: *William Siqueira*.

Also, the authors would like to thank *Lubos Neslušan* for providing the algorithm for calculating the theoretical radiant (Neslušan et al., 1998) and the Western Meteor Physics Group for the dissimilarity criterion algorithms implementation (Vida., 2019).

References

Amaral L. S., Trindade, L. S., Bella C. A. P. B., Zurita M. L. P. V., Poltronieri R. C., Silva G. G., Faria C. J. L., Jung C. F., and Koukal J. A. (2018). "Brazilian Meteor Observation Network: History of creation and first developments". In Gyssens M. and Rault J.-L., editors, *Proceedings of the International Meteor Conference,* Petnica, Serbia, 21–24 September, 2017. IMO. pages 171–175.

Bhatnagar K. B., Saha L. M. (1993). "N-Body problem". *Astronomical Society of India, Bulletin*, **21**, 1–25.

Brown P., Jones J. (1998). "Simulation of the Formation and Evolution of the Perseid Meteoroid Stream". *Icarus*, **133**, 36–68.

Chambers J. E. (1999). "A Hybrid Symplectic Integrator that Permits Close Encounters Between Massive Bodies". *Monthly Notices of the Royal Astronomical Society*, **304**, 793–799.

Clube S. V. M., Napier W. M. (1984). "The microstructure of terrestrial catastrophism". *Monthly Notices of the Royal Astronomical Society*, **211**, 953–968.

Drummond J. D. (1981). "A test of comet and meteor shower associations". *Icarus*, **45**, 545–553.

Egal A., Gural P. S., Vaubaillon J., Colas F., Thuillot W. (2017). "The challenge associated with the robust computation of meteor velocities from video and photographic records". *Icarus*, **294**, 43–57.

Guennoun M., Vaubaillon J., Čapek D., Koten P., Benkaldoun Z. (2019). "A robust method to identify meteor showers new parent bodies from the SonotaCo and EDMOND meteoroid orbit databases". *Astronomy & Astrophysics*, **622**, id. A84, 9 pp.

Hirayama K. (1918). "Groups of asteroids probably of common origin". *Astronomical Journal*, **31**, iss. 743, 185–188.

Jenniskens P. (2004). "2003 EH_1 Is the Quadrantid Shower Parent Comet". *Astronomical Journal*, **127**, 3018–3022.

Jenniskens P. (2007). "The IAU Meteor Shower Nomenclature Rules". In: Trigo-Rodríguez J.M., Rietmeijer F.J.M., Llorca J., Janches D., editors, *Advances in Meteoroid and Meteor Science*. Springer, New York, NY. Pages 5–6.

Jenniskens P. (2008). "The IAU Meteor Shower Nomenclature Rules". *Earth, Moon, and Planets*, **102**, 5–9.

Jenniskens P., Jopek T. J., Janches D., Hajduková M., Kokhirova G. I., Rudawska R. (2020). "On removing showers from the IAU Working List of Meteor Showers". *Planetary and Space Science*, **182**, article id. 104821 (3 pages).

Jewitt D., Hsieh H., Agarwal J. (2015). "The Complex History of Trojan Asteroids". In: P. Michel, F. DeMeo, W. Bottke, editors, *Asteroids IV*. University of Arizona Space Science Series. pages 203–220.

Jopek T. J. (1993). "Remarks on the meteor orbital similarity D-criterion". *Icarus*, **106**, 603–607.

Jopek T. J. and Williams I. P. (2013). "Stream and sporadic meteoroids associated with near-Earth objects". *Monthly Notices of the Royal Astronomical Society*, **430**, 2377–2389.

Kinoshita H., Yoshida H., Nakai H. (1991). "Symplectic integrators and their application to dynamical astronomy". *Celestial Mechanics and Dynamical Astronomy*, **50**, 59–71.

Micheli M., Bernardi F., Tholen D. J. (2008). "Updated analysis of the dynamical relation between asteroid 2003 EH1 and comets C/1490 Y1 and C/1385 U1". *Monthly Notices of the Royal Astronomical Society*, **390**, L6–L8.

Neslušan L., Svoren J., Porubčan V. (1998). "A computer program of calculation of a theoretical meteor-stream radiant". *Astronomy and Astrophysics*, **331**, 411–413.

Porubčan V., Williams I. P., Kornoš L. (2004). "Associations Between Asteroids and Meteoroid Streams". *Earth, Moon, and Planets*, **95**, 697–712.

Porubčan V., Kornoš L., Williams I. P. (2006). "The Taurid complex meteor showers and asteroids". *Contributions of the Astronomical Observatory Skalnate Pleso*, **36**, 103–117.

Rein H., Liu S.-F. (2012). "REBOUND: An open-source multi-purpose N-body code for collisional dynamics". *Astronomy and Astrophysics*, **537**, 10 pages. 10.1051/0004-6361/201118085.

Rein H., Tamayo D. (2015). "WHFAST: a fast and unbiased implementation of a symplectic Wisdom–Holman integrator for long-term gravitational simulations". *Monthly Notices of the Royal Astronomical Society*, **452**, 376–388.

Rudawska R., Vaubaillon J., Atreya P. (2012). "Association of individual meteors with their parent bodies". *Astronomy & Astrophysics*, **541**, id. A2, 5 pp.

Schiaparelli G. V. (1867a). "Sur la relation qui existe entre les Comètes et les Etoiles filantes". *Monthly Notices of the Royal Astronomical Society,* **27**, 246–247.

Schiaparelli G. V. (1867b). "Sur la relation qui existe entre les comètes et les étoiles filantes". *Astronomische Nachrichten*, **68**, 331–332.

Šegon D., Gural P., Andreić Ž., Skokić I., Korlević K., Vida D., Novoselnik F. (2014). "A parent body search across several video meteor data bases". In: T.J. Jopek, F.J.M. Rietmeijer, J. Watanabe, I.P. Williams, editors, *Meteoroids 2013*, Proceedings of the Astronomical Conference held at A.M. University, Poznań, Poland, Aug. 26-30, 2013. A.M. University Press, pages 251–262.

Southworth R. R. and Hawkins G. S. (1963). "Statistics of meteor streams". *Smithson. Contrib. Astrophys.*, **7**, 261–286.

Svoren J., Neslušan L., Porubčan V. (1993). "Applicability of meteor radiant determination methods depending on orbit type. I. High-eccentric orbits". *Contributions of the Astronomical Observatory Skalnate Pleso*, **23**, 23–44.

Svoren J., Neslušan L., Porubčan V. (1994). "Applicability of meteor radiant determination methods depending on orbit type. II. Low-eccentric orbits". *Contributions of the Astronomical Observatory Skalnate Pleso*, **24**, 5–18.

Vida D., Brown P. G., Campbell-Brown M. (2018). "Modelling the measurement accuracy of pre-atmosphere velocities of meteoroids". *Monthly Notices of the Royal Astronomical Society*, **479**, 4307–4319.

Vida D., Gural P. S., Brown P. G., Campbell-Brown M., Wiegert P. (2019). "Estimating trajectories of meteors: an observational Monte Carlo approach–I theory". *Monthly Notices of the Royal Astronomical Society*, **491**, 2688–2705.

Weiss E. (1868). "Beiträge zur Kenntniss der Sternschnuppen". *Astronomische Nachrichten*, **72**, 81–102.

Whipple F. L., El-Din Hamid S. (1952). "On the Origin of the Taurid Meteor Streams". *Helwan Institute of Astronomy and Geophysics Bulletins*. **41**. 3–30.

Whipple F. L. (1983). "1983 TB and the Geminid Meteors". IAU Circ., No. 3881, #1 (1983). Edited by Marsden B. G.

Williams I. P., Ryabova G. O., Baturin A. P. and Chernitsov A. M. (2004). "The parent of the Quadrantid meteoroid stream and asteroid 2003 EH1". *Monthly Notices of the Royal Astronomical Society*, **355**, 1171–1181.

Williams I. P., Jones D. C. (2007). "How useful is the 'mean stream' in discussing meteoroid stream evolution?" *Monthly Notices of the Royal Astronomical Society*, **375**, 593–603.

Yeomans D. K., Yau K. K., Weissman P. R. (1996). "The impending appearance of comet Tempel-Tuttle and the Leonid meteors". *Icarus*, **124**, 407–413.

Zurita M., Damiglê R., Di Pietro C., Trindade L., Silva G. G., Lima A., Mota A., Arthur R. and Betzler A. S. (2019). "A bright fireball over the coast of the state of Bahia". *Boletim da Sociedade Astronômica Brasileira*, **31**, 14–16.

Bright fireballs recorded along February 2021 in the framework of the Southwestern Europe Meteor Network

J.M. Madiedo[1], J.L. Ortiz[1], J. Izquierdo[2], P. Santos-Sanz[1], J. Aceituno[3], E. de Guindos[3], P. Yanguas[4] and J. Palacián[4]

[1] **Solar System Department, Institute of Astrophysics of Andalusia (IAA-CSIC), 18080 Granada, Spain**
madiedo@cica.es, ortiz@iaa.es, psantos@iaa.es

[2] **Departamento de Física de la Tierra y Astrofísica, Universidad Complutense de Madrid, 28040 Madrid, Spain**
jizquierdo9@gmail.com

[3] **Observatorio Astronómico de Calar Alto (CAHA), E-04004, Almería, Spain**
aceitun@caha.es, guindos@caha.es

[4] **Departamento de Estadística, Informática y Matemáticas e Instituto de investigación en materiales avanzados, Universidad Pública de Navarra, 31006 Pamplona, Navarra, Spain**
yanguas@unavarra.es, palacian@unavarra.es

This work focuses on the analysis of some of the brightest bolides recorded along February 2021 by the meteor-observing stations operating in the framework of the Southwestern Europe Meteor Network (SWEMN). Some of them were produced by meteoroids belonging to recently discovered and poorly-known streams. The absolute magnitude of these fireballs, which were observed over the Iberian Peninsula, ranged between –7 and –10. The emission spectra produced by some of these events are also presented and discussed.

1 Introduction

This work discusses a series of bright fireballs recorded over Spain by the Southwestern Europe Meteor Network (SWEMN) along February 2021. Weather conditions were not very favorable over most of the Iberian Peninsula during this period, mainly during the last two weeks of that month. This of course was a serious issue for SWEMN meteor stations, and these recorded less meteor events than average.

SWEMN was started by the Institute of Astrophysics of Andalusia (IAA-CSIC) with the aim to analyze the behavior and properties of meteoroids entering the Earth's atmosphere. For this purpose, SWEMN develops the Spectroscopy of Meteoroids by means of Robotic Technologies (SMART) survey. SMART, which started operation in 2006, is currently being carried out at 10 meteor-observing stations in Spain operated from IAA-CSIC (Madiedo, 2014; Madiedo, 2017). In 2021, four additional stations joined the project. These are operated from two universities in Spain: Public University of Navarra (UPNA) and Complutense University of Madrid (UCM).

SMART employs an array of automated cameras and spectrographs to determine the atmospheric trajectories of meteors and the orbit of their parent meteoroids, but also to analyze the composition of these particles from the emission spectrum produced by these meteors (see, e.g., Madiedo et al., 2013; Madiedo et al., 2014). It is worth mentioning that SMART works in close connection with the Moon Impacts Detection and Analysis System (MIDAS), which is a project conducted by the Institute of Astrophysics of Andalusia (Ortiz et al., 2015; Madiedo et al., 2018). The aim of the MIDAS survey is the identification and analysis of flashes generated when meteoroids hit the lunar ground, and the information provided by SMART allows to identify the most likely source of meteoroids impacting the Moon (Madiedo et al. 2015a,b; Madiedo et al. 2019).

Figure 1 – Stacked image of the SWEMN20210202_033000 "Albacete" fireball as recorded from La Sagra.

The bolides described here reached a peak absolute magnitude ranging from –7 to –10. All of them were simultaneously recorded from several SWEMN meteor-observing stations. In this way, their atmospheric path could be triangulated and the position of their radiant could be derived. We found that some of the bolides were associated with recently discovered and poorly-known meteoroid streams. The orbital elements of the meteoroids that gave rise to these meteor events were also calculated. In addition, we present the emission spectrum produced by some of these fireballs.

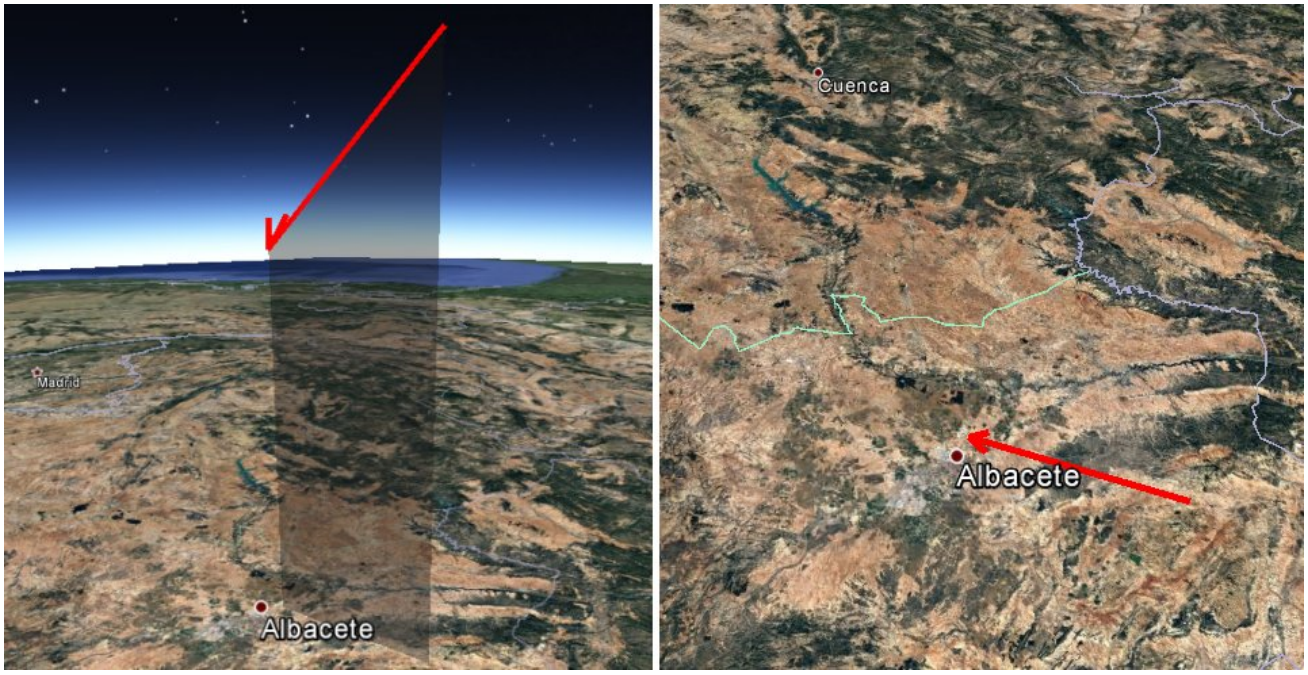

Figure 2 – Atmospheric path (left) and projection on the ground (right) of the trajectory of the SWEMN20210202_033000 "Albacete" fireball.

2 Instrumentation and methods

The bolides analyzed in this work were recorded by means of an array of black and white low-lux analog CCD video cameras manufactured by Watec Co. (models 902H and 902H2 Ultimate). To record meteor emission spectra, some of these devices are configured as spectrographs by attaching holographic 1000 lines/mm diffraction gratings to their objective lens. These Watec cameras have a resolution of 720 × 576 pixels, and their field of view ranges, approximately, from 62 × 50 degrees to 14 × 11 degrees in order to get a good accuracy in the calculation of meteor positions and velocities. We have also employed digital CMOS color cameras (models Sony A7S and A7SII) operating in HD video mode (1920 × 1080 pixels). These cover a field of view of around 90 × 40 degrees. A detailed description of this hardware was given elsewhere (Madiedo, 2017).

At each meteor-observing station the cameras monitor the night sky and operate in a fully autonomous way. The atmospheric trajectory and radiant of meteors, and also the orbit of their parent meteoroids, were obtained with the Amalthea software, developed by J.M. Madiedo (Madiedo, 2014). This program employs the planes-intersection method to obtain the path of meteors in the atmosphere (Ceplecha, 1987). However, for Earth-grazing events atmospheric trajectories are obtained by Amalthea by means of a modification of this classical method (Madiedo et al., 2016). Emission spectra were analyzed with the ChiMet software (Madiedo, 2015a).

3 The 2021 February 2 bolide

On the night of 2021 February 2, at $3^h30^m00.0 \pm 0.1^s$ UTC, a fireball with a peak absolute magnitude of -7 ± 1 was recorded from the SWEMN meteor-observing stations located at the astronomical observatories of Calar Alto, La Sagra, La Hita, Sierra Nevada and Sevilla (*Figure 1*). This bolide was labeled in our meteor database with the code SWEMN20210202_033000.

Atmospheric path, radiant and orbit

The analysis of the atmospheric path of the bolide has been performed by taking into account the recordings from the different meteor-observing stations that observed the event. Our calculations reveal that it overflew the province of Albacete (*Figure 2*). The estimated pre-atmospheric velocity of the meteoroid is $v_\infty = 63.0 \pm 0.4$ km/s, with the apparent radiant located at the equatorial coordinates $\alpha = 226.2^o$, $\delta = +14.4^o$. The luminous event began at a height $H_b = 112.6 \pm 0.5$ km, and ended at an altitude $H_e = 75.9 \pm 0.5$ km. At its terminal point the bolide was almost over the vertical of the city of Albacete, and so it was named after this location. The atmospheric path of the fireball and its projection on the ground are shown in *Figure 2*.

Table 1 – Orbital data (J2000) of the progenitor meteoroid of the SWEMN20210202_033000 "Albacete" fireball.

a (AU)	6.8 ± 1.6	ω (º)	185.9 ± 0.4
e	0.85 ± 0.03	Ω (º)	313.21583 ± 10^{-5}
q (AU)	0.9830 ± 0.0003	i (º)	119.8 ± 0.2

The calculated geocentric velocity of the meteoroid yields $v_g = 61.7 \pm 0.4$ km/s. The orbital parameters of the parent meteoroid before its encounter with our planet are listed in *Table 1*. This heliocentric orbit is shown in *Figure 3*. The value of the Tisserand parameter with respect to Jupiter ($T_J = -0.1$) reveals that the meteoroid followed a cometary orbit before entering the Earth's atmosphere. Radiant and orbital data reveal that said meteoroid belonged to the 12-Bootids stream (TBO#0607). This recently discovered

and poorly known annual shower peaks around January 18 (Segon et al., 2014). The orbital elements listed in *Table 1* are in very good agreement with orbital parameters included in the IAU meteor database[2].

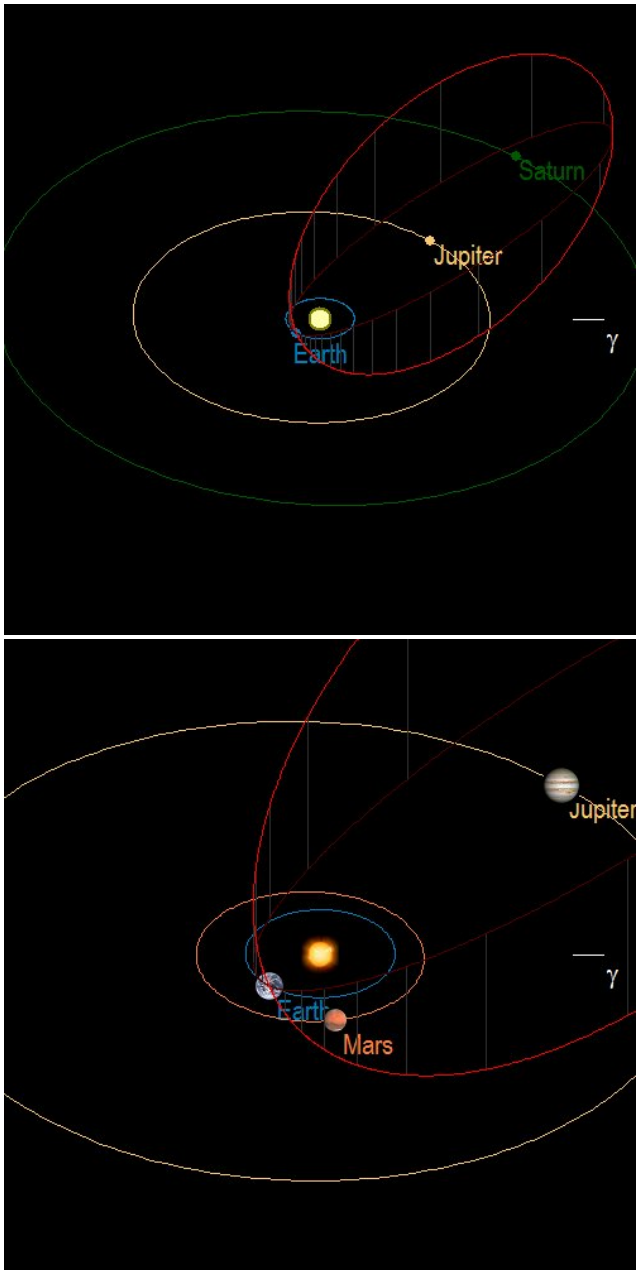

Figure 3 – Up: orbit (red line) of the parent meteoroid of the SWEMN20210202_033000 fireball, and projection of this orbit (dark red line) on the ecliptic plane; Down: close-up view of the orbit.

Emission spectrum

The emission spectrum of the fireball was recorded by one of our videospectrographs from Sierra Nevada. Meteor spectra with the resolution provided by our instruments typically allows to identify lines produced by Na, Mg, Ni, Fe, Ca and some metal oxides in the meteoroid, together with the contributions of atmospheric oxygen and nitrogen (see, for instance, Madiedo, 2014; Madiedo et al. 2021). Previous works performed from the Calar Alto Astronomical Observatory have shown that higher resolution spectra have proven to be useful to identify additional species, such as Ti, Cr, Zr, Pd and W (Passas et al., 2016).

As in previous works (Madiedo, 2015b), the spectrum was calibrated in wavelength and corrected by taking into account the spectral sensitivity of the device. The calibrated spectrum is shown in *Figure 4*, where the most significant lines have been highlighted. The majority of these contributions correspond to neutral iron (Fe I), which is typical in meteor spectra (Borovička, 1993; Madiedo, 2014). In this case, several multiplets of Fe I have been identified. The most important ones are Fe I-4 at 393.3 nm (which appears blended with the Mg I-3 line at 383.2 nm), Fe I-43 and Fe I-15. The most important contributions, however, correspond to the H and K lines of Ca II-1, which also appear blended in the signal. The emission lines of the Na I-1 doublet (588.9 nm) and the Mg I-2 triplet (516.7 nm) are also very significant. The contribution from Ca I-2 at 422.6 nm was also observed. Atmospheric N_2 bands were identified in the red region of the spectrum, together with the contribution from N I and the O I line at 777.1 nm. The analysis of the relative intensities of these lines will provide key information about the nature of the meteoroid.

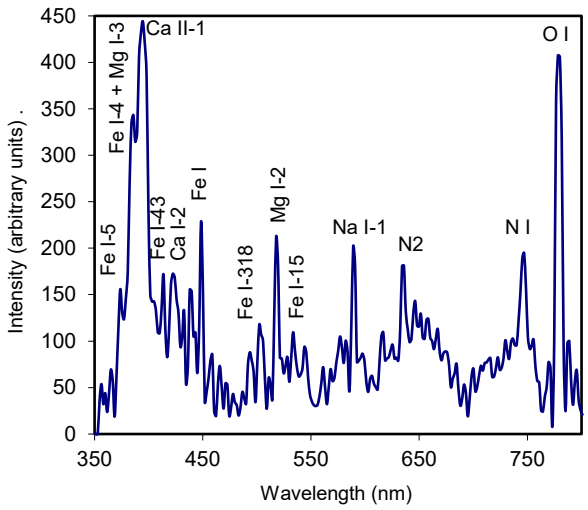

Figure 4 – Calibrated emission spectrum of the SWEMN20210202_033000 "Albacete" fireball.

4 The 2021 February 15 fireball

This event was detected by SWEMN systems on 2021 February 15 at $21^h38^m19.8 \pm 0.1^s$ UTC. Its peak absolute magnitude was –7 ± 1 (*Figure 5*). The bolide was recorded from the meteor-observing stations operating at La Sagra, Sierra Nevada, Calar Alto, El Arenosillo, and Sevilla. The fireball, which can be viewed on this YouTube video[3], was included in the SWEMN meteor database under the code SWEMN20210215_213819.

Atmospheric path, radiant and orbit

According to our calculations, this fireball overflew the provinces of Córdoba and Jaén, located in Andalusia (south of Spain). The meteoroid that gave rise to this luminous event entered the atmosphere with an initial velocity

[2] http://www.astro.amu.edu.pl/~jopek/MDC2007/

[3] https://youtu.be/xWpdDZWss5o

$v_\infty = 14.4 \pm 0.3$ km/s. The apparent radiant of the meteor was located at the equatorial coordinates $\alpha = 58.6º$, $\delta = -17.3º$. The bolide began at an altitude $H_b = 92.1 \pm 0.4$ km over the south of the province of Córdoba. The terminal point of the fireball was reached at a height $H_e = 64.0 \pm 0.5$ km over the province of Jaén, next to the vertical of Arjona. For this reason, we named this event after this town. The atmospheric trajectory of this slow bolide and its projection on the ground are shown in *Figure 6*.

Figure 5 – Stacked image of the SWEMN20210215_213819 "Arjona" fireball over one of the domes of the Sierra Nevada Astronomical Observatory.

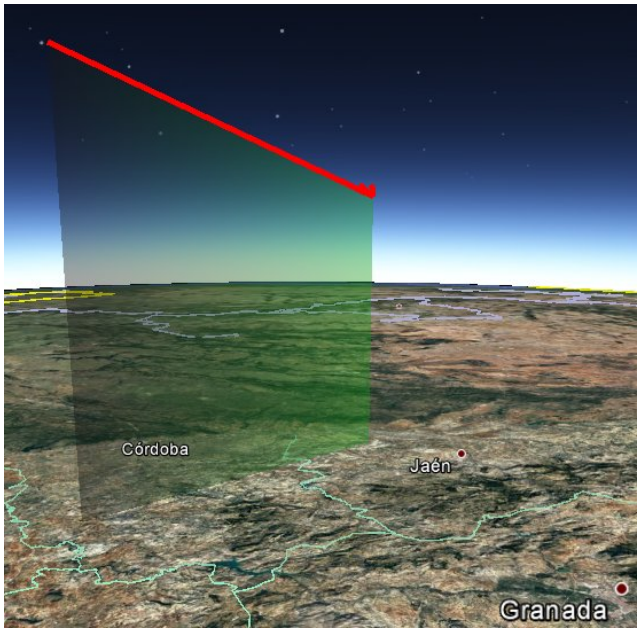

Figure 6 – Atmospheric path and projection on the ground of the trajectory of the SWEMN20210215_213819 "Arjona" fireball.

Once the atmospheric path was characterized, the orbital elements of the progenitor meteoroid were calculated. *Table 2* contains the orbital parameters obtained for this particle. This orbit is shown in *Figure 7*. The calculated geocentric velocity yields $v_g = 9.6 \pm 0.4$ km/s. The value of the Tisserand parameter with respect to Jupiter ($T_J = 3.5$) shows that the meteoroid followed an asteroid-like orbit before its encounter with our planet. According to radiant and orbital data, this meteoroid belonged to the sporadic background.

Table 2 – Orbital data (J2000) of the progenitor meteoroid of the SWEMN20210215_213819 "Arjona" fireball.

a (AU)	2.0 ± 0.1	ω (º)	343.5 ± 0.8
e	0.53 ± 0.03	Ω (º)	147.13489 ± 10^{-5}
q (AU)	0.9738 ± 0.0008	i (º)	10.5 ± 0.3

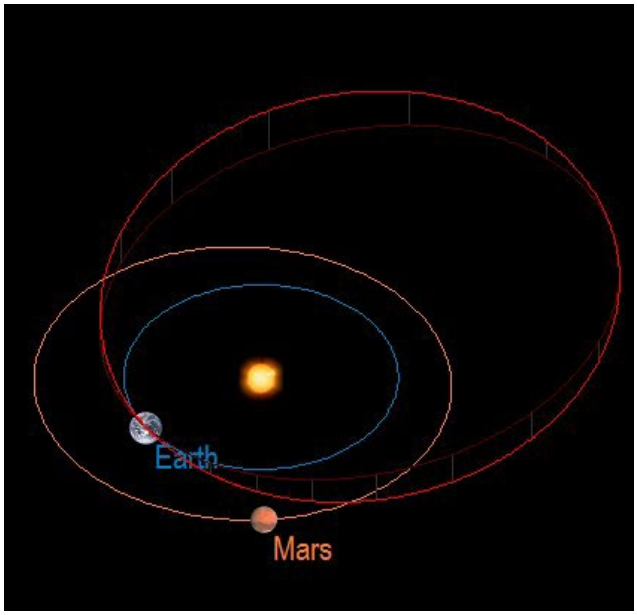

Figure 7 – Orbit (red line) of the parent meteoroid of the SWEMN20210215_213819 fireball, and its projection (dark red line) on the ecliptic plane.

5 The 2021 February 16 fireball

On the night of 2021 February 16, at $5^h00^m32.9 \pm 0.1^s$ UTC, a bolide with a peak absolute magnitude of -8 ± 1 was recorded by SWEMN systems operating from the astronomical observatories of La Hita, Sierra Nevada, El Arenosillo, Calar Alto, La Sagra, Sevilla and Madrid (*Figure 8*). A video showing this event was uploaded to YouTube[4]. After its appearance date and time, the fireball was included in our meteor database with the code SWEMN20210216_050033.

Atmospheric path, radiant and orbit

From the analysis of the recordings, we obtained that the event overflew the province of Badajoz (southwest of Spain). The pre-atmospheric velocity measured from the recordings was $v_\infty = 61.8 \pm 0.3$ km/s. The bolide began at an altitude $H_b = 117.7 \pm 0.5$ km over Badajoz and ended at a height $H_e = 82.7 \pm 0.5$ km over the same province. We named this event "Villafranco del Guadiana", since the terminal point of its atmospheric path was located almost

[4] https://youtu.be/2cU4kn5tHBs

over the vertical of this town. The apparent radiant of the meteor was located at the equatorial coordinates $\alpha = 196.9^{\circ}$, $\delta = -17.7^{\circ}$. The atmospheric trajectory of the fireball and its projection on the ground are shown in *Figure 9*.

Figure 8 – Stacked image of the SWEMN20210216_050032 "Villafranco del Guadiana" fireball as recorded from Sevilla.

Figure 9 – Atmospheric path and projection on the ground of the trajectory of the SWEMN20210216_050032 fireball.

Table 3 – Orbital data (J2000) of the progenitor meteoroid of the SWEMN20210216_050033 "Villafranco del Guadiana" fireball.

a (AU)	6.1 ± 0.9	ω (º)	118.9 ± 0.9
e	0.955 ± 0.005	Ω (º)	147.45544 ± 10^{-5}
q (AU)	0.271 ± 0.005	i (º)	148.7 ± 0.2

From the calculation of the orbital parameters of the progenitor meteoroid we derived the values listed in *Table 3*. The geocentric velocity yields $v_g = 60.9 \pm 0.3$ km/s. The orbit is shown in *Figure 10*. The calculated value of the Tisserand parameter with respect to Jupiter ($T_J = 0.3$) shows that this particle followed a cometary orbit before its encounter with our planet. Besides, radiant and orbital data reveal that the bolide was produced by a sporadic meteoroid.

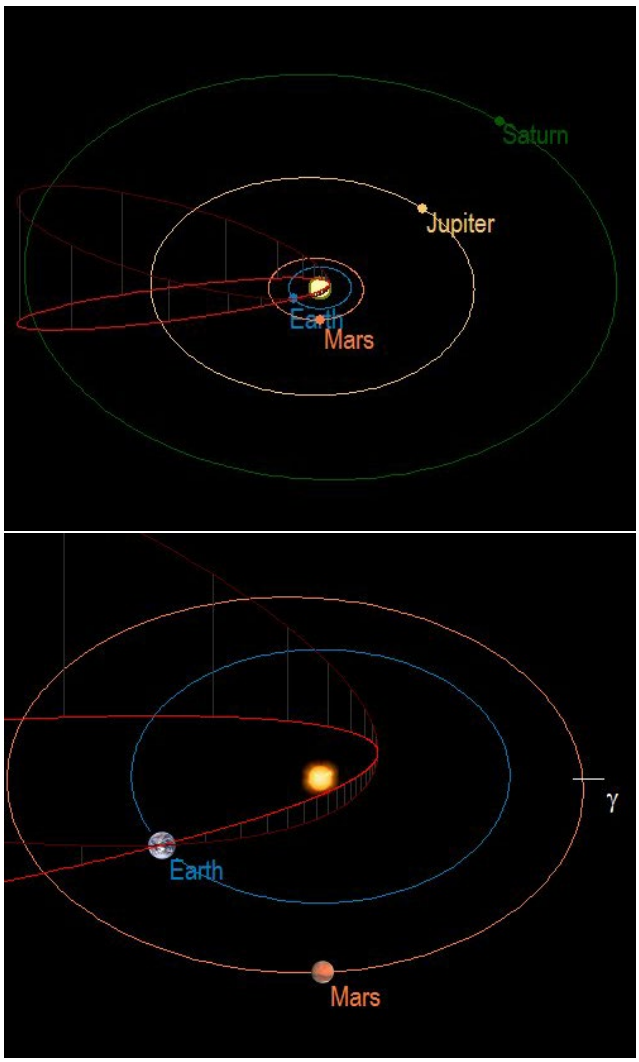

Figure 10 – Up: orbit (red line) of the parent meteoroid of the SWEMN20210216_050032 fireball, and its projection (dark red line) on the ecliptic plane; Down: close-up view of the orbit.

6 The 2021 February 17 fireball

This bolide was observed at $20^{h}35^{m}36.5 \pm 0.1^{s}$ UTC on 2021 February 17 (*Figure 11*). It exhibited several flares along its atmospheric trajectory as a consequence of the disruption of the progenitor meteoroid. The fireball reached a peak absolute magnitude of -10 ± 1. This event was spotted from the meteor-observing stations operating at the astronomical observatories of La Hita, La Sagra, Calar Alto, Sierra Nevada, El Arenosillo and Sevilla. It was recorded by our HD cameras. A video showing this fireball and its trajectory can be viewed on YouTube[5]. The bolide was included in our meteor database with the code SWEMN20210217_203536.

Atmospheric path, radiant and orbit

According to our calculation, the meteor was produced by a meteoroid that entered the atmosphere with an initial velocity $v_\infty = 27.6 \pm 0.3$ km/s. Its apparent radiant was located at the equatorial coordinates $\alpha = 146.8^{\circ}$, $\delta = +9.5^{\circ}$. This fireball also overflew the province of Badajoz, as the

[5] https://youtu.be/gvED_SpoX84

above-described event recorded the day before did. Thus, the bolide began at an altitude $H_b = 94.6 \pm 0.5$ km over Badajoz, and ended its luminous phase at a height $H_e = 43.9 \pm 0.4$ km over the same province. We named this fireball "Mérida", since it overflew this city. *Figure 12* shows the atmospheric trajectory of this meteor and its projection on the ground.

Figure 11 – Stacked image of the SWEMN20210217_203536 "Mérida" fireball as recorded from Sevilla.

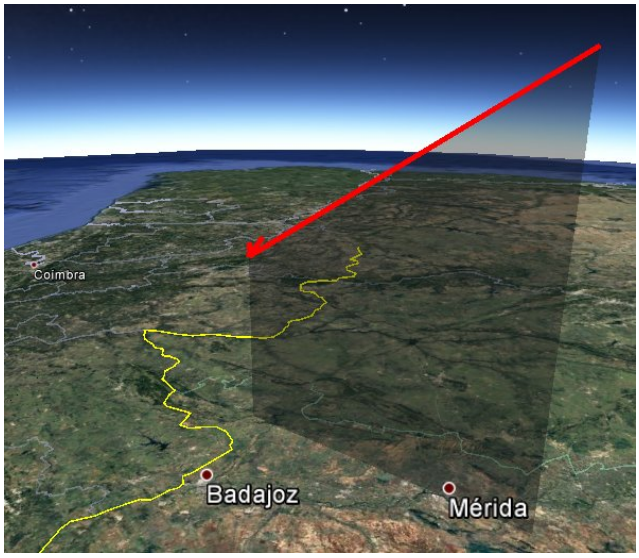

Figure 12 – Atmospheric path and projection on the ground of the trajectory of the SWEMN20210217_203536 "Mérida" fireball.

The results of the computation of the orbital elements of the meteoroid are listed in *Table 4*. The projection on the ecliptic plane of this orbit has been drawn in *Figure 13*. The geocentric velocity of the meteoroid yields $v_g = 25.1 \pm 0.3$ km/s. According to the data provided by the IAU meteor database, these results point to an association of this fireball with the February π-Leonids (FPL#0501), which peaks around February 6 (Rudawska and Jenniskens, 2014). The Tisserand parameter with respect to Jupiter, which yields $T_J = 2.19$, shows that the meteoroid followed a cometary orbit before its encounter with Earth, and suggests that this meteoroid stream is produced by a Jupiter family comet (JFC).

Table 4 – Orbital data (J2000) of the progenitor meteoroid of the SWEMN20210217_203536 "Mérida" fireball.

a (AU)	4.0 ± 0.3	ω (º)	84.63 ± 0.08
e	0.85 ± 0.01	Ω (º)	149.09629 ± 10^{-5}
q (AU)	0.574 ± 0.002	i (º)	3.8 ± 0.1

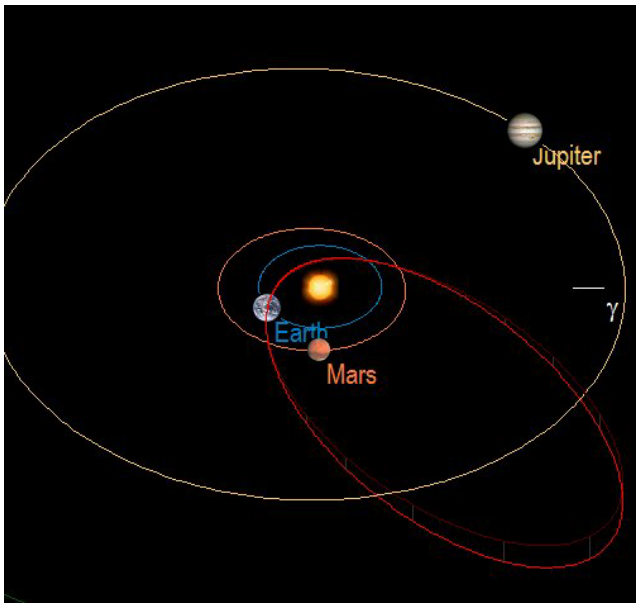

Figure 13 – Orbit (red line) of the parent meteoroid of the SWEMN20210217_203536 "Mérida" fireball, and its projection (dark red line) on the ecliptic plane.

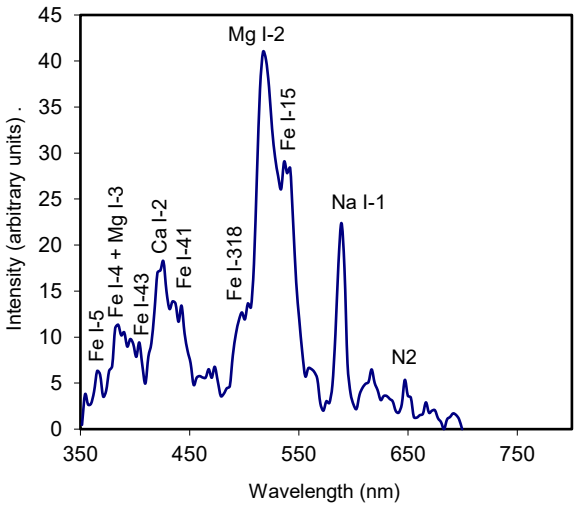

Figure 14 – Calibrated emission spectrum of the SWEMN20210217_203536 "Mérida" fireball.

Emission spectrum

The emission spectrum of the "Mérida" fireball was recorded from the meteor-observing station located at La Hita Astronomical Observatory. *Figure 14* shows this signal, which was corrected by taking into account the sensitivity of the spectrograph and calibrated in wavelength by means of the ChiMet software (Madiedo, 2015a). As can be noticed, the most relevant contributions correspond to the Na-I doublet (588.9 nm), the Mg I-2 triplet (516.7 nm), and the Fe I-15 emission. The contribution from Fe I-4 (393.3 nm) appears blended with the line produced by Mg

I-3 at 383.2 nm. Other neutral Fe multiplets have been identified, as for instance those of Fe I-5, Fe I-43, Fe I-41, and Fe I-318. The line of Ca I-2 at 422.6 nm was also found. Molecular bands produced by atmospheric N_2 are present in the red region of the spectrum.

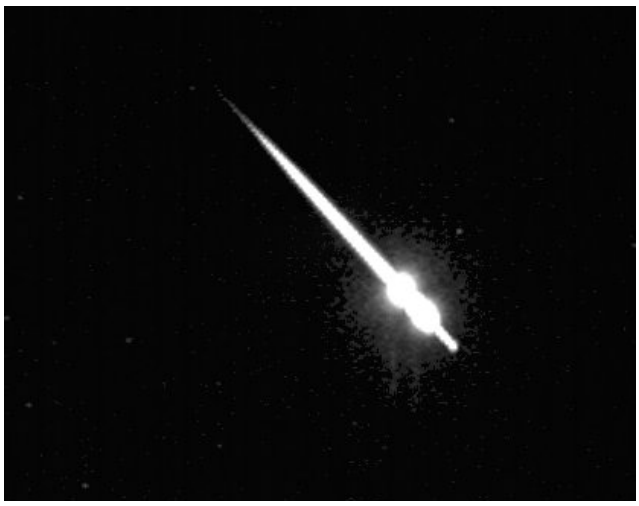

Figure 15 – Stacked image of the SWEMN20210218_043509 "Helechal" fireball as recorded from La Hita meteor station.

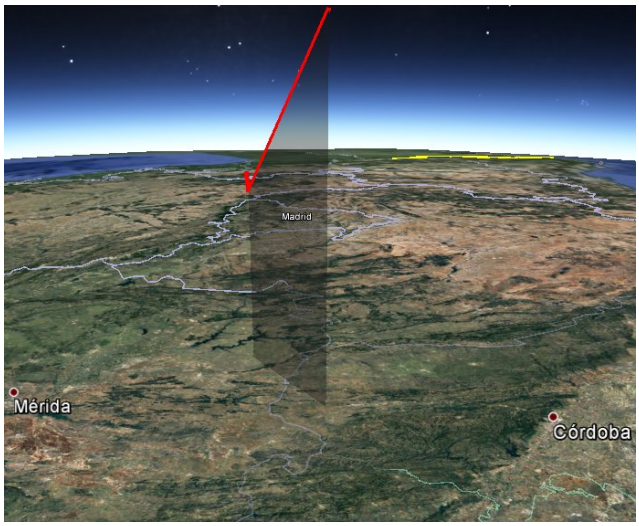

Figure 16 – Atmospheric path and projection on the ground of the trajectory of the SWEMN20210218_043509 fireball.

7 The 2021 February 18 fireball

This bolide reached a peak absolute magnitude of -9 ± 1, and was recorded at $4^h35^m09.4 \pm 0.1^s$ UTC on 2021 February 18. It experienced two bright flares, as can be seen in *Figure 15*. The event was spotted from the SWEMN meteor-observing stations deployed at La Hita, La Sagra, Calar Alto, Sevilla, Madrid, Sierra Nevada and El Arenosillo. A video showing this fireball was uploaded to YouTube[6]. The bolide was included in our meteor database with the code SWEMN20210218_043509.

Atmospheric path, radiant and orbit

The triangulation of the atmospheric trajectory of the meteor reveals that the meteoroid entered the atmosphere with an initial velocity $v_\infty = 67.4 \pm 0.5$ km/s. The apparent radiant was located at the equatorial coordinates $\alpha = 223.1^o$, $\delta = +1.4^o$. The bolide began at an altitude $H_b = 124.2 \pm 0.5$ km over the north of the province of Córdoba, and ended its luminous phase over the province of Badajoz, at a height $H_e = 63.4 \pm 0.5$ km. The event exhibited its first major flare when it overflew Helechal, a village in the province of Badajoz. For this reason, we named the fireball after this location. *Figure 16* shows the atmospheric trajectory of the "Helechal" bolide and its projection on the ground.

Table 5 – Orbital data (J2000) of the progenitor meteoroid of the SWEMN20210218_043509 "Helechal" fireball.

a (AU)	9.4 ± 4.0	ω (º)	244.5 ± 1.6
e	0.92 ± 0.03	Ω (º)	329.45156 ± 10^{-5}
q (AU)	0.717 ± 0.007	i (º)	147.1 ± 0.2

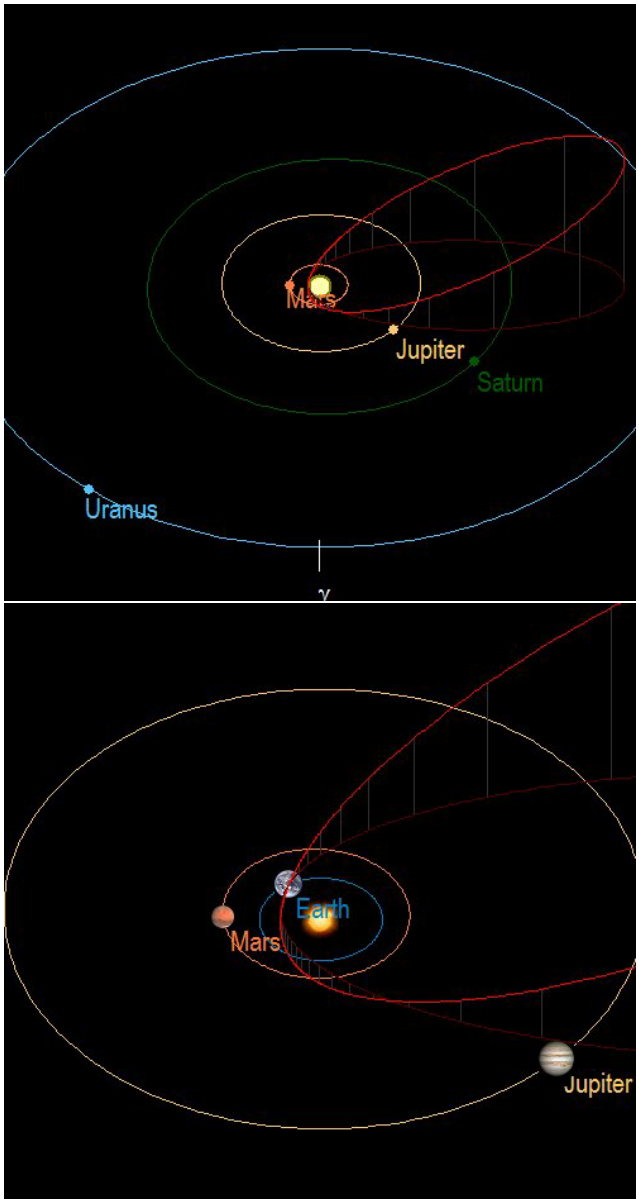

Figure 17 – Up: orbit (red line) of the parent meteoroid of the SWEMN20210218_043509 fireball, and its projection (dark red line) on the ecliptic plane; Down: close-up view of the orbit.

The Amalthea software provided the values listed in *Table 5* for the orbital elements of the progenitor meteoroid. The

[6] https://youtu.be/91izm6gYv0g

projection on the ecliptic plane of this heliocentric orbit is shown in *Figure 17*. The calculated value of the geocentric velocity of this particle yields $v_g = 66.4 \pm 0.5$ km/s. According to the information found in the IAU meteor database, these results show that the meteoroid belonged to the February μ-Virginids (FMV#0516). This poorly-known meteoroid stream produces a display of meteors peaking around February 15 (Segon et al., 2013). The calculated value of the Tisserand parameter with respect to Jupiter ($T_J = -0.3$) shows that this meteoroid followed a cometary orbit before entering our atmosphere.

Emission spectrum

Four SWEMN spectrographs located at La Hita, La Sagra, and El Arenosillo recorded the emission spectrum of the "Helechal" bolide. The signal (*Figure 18*) was calibrated in wavelength and then corrected by taking into account the sensitivity of the recording device. As in previous cases, most features in the spectrum are associated with the emission of neutral iron. Thus, we have identified lines produced by Fe I-23, Fe I-5, Fe I-4, Fe I-318, Fe I-16 and Fe I-15. However, the most remarkable emission corresponds to the H and K lines of ionized calcium (Ca II-1 multiplet). Other relevant contributions are due to the Na-I doublet (588.9 nm), the Mg I-2 triplet (516.7 nm), Ca I-2 (422.6 nm), and Mg I-3 (383.2 nm). The latter is blended with the line produced by Fe I-4 at 393.3 nm. Molecular bands from atmospheric N_2 are also present in this case. A deeper analysis of this spectrum is currently in progress to derive information about the nature of the meteoroid.

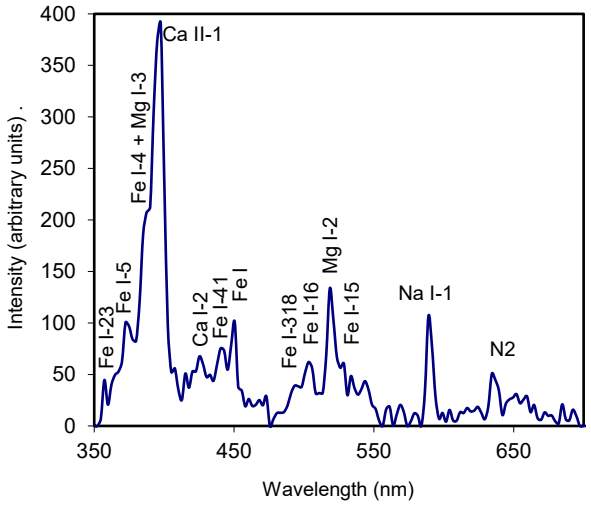

Figure 18 – Calibrated emission spectrum of the SWEMN20210218_043509 "Helechal" fireball.

8 Conclusion

We have presented here the five most relevant bolides recorded over Spain along February 2021 in the framework of the Southwestern Europe Meteor Network (SWEMN). The peak absolute magnitude of these fireballs ranged from –7 to –10. Our analysis has revealed that these events were produced by meteoroids belonging to the sporadic background, but also by members of recently-discovered meteoroid streams. So, our research has provided valuable information about the properties of poorly-known meteor showers.

The bolide recorded on February 2 (named "Albacete") was associated with the 12 Bootids (TBO#0607), a recently discovered meteoroid stream which peaks around January 18. It reached a peak absolute magnitude of –7. and the meteoroid followed a cometary orbit before hitting the Earth's atmosphere.

The bolide "Arjona", which was recorded on February 15, was produced by a sporadic meteoroid following an asteroidal orbit. This fireball overflew the provinces of Córdoba and Jaén, and reached a peak absolute magnitude of –7.

Another sporadic fireball (named "Villafranco del Guadiana") was spotted on February 16. In this case, the meteoroid followed a cometary orbit before entering the atmosphere. This event, which had a peak absolute magnitude of –8, overflew the province of Badajoz.

The mag. –10 "Merida" bolide, which also overflew the province of Badajoz, was recorded on February 17. It was associated with the February π-Leonids (FPL#0501), a poorly-known meteor shower which peaks around February 6. According to our results, the meteoroid followed a Jupiter family comet orbit before entering the atmosphere.

Finally, the mag. –9 "Helechal" fireball was found to be generated by a meteoroid belonging to the February μ-Virginid meteoroid stream. This bolide, which overflew the provinces of Córdoba and Badajoz, was recorded on February 18, three days after the peak of this meteor shower.

We have also recorded and presented the emission spectra obtained for the three shower bolides described in this work: "Albacete", "Mérida" and "Helechal". The main emission lines appearing in these spectra have been identified, and most of them were found to be produced by several neutral iron multiplets. The contributions from other chemical species contained in the progenitor meteoroids, such as those of Na I, Mg I, Ca I, and Ca II, were also identified. Atmospheric contributions were present in these signals too. Further analysis of these spectra is being performed to derive chemical information about the the 12-Bootids, the February π-Leonids, and the February μ-Virginids. This will allow us to improve our knowledge about these recently-discovered and poorly-known meteoroid streams.

Acknowledgment

We acknowledge support from the Spanish Ministry of Science and Innovation (project PID2019-105797GB-I00). We also acknowledge financial support from the State Agency for Research of the Spanish MCIU through the "Center of Excellence Severo Ochoa award to the Instituto de Astrofísica de Andalucía (SEV-2017-0709)". P.S-S. acknowledges financial support by the Spanish grant AYA-RTI2018-098657-J-I00 "LEO-SBNAF" (MCIU / AEI / FEDER, UE).

References

Borovička J. (1993). "A fireball spectrum analysis". *Astronomy and Astrophysics*, **279**, 627–645.

Ceplecha Z. (1987). "Geometric, dynamic, orbital and photometric data on meteoroids from photographic fireball networks". *Bull. Astron. Inst. Cz.*, **38**, 222–234.

Madiedo J. M., Trigo-Rodríguez J. M., Lyytinen E., Dergham J., Pujols P., Ortiz J. L. and Cabrera J. (2013). "On the activity of the γ-Ursae Minorids meteoroid stream in 2010 and 2011". *Monthly Notices of the Royal Astronomical Society*, **431**, 1678–1685.

Madiedo J. M. (2014). "Robotic systems for the determination of the composition of solar system materials by means of fireball spectroscopy". *Earth, Planets & Space*, **66**, 70.

Madiedo J. M., Ortiz J. L., Trigo-Rodríguez J. M., Dergham J. and Castro-Tirado A.J. (2014). "Analysis of bright Taurid fireballs and their ability to produce meteorites". *Icarus*, **231**, 356–364.

Madiedo J. M. (2015a). "Spectroscopy of a κ-Cygnid fireball afterglow". *Planetary and Space Science*, **118**, 90–94.

Madiedo J. M. (2015b). "The ρ-Geminid meteoroid stream: orbits, spectroscopic data and implications for its parent body". *Monthly Notices of the Royal Astronomical Society*, **448**, 2135–2140.

Madiedo J. M., Ortiz J. L., Organero F., Ana-Hernández L., Fonseca F., Morales N. and Cabrera-Caño J. (2015a). "Analysis of Moon impact flashes detected during the 2012 and 2013 Perseids". *Astronomy and Astrophysics*, **577**, A118.

Madiedo J. M., Ortiz J. L., Morales N. and Cabrera-Caño J. (2015b). "MIDAS: Software for the detection and analysis of lunar impact flashes". *Planetary and Space Science*, **111**, 105–115.

Madiedo J. M., Espartero F., Castro-Tirado A. J., Pastor S., and De los Reyes J. A. (2016). "An Earth-grazing fireball from the Daytime ζ-Perseid shower observed over Spain on 2012 June 10". *Monthly Notices of the Royal Astronomical Society*, **460**, 917–922.

Madiedo J. M. (2017). "Automated systems for the analysis of meteor spectra: The SMART Project". *Planetary and Space Science*, **143**, 238–244.

Madiedo J. M., Ortiz J. L. and Morales N. (2018). "The first observations to determine the temperature of a lunar impact flash and its evolution". *Monthly Notices of the Royal Astronomical Society*, **480**, 5010–5016.

Madiedo J. M., Ortiz J. L., Santos-Sanz P., Aceituno J. and de Guindos E. (2021). "Bright fireballs recorded during January 2021 in the framework of the Southwestern Europe Meteor Network". *eMetN*, **6**, 247-254.

Madiedo J. M., Ortiz J. L., Yanagisawa M., Aceituno J. and Aceituno F. (2019). "Impact flashes of meteoroids on the Moon". *Meteoroids: Sources of Meteors on Earth and Beyond*, Ryabova G. O., Asher D. J., and Campbell-Brown M. D. (eds.), Cambridge, UK. Cambridge University Press, ISBN 9781108426718, 2019, p. 136–158.

Ortiz J. L., Madiedo J. M., Morales N., Santos-Sanz P. and Aceituno F. J. (2015). "Lunar impact flashes from Geminids: analysis of luminous efficiencies and the flux of large meteoroids on Earth". *Monthly Notices of the Royal Astronomical Society*, **454**, 344–352.

Passas M., Madiedo J. M., Gordillo-Vázquez F. J. (2016). "High resolution spectroscopy of an Orionid meteor from 700 to 800 nm". *Icarus*, **266**, 134–141.

Rudawska R. and Jenniskens P. (2014). "New meteor showers identified in the CAMS and SonotaCo meteoroid orbit surveys". *The Meteoroids 2013, Proceedings* of the Astronomical Conference held at A.M. University, Poznań, Poland, Aug. 26-30, 2013. Eds.: T.J. Jopek, F.J.M. Rietmeijer, J. Watanabe, I.P. Williams, A.M. University Press, 2014, p. 217–224.

Segon D., Andreic Z., Korlevic K., Novoselnik F., Vida D. and Skokic I. (2013). "8 new showers from Croatian Meteor Network data". *WGN, Journal of the International Meteor Organization*, **41**, 70–74.

Segon D., Andreic Z., Gural P., Skokic I., Korlevic K., Vida D., Novoselnik F. and Gostinski D. (2014). "Results of CMN 2013 search for new showers across CMN and SonotaCo databases III". *WGN, Journal of the International Meteor Organization*, **42**, 227–233.

Bright fireballs recorded along March 2021 in the framework of the Southwestern Europe Meteor Network

J. M. Madiedo[1], J. L. Ortiz[1], J. Izquierdo[2], P. Santos-Sanz[1], J. Aceituno[3], E. de Guindos[3], P. Yanguas[4] and J. Palacián[4]

[1] **Solar System Department, Institute of Astrophysics of Andalusia (IAA-CSIC), 18080 Granada, Spain**
madiedo@cica.es, ortiz@iaa.es, psantos@iaa.es

[2] **Departamento de Física de la Tierra y Astrofísica, Universidad Complutense de Madrid, 28040 Madrid, Spain**
jizquierdo9@gmail.com

[3] **Observatorio Astronómico de Calar Alto (CAHA), 04004, Almería, Spain**
aceitun@caha.es, guindos@caha.es

[4] **Departamento de Estadística, Informática y Matemáticas e Institute for Advanced Materials and Mathematics, Universidad Pública de Navarra, 31006 Pamplona, Navarra, Spain**
yanguas@unavarra.es, palacian@unavarra.es

The most relevant bolides recorded along March 2021 in the framework of the Southwestern Europe Meteor Network (SWEMN) and the SMART project are presented here. These fireballs, which overflew the Iberian Peninsula and neighboring areas, had an absolute peak luminosity ranging between magnitude –8 and –11. We also analyze the main features appearing in the emission spectra recorded for some of these bright meteors.

1 Introduction

We present here the most remarkable bolides recorded during March 2021 over Spain and neighboring areas by the Southwestern Europe Meteor Network (SWEMN). Because of adverse weather conditions during the first two weeks of this month, the most remarkable fireball activity was spotted by our systems during the second half of March.

SWEMN is a research network coordinated by the Institute of Astrophysics of Andalusia (IAA-CSIC) with the aim to analyze the Earth's meteoric environment. Currently the network is also integrated by researchers from the Complutense University of Madrid (UCM), the Public University of Navarre (UPNA), and the Calar Alto Observatory (CAHA). We also receive input from amateur astronomers who collaborate with this meteor network.

To identify and analyze meteors in the Earth's atmosphere, SWEMN develops the Spectroscopy of Meteoroids by means of Robotic Technologies (SMART) survey (Madiedo, 2014; Madiedo, 2017). To obtain a much more complete insight into the properties of the Earth-Moon meteoric environment, SMART works in close connection with another project conducted by the Institute of Astrophysics of Andalusia: The Moon Impacts Detection and Analysis System (MIDAS) (Ortiz et al., 2015; Madiedo et al., 2018). Thus, SMART employs our atmosphere as a detector to identify meteors generated by meteoroids crossing the Earth's orbit. At the same time, MIDAS considers the Moon as a laboratory that provides information about meteoroids hitting the lunar ground (Madiedo et al., 2019a). Previous works showed that there exists a strong synergy between both systems (Madiedo et al. 2015a, b; Madiedo et al. 2019b).

The bolides presented in this work reached a peak absolute magnitude ranging from –8 to –11. The results obtained from the analysis of their atmospheric path and radiant are discussed below. The orbital elements of the progenitor meteoroids were also obtained. As in previous reports (Madiedo et al., 2021), we also present the emission spectrum recorded for some of these bright meteors.

2 Instrumentation and methods

The meteors described here were recorded by means of analog CCD video cameras manufactured by Watec. (models 902H and 902H2 Ultimate). Their field of view ranges from 62 × 50 degrees to 14 × 11 degrees. To record meteor spectra, we have attached holographic diffraction gratings (1000 lines/mm) to the lens of some of these cameras. We have also employed digital CMOS color cameras (models Sony A7S and A7SII) operating in HD video mode (1920 × 1080 pixels). These cover a field of view of around 90 × 40 degrees. A detailed description of this hardware and the way it operates was given in previous works (Madiedo, 2017).

The atmospheric path and radiant of meteors, and also the orbit of their parent meteoroids, were obtained with the Amalthea software, developed by J.M. Madiedo (Madiedo, 2014). This program employs the planes-intersection method (Ceplecha, 1987). However, for Earth-grazing events atmospheric trajectories are obtained by Amalthea by means of a modification of this classical method (Madiedo

et al., 2016). Emission spectra were analyzed with the ChiMet software (Madiedo, 2015a).

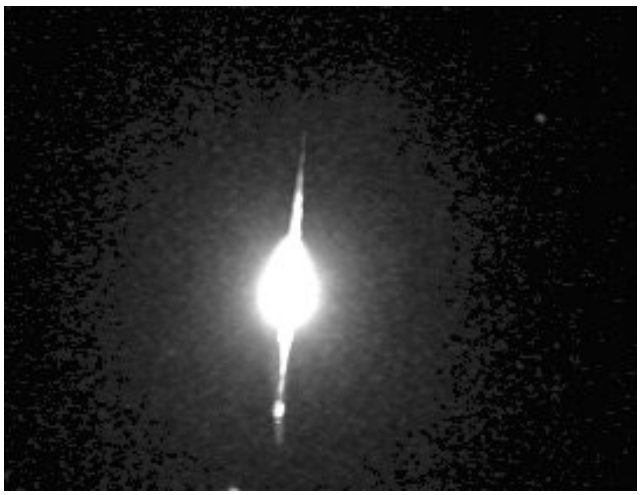

Figure 1 – Stacked image of the SWEMN20210312_233300 "Azuaga" fireball as recorded from the SWEMN meteor-observing station deployed at La Hita Astronomical Observatory.

Figure 2 – Atmospheric path and projection on the ground of the trajectory of the SWEMN20210312_233300 "Azuaga" fireball.

3 The 2021 March 12 meteor event

The first remarkable bolide spotted by our meteor-observing stations on March 2021 was observed on the 12th day of that month, at $23^h33^m00.5 \pm 0.1^s$ UTC (*Figure 1*). The event, which had a peak absolute magnitude of -11 ± 1, was recorded by the cameras deployed at Calar Alto, Sierra Nevada, La Sagra, La Hita, Sevilla, El Arenosillo, and Madrid. This event was labeled in our meteor database with the code SWEMN20210312_233300. A video showing images of the fireball and its trajectory was uploaded to YouTube[7].

Atmospheric trajectory, radiant and orbit

From the analysis of the atmospheric trajectory of the fireball we concluded that it overflew the province of Badajoz (*Figure 2*). The observed pre-atmospheric velocity of the meteoroid is $v_\infty = 20.2 \pm 0.3$ km/s, with the apparent radiant located at the equatorial coordinates $\alpha = 163.03^o$, $\delta = +48.94^o$. The meteor began at a height $H_b = 99.9 \pm 0.5$ km, and ended at an altitude $H_e = 62.9 \pm 0.5$ km. The zenith angle of this trajectory was of about 11 degrees. At its terminal point the bolide was close to the vertical of the town of Azuaga, and so we named the fireball after this location. The atmospheric path of the bolide and its projection on the ground are shown in *Figure 2*.

Table 1 – Orbital data (J2000) of the progenitor meteoroid of the SWEMN20210312_233300 "Azuaga" fireball.

a (AU)	4.8 ± 0.5	ω (º)	215.22 ± 0.07
e	0.81 ± 0.02	Ω (º)	352.32460 ± 10^{-5}
q (AU)	0.912 ± 0.001	i (º)	15.6 ± 0.2

The meteoroid had a geocentric velocity $v_g = 16.9 \pm 0.3$ km/s. Its orbital parameters before its encounter with our planet are shown in *Table 1*, and this orbit is drawn in *Figure 3*. According to the calculated value of the Tisserand parameter with respect to Jupiter ($T_J = 2.1$), the meteoroid followed a Jupiter family comet (JFC) orbit before entering the Earth's atmosphere. Radiant and orbital data do not match any of the meteoroid streams listed in the IAU meteor database[8]. So, we concluded that this event was produced by the sporadic background.

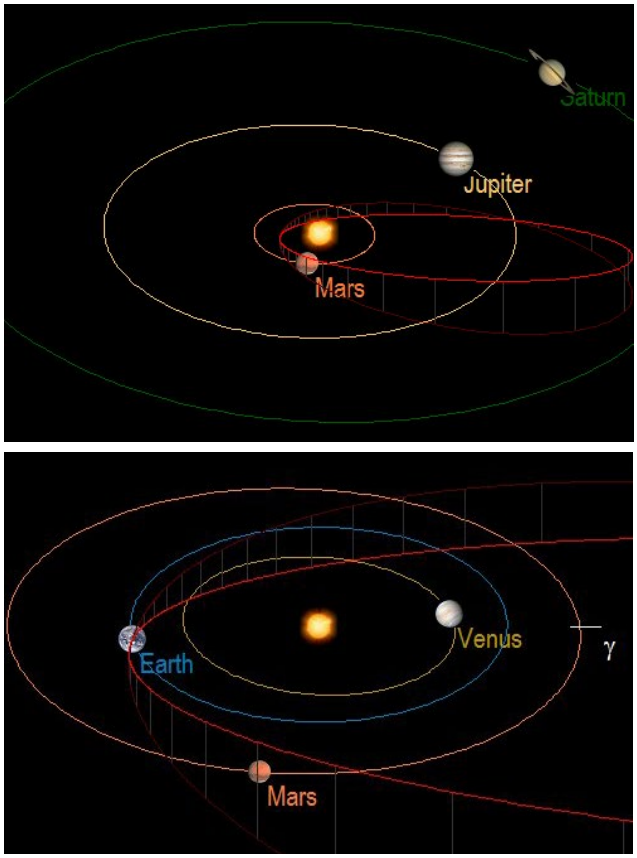

Figure 3 – Up: orbit (red line) of the parent meteoroid of the SWEMN20210312_233300 fireball, and projection of this orbit (dark red line) on the ecliptic plane; Down: close-up view of the orbit.

[7] https://youtu.be/iYAiTSkuriY

[8] http://www.astro.amu.edu.pl/~jopek/MDC2007/

Emission spectrum

The emission spectrum of the fireball was recorded by our spectrographs from the astronomical observatories of Calar Alto, La Hita, and El Arenosillo. It was analyzed with the ChiMet software, which calibrates the signal in wavelength and then corrects it by taking into account the spectral sensitivity of the device (Madiedo et al., 2014; Madiedo, 2015b). The calibrated spectrum and the most significant emission lines identified with ChiMet are shown in *Figure 4*. As usual in meteor spectra, most of these lines correspond to neutral iron (Borovička, 1993; Madiedo, 2014; Espartero and Madiedo, 2016). In this case we have identified the emissions from Fe I-23, Fe I-4, Fe I-43, Fe I-42, Fe I-41, Fe I-318, and Fe I-15. The most significant emission, however, is that of the Na I-1 doublet (588.9 nm), followed by the contribution corresponding to the Mg I-2 triplet (516.7 nm). Further analysis of the relative intensities of these lines will provide information about the nature of the meteoroid.

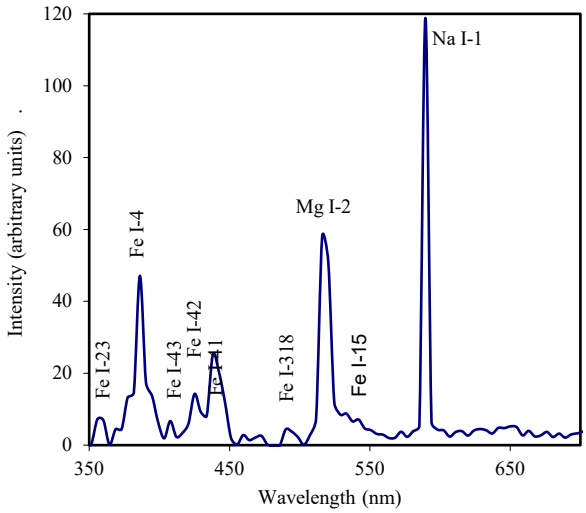

Figure 4 – Calibrated emission spectrum of the SWEMN20210312_233300 "Azuaga" fireball.

4 The 2021 March 15 fireball

This fireball event was recorded by SWEMN systems on 2021 March 15 at $0^h51^m08.8 \pm 0.1^s$ UTC, and its peak absolute magnitude was -11 ± 1 (*Figure 5*). It was spotted from the meteor-observing stations operating at La Sagra, Sierra Nevada, Calar Alto, Madrid, and Sevilla. The fireball, which can be viewed on this YouTube video[9], was included in the SWEMN meteor database under the code SWEMN20210315_005108.

Atmospheric path, radiant and orbit

The analysis of the images revealed that the fireball overflew the Mediterranean Sea, between the coasts of Andalusia (Spain) and Morocco. The parent meteoroid of this bolide entered the atmosphere with an initial velocity $v_\infty = 36.9 \pm 0.4$ km/s. The apparent radiant of the meteor was located at the equatorial coordinates $\alpha = 253.1^o$, $\delta = +48.4^o$. The bolide began at an altitude $H_b = 111.3 \pm 0.5$ km over the Mediterranean Sea, over the vertical of a point located at about 74 km of the coast of Spain and 62 km of the coast of Morocco. The terminal point of the trajectory was reached at a height $H_e = 59.1 \pm 0.5$ km over the sea. This trajectory and its projection on the ground are shown in *Figure 6*. We named this event "Alborán", since it began over the Alborán Ridge.

Figure 5 – Stacked image of the SWEMN20210315_005108 "Alborán" fireball over one of the domes of the Calar Alto Astronomical Observatory.

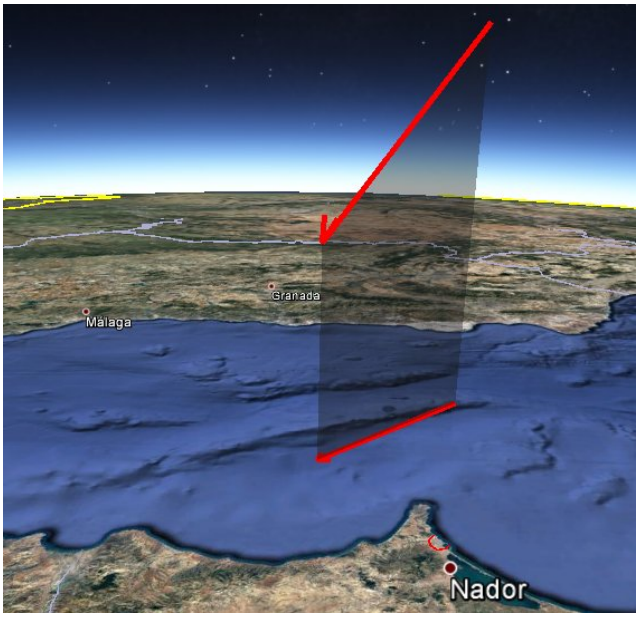

Figure 6 – Atmospheric path and projection on the ground of the trajectory of the SWEMN20210215_005108 "Alborán" fireball.

The calculation of the orbital elements of the progenitor meteoroid yields the results listed in *Table 2*, and the corresponding heliocentric orbit is shown in *Figure 7*. The value derived for the geocentric velocity is $v_g = 34.9 \pm 0.4$ km/s. The value of the Tisserand parameter with respect to Jupiter ($T_J = 2.3$) shows that this meteoroid also followed a cometary orbit (JFC type). According to radiant and orbital information listed in the IAU Meteor

[9] https://youtu.be/k6mv4IEOaBw

Data Center, this meteoroid belonged to the x-Herculid meteoroid stream (XHE#0346), which produces an annual display of meteors with a peak activity around March 12 (Jenniskens et al., 2016).

Table 2 – Orbital data (J2000) of the progenitor meteoroid of the SWEMN20210215_005108 "Alborán" fireball.

a (AU)	2.9 ± 0.2	ω (º)	197.5 ± 0.8
e	0.67 ± 0.02	Ω (º)	354.37180 ± 10^{-5}
q (AU)	0.975 ± 0.001	i (º)	59.4 ± 0.4

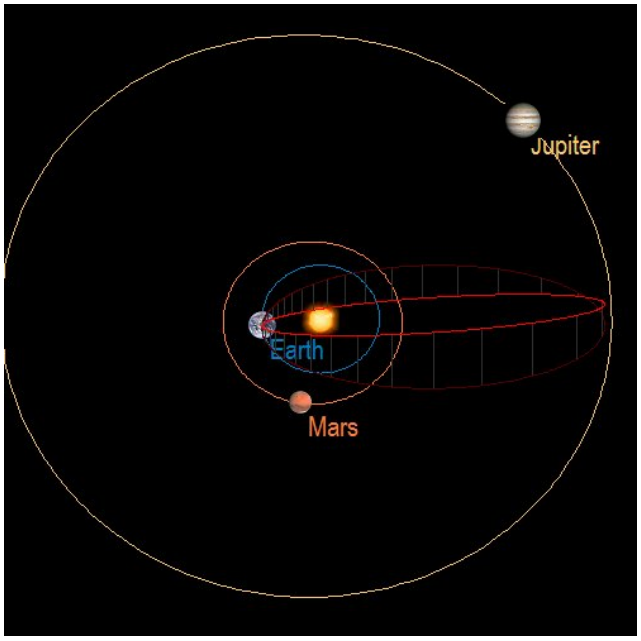

Figure 7 – Orbit (red line) of the parent meteoroid of the SWEMN20210215_005108 fireball, and its projection (dark red line) on the ecliptic plane.

5 The 2021 March 17 fireball

At $5^h06^m59.4 \pm 0.1^s$ UTC on March 17, our cameras recorded a bolide with a peak absolute magnitude of –8 ± 1 from the meteor-observing stations located at La Hita, Sierra Nevada, El Arenosillo, Calar Alto, La Sagra, Sevilla and Madrid (*Figure 8*). A video showing this event was uploaded to YouTube[10]. This bright meteor was included in our database with the code SWEMN20210317_050659.

Atmospheric path, radiant and orbit

By analyzing our recordings we obtained that the event overflew the provinces of Jaén and Ciudad Real. The pre-atmospheric velocity observed for this meteor was $v_\infty = 28.9 \pm 0.3$ km/s. The bolide began at an altitude $H_b = 99.9 \pm 0.5$ km over the north of the province of Jaén and ended at a height $H_e = 52.1 \pm 0.5$ km over the south of the province of Ciudad Real. We named this meteor "Villamanrique", since this final stage was located almost over the vertical of this town. The apparent radiant of the bolide was located at the equatorial coordinates $\alpha = 188.9º$, $\delta = +5.2º$. The atmospheric trajectory of the fireball and its projection on the ground are shown in *Figure 9*.

Figure 8 – Stacked image of the SWEMN20210317_050659 "Villamanrique" fireball as recorded from La Hita Observatory.

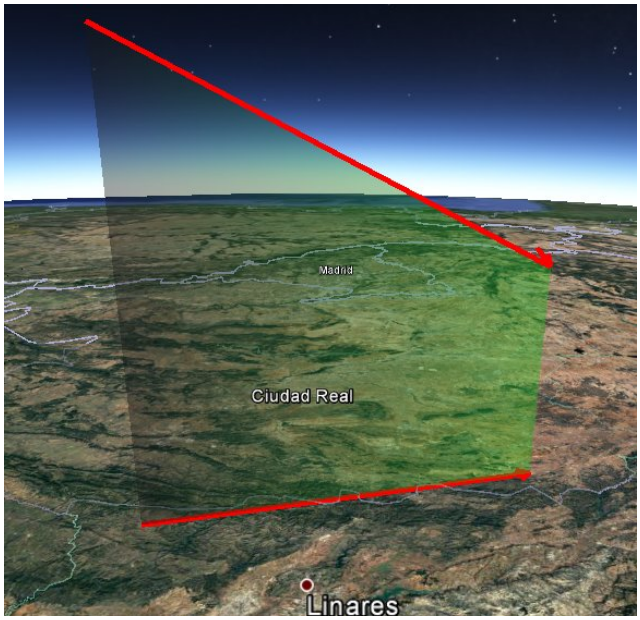

Figure 9 – Atmospheric path and projection on the ground of the trajectory of the SWEMN20210317_050659 fireball.

Table 3 – Orbital data (J2000) of the progenitor meteoroid of the SWEMN20210317_050659 "Villamanrique" fireball.

a (AU)	2.26 ± 0.08	ω (º)	285.24 ± 0.06
e	0.809 ± 0.008	Ω (º)	356.54225 ± 10^{-5}
q (AU)	0.433 ± 0.003	i (º)	5.6 ± 0.1

The heliocentric orbit of the meteoroid is shown in *Figure 10*, and the value of the corresponding orbital parameters are listed in *Table 3*. The geocentric velocity obtained in this case is $vg = 27.1 \pm 0.3$ km/s. We concluded that this meteoroid followed an asteroidal orbit before its encounter with our planet, since the Tisserand parameter with respect to Jupiter yields $T_J = 3.06$. However, this value is in the limit between asteroidal and Jupiter family cometary orbits. Radiant and orbital data reveal that the

[10] https://youtu.be/3yd1TlLEbC8

bolide was an η-Virginid (EVI#0011). This meteor shower peaks around March 14 (Jenniskens et al., 2016).

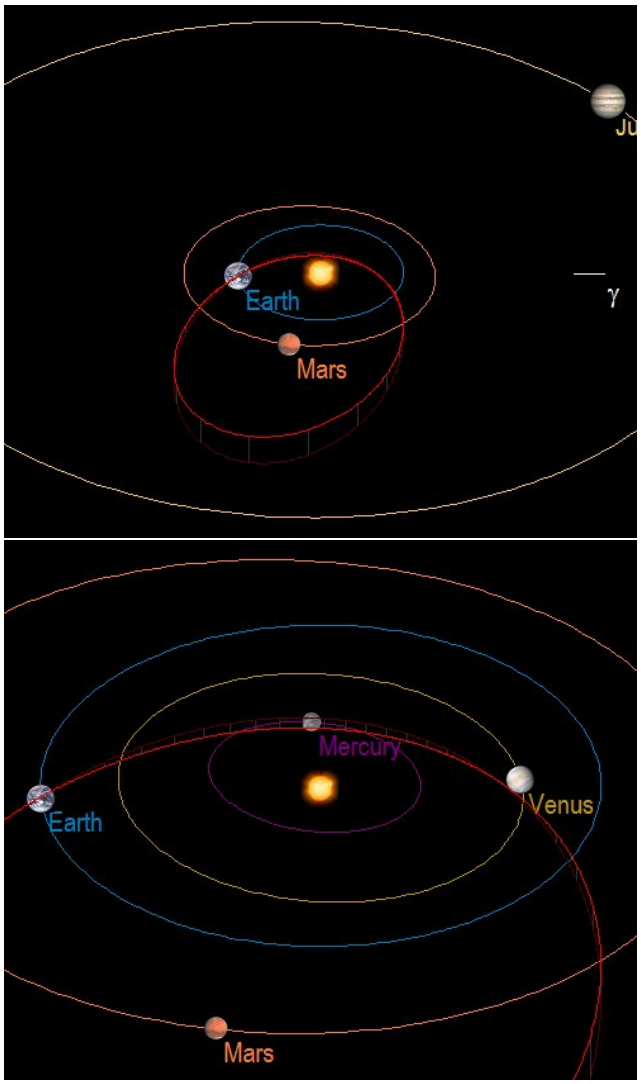

Figure 10 – Up: orbit (red line) of the parent meteoroid of the SWEMN20210317_050659 fireball, and its projection (dark red line) on the ecliptic plane; Down: close-up view of the orbit.

6 The 2021 March 21 fireball

The bolide observed on the 21st of this month was recorded at $20^h58^m34.7 \pm 0.1^s$ UTC and reached a peak absolute magnitude of -8 ± 1. As can be seen in *Figure 11*, it exhibited several flares along its atmospheric trajectory as a consequence of the disruption of the meteoroid. The event was spotted from the meteor-observing stations operated by the SWEMN network at the astronomical observatories of La Hita, Calar Alto, and El Arenosillo. It was included in our meteor database with the code SWEMN20210321_205834.

Atmospheric path, radiant and orbit

The observed initial velocity of the meteoroid was $v_\infty = 30.6 \pm 0.4$ km/s, and the apparent radiant of the event was located at the equatorial coordinates $\alpha = 190.0^o$, $\delta = +1.5^o$. It overflew the Mediterranean Sea, between the coasts of Andalusia (Spain) and Africa. Thus, the bolide began at an altitude $H_b = 88.6 \pm 0.4$ km over the sea. At this stage it was over the vertical of a point located at about 26 km from the coast of Algeria and 133 km from the coast of Spain. The fireball ended at a height $H_e = 58.8 \pm 0.4$ km over a point located at about 51 km from the coast of Morocco and 100 km from the coast of Spain. We named this fireball "Cábliers", since it overflew the Cábliers Bank, located under the Mediterranean Sea. *Figure 12* shows the atmospheric trajectory of this meteor and its projection on the ground.

The computed orbital elements are shown in *Table 4*, and the heliocentric orbit is drawn in *Figure 13*. The geocentric velocity of the meteoroid yields $v_g = 28.1 \pm 0.3$ km/s. According to the data provided by the IAU meteor database, we concluded that this fireball was also associated with the η-Virginids (EVI#0011), as we found for the previously described SWEMN20210317_050659 bolide. In this case the Tisserand parameter with respect to Jupiter yields $T_J = 3.04$, which shows that the meteoroid followed an asteroidal orbit before its encounter with Earth. Nevertheless, this value is in the limit between asteroidal and Jupiter family cometary orbits.

Table 4 – Orbital data (J2000) of the progenitor meteoroid of the SWEMN20210321_205834 "Cábliers" fireball.

a (AU)	2.3 ± 0.1	ω (º)	288.4 ± 0.2
e	0.827 ± 0.008	Ω (º)	1.17314 ± 10^{-5}
q (AU)	0.402 ± 0.002	i (º)	4.8 ± 0.1

Figure 11 – Stacked image of the SWEMN20210321_205834 "Cábliers" fireball as recorded from Calar Alto.

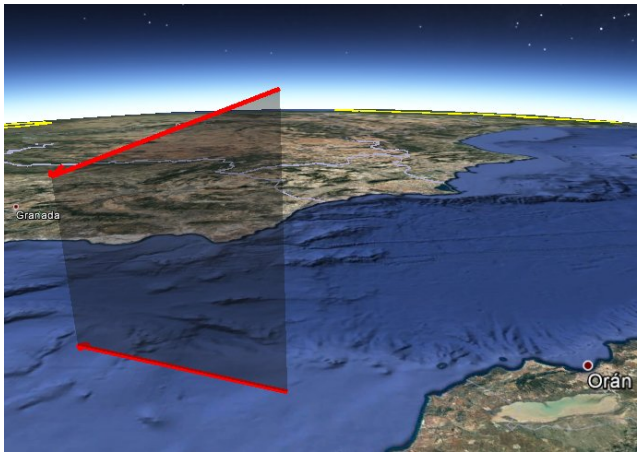

Figure 12 – Atmospheric path and projection on the ground of the trajectory of the SWEMN20210321_205834 fireball.

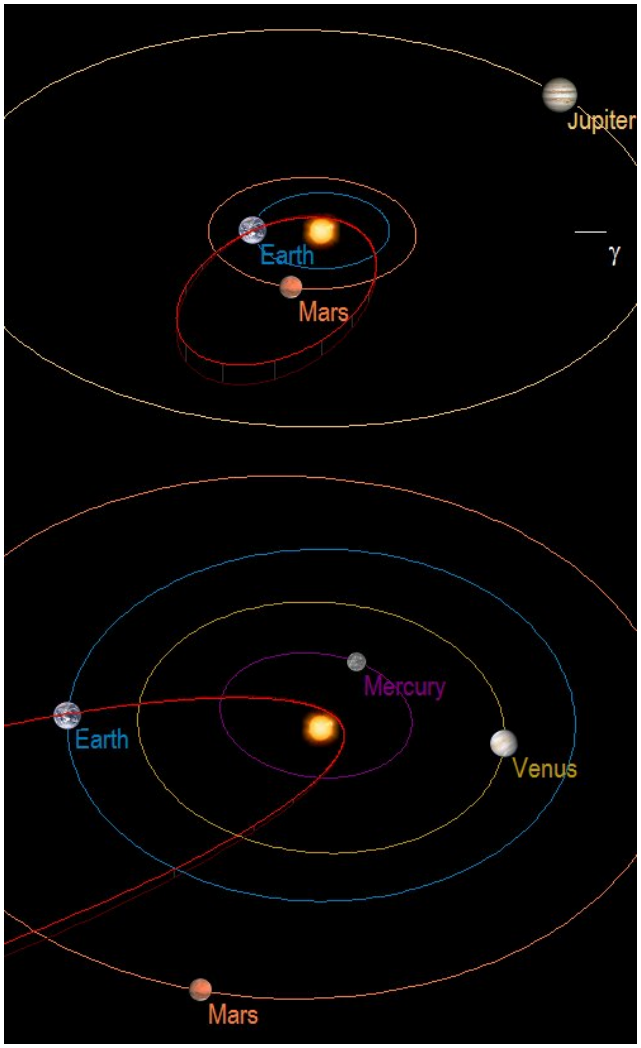

Figure 13 – Up: orbit (red line) of the parent meteoroid of the SWEMN20210321_205834 fireball, and its projection (dark red line) on the ecliptic plane; Down: close-up view of the orbit.

Figure 14 – Stacked image of SWEMN20210325_004454 "Alcira" fireball as recorded from Calar Alto.

7 The 2021 March 25 fireball

This bright meteor was detected at $0^h44^m54.0 \pm 0.1^s$ UTC on 2021 March 25, and reached a peak absolute magnitude of -9 ± 1 (*Figure 14*). The bolide was spotted from the SWEMN meteor-observing stations located at La Hita, La Sagra, Calar Alto, Madrid, and Sierra Nevada. A video showing this fireball was uploaded to YouTube[11]. It was included in the SWEMN meteor database with the code SWEMN20210325_004454.

Atmospheric path, radiant and orbit

The analysis of the atmospheric trajectory reveals that the meteoroid entered the atmosphere with an initial velocity $v_\infty = 42.0 \pm 0.4$ km/s. The apparent radiant of the meteor was located at the equatorial coordinates $\alpha = 209.0^\circ$, $\delta = -9.8^\circ$. The luminous event began at an altitude $H_b = 96.6 \pm 0.5$ km over the north of the province of Alicante, and ended over the province of Valencia, at a height $H_e = 50.0 \pm 0.5$ km. The meteor overflew Alcira, a town located in the province of Valencia. For this reason we named the fireball after this place. *Figure 15* shows its atmospheric trajectory and the projection on the ground of this path.

Table 5 – Orbital data (J2000) of the progenitor meteoroid of the SWEMN20210325_004454 "Alcira" fireball.

a (AU)	2.5 ± 0.1	ω (°)	329.4 ± 0.2
e	0.967 ± 0.003	Ω (°)	4.30143 ± 10^{-5}
q (AU)	0.084 ± 0.002	i (°)	3.0 ± 0.1

Figure 15 – Atmospheric path and projection on the ground of the trajectory of the SWEMN20210325_004454 fireball.

By means of the Amalthea software we derived the values listed in *Table 5* for the orbital elements of the parent meteoroid. This orbit is plotted in *Figure 16*. The calculated value of the geocentric velocity of this particle yields $v_g = 40.4 \pm 0.4$ km/s. According to the information found in the IAU meteor database, these results show that the fireball was a κ-Virginid (KVI#0509). This poorly-known meteoroid stream produces every year a display of meteors peaking around March 26 (Segon et al., 2013). So, this event was recorded one day before this peak. The Tisserand parameter with respect to Jupiter yields $T_J = 2.3$, which shows that this meteoroid followed a cometary orbit (JFC type) before entering our atmosphere.

[11] https://youtu.be/f5FN0TDUoKs

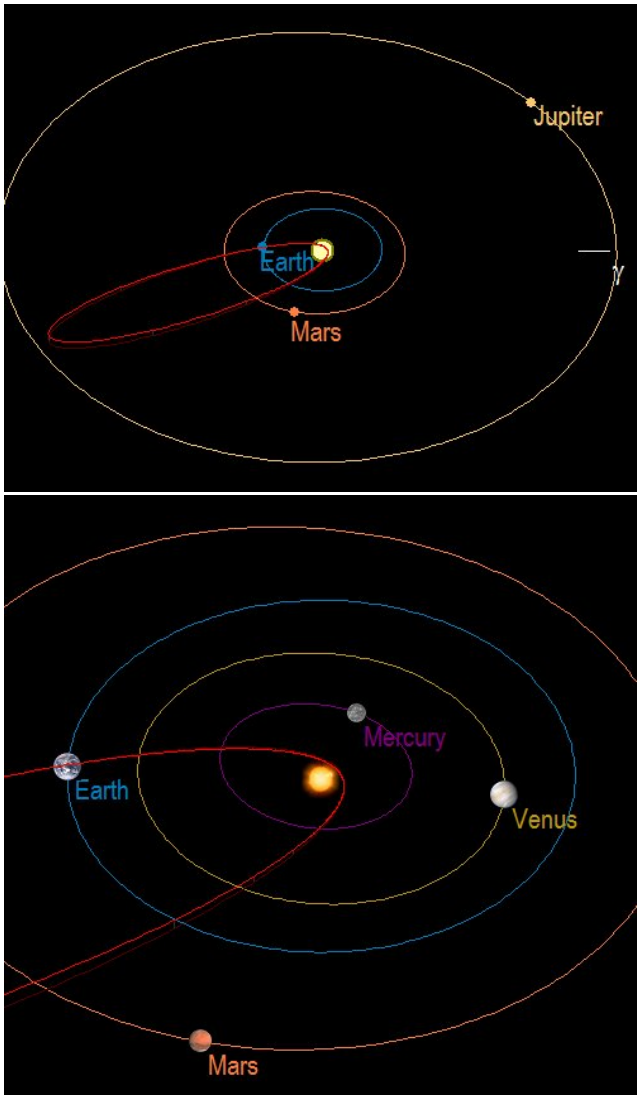

Figure 16 – Up: orbit (red line) of the parent meteoroid of the SWEMN20210325_004454 fireball, and its projection (dark red line) on the ecliptic plane; Down: close-up view of the orbit.

Figure 17 – Stacked image of the SWEMN20210328_042115 "Villacarrillo" fireball over the domes of the Calar Alto Astronomical Observatory.

8 The 2021 March 28 fireball

The last event in this report was recorded on 2021 March 28 at $4^h21^m15.8 \pm 0.1^s$ UTC (*Figure 17*). It reached a peak absolute magnitude of -10 ± 1. Despite non favorable weather conditions, it was recorded from several SWEMN stations: La Hita, La Sagra, Calar Alto, Sevilla, Madrid, and Sierra Nevada. A video showing images and the trajectory of this fireball was uploaded to YouTube[12]. The event was included in our meteor database with the code SWEMN20210328_042115.

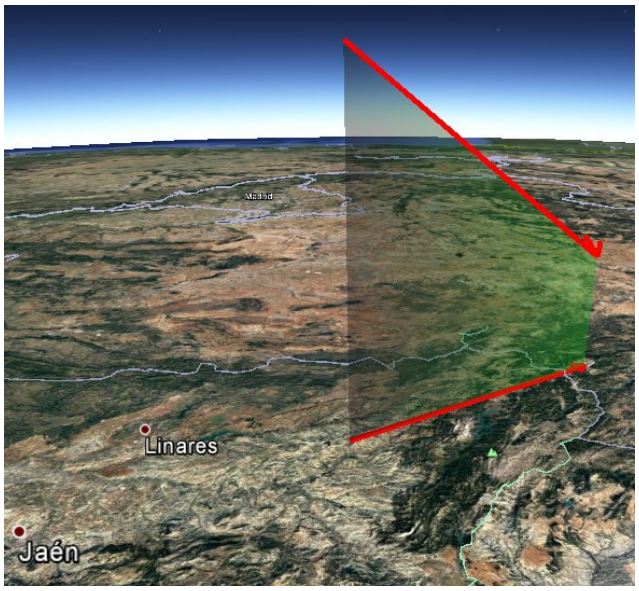

Figure 18 – Atmospheric path and projection on the ground of the trajectory of the SWEMN20210328_042115 fireball.

Atmospheric path, radiant and orbit

From the calculation of the atmospheric trajectory of the meteor we concluded that this event overflew the regions of Andalusia and Castilla-La Mancha (south of Spain). The parent meteoroid entered the atmosphere with an initial velocity $v_\infty = 24.5 \pm 0.3$ km/s, and the apparent radiant was located at the equatorial coordinates $\alpha = 195.0^o$, $\delta = +5.1^o$. The bolide began at an altitude $H_b = 89.6 \pm 0.5$ km. At this initial stage the event was located almost over the vertical of Villacarrillo, a village located in the province of Jaén (Andalusia). For this reason we named this bolide after this location. The terminal point was located over the province of Albacete (Castilla-La Mancha), at a height $H_e = 29.3 \pm 0.5$ km. *Figure 18* shows the atmospheric trajectory of the "Villacarrillo" bolide and its projection on the ground.

Table 6 – Orbital data (J2000) of the progenitor meteoroid of the SWEMN20210328_042115 "Villacarrillo" fireball.

a (AU)	1.95±0.05	ω (º)	272.9±0.1
e	0.71±0.01	Ω (º)	7.42063 ± 10^{-5}
q (AU)	0.561±0.004	i (º)	5.2±0.1

The calculation of the orbital elements of the meteoroid yields the results listed in *Table 6*. The corresponding orbit

[12] https://youtu.be/FJmgkYGTUWA

is drawn in *Figure 19*. The geocentric velocity derived for this case was $v_g = 22.2 \pm 0.3$ km/s, and the Tisserand parameter with respect to Jupiter ($T_J = 3.5$) indicates that the meteoroid followed an asteroidal orbit. According to the information included in the IAU meteor database, from these results we concluded that the fireball was a σ-Leonid (SLE#136). This is a poorly-known meteoroid stream whose meteor activity peaks around March 29 (Molau and Rendtel, 2009).

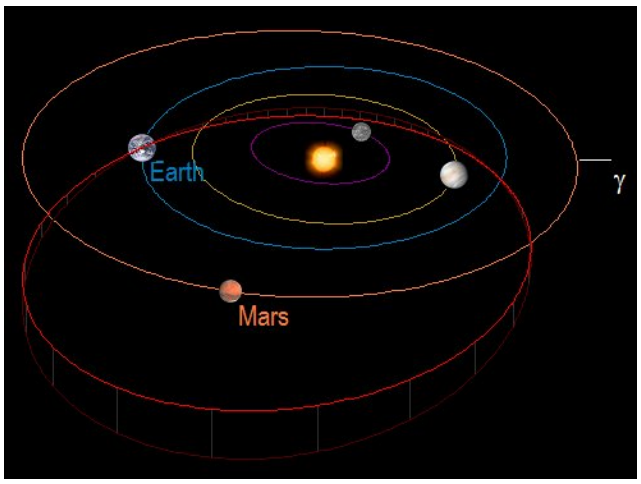

Figure 19 – Orbit (red line) of the parent meteoroid of the SWEMN20210328_042115 fireball, and its projection (dark red line) on the ecliptic plane.

Emission spectrum

Our spectrographs located at La Hita and La Sagra meteor-observing stations recorded the emission spectrum of this fireball. *Figure 20* shows the calibrated signal, together with the most important emissions present in this spectrum. As can be noticed, we have identified lines produced by several Fe I multiplets, as those of Fe I-318 and Fe I-15. The latter is the most remarkable emission together with those of Mg I-2 and Na I-1. In addition to this line of neutral sodium, the emission of Na I-6 at 562.8 nm was also identified. The lines of Ca I-21 (559.9 nm) and Ca I-3 (649.3 nm) are also present in the signal, together with several contributions of atmospheric N_2 in the red region of the spectrum.

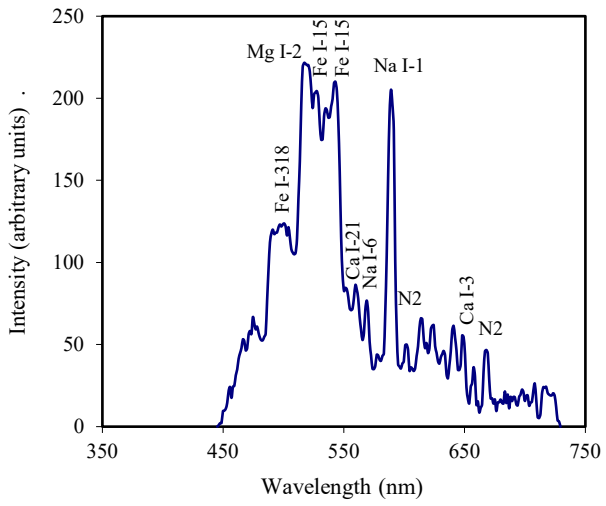

Figure 20 – Calibrated emission spectrum of the SWEMN20210328_042115 "Villacarrillo" fireball.

A deeper analysis of this spectrum will be performed in order to obtain information about the chemical nature of meteoroids in the σ-Leonid stream. Thus, the analysis of emission spectra produced by events associated with poorly-known streams is one of the aims of the SMART survey (see, for instance, Madiedo et al., 2013; Madiedo 2014).

9 Conclusion

The most remarkable bolides recorded during March 2021 in the framework of the Southwestern Europe Meteor Network (SWEMN) have been described. The absolute magnitude of these bright meteors during their peak luminosity ranged from –8 to –11. Our analysis has revealed that these events were produced by meteoroids belonging to the sporadic background and several minor and poorly-known streams.

The "Azuaga" fireball, recorded on March 12, overflew the province of Badajoz and was associated with the sporadic background. It reached a peak absolute magnitude of –11. The meteoroid followed a cometary orbit (JFC orbit) before hitting the Earth's atmosphere. In the spectrum of this meteor we have identified the emissions from several neutral iron multiplets (Fe I-23, Fe I-4, Fe I-43, Fe I-42, Fe I-41, Fe I-318, and Fe I-15). The most significant contributions in this signal are the corresponding to the Na I-1 doublet and the Mg I-2 triplet.

The "Alborán" bolide, spotted on March 15, overflew the Mediterranean Sea and reached a peak absolute magnitude of –11. It was produced by a member of the x-Herculid meteoroid stream (XHE#0346), which produces an annual display of meteors with a peak activity around March 12. Our results show that meteoroids in this stream follow a JFC orbit.

Another bright meteor was spotted by our network on March 17. This bolide, which was named "Villamanrique", overflew the south of Spain and had a luminosity equivalent to magnitude –8. It was associated with the η-Virginids (EVI#0011). Our results suggest an asteroidal origin for this stream. However, the value of the Tisserand parameter with respect to Jupiter is in the limit between asteroidal and JFC orbits.

The Mediterranean Sea was flown over by another mag. –8 η-Virginid fireball on March 21. This bright meteor was named "Cábliers". Again, the value of the Tisserand parameter with respect to Jupiter is in the limit between asteroidal and JFC orbits, and so our results cannot clarify the nature (asteroidal or cometary) of the parent body of this stream.

The "Alcira" bolide, with a peak absolute magnitude of –9, was spotted on March 25 and overflew the provinces of Alicante and Valencia. It was produced by a meteoroid belonging to the κ-Virginid stream (KVI#0509). This is recently-discovered and poorly-known meteoroid stream which produces an annual meteor shower that peaks around

March 26. According to our results, the meteoroid followed a Jupiter family comet orbit before entering the Earth's atmosphere.

The last fireball presented in this report was recorded on March 28 and had a peak absolute luminosity equivalent to magnitude –10. It overflew the regions of Andalusia and Castilla-La Mancha, and was generated by a meteoroid from the σ-Leonids (SLE#136). This is a poorly-known meteoroid stream whose meteor activity peaks around March 29. Our calculation reveals that this meteoroid followed an asteroidal orbit before hitting our atmosphere. The most remarkable contributions in the spectrum of this bolide are those of Fe I-15, Mg I-2, and Na I-1. The lines of Na I-6, Ca I-21 and Ca I-3 have been also found. A deeper analysis of this spectrum will provide key information about the composition of meteoroids in this stream.

Acknowledgment

We acknowledge support from the Spanish Ministry of Science and Innovation (project PID2019-105797GB-I00). We also acknowledge financial support from the State Agency for Research of the Spanish MCIU through the "Center of Excellence Severo Ochoa" award to the Instituto de Astrofísica de Andalucía (SEV-2017-0709)". P.S-S. acknowledges financial support by the Spanish grant AYA-RTI2018-098657-J-I00 "LEO-SBNAF" (MCIU / AEI / FEDER, UE).

References

Borovička J. (1993). "A fireball spectrum analysis". *Astronomy and Astrophysics*, **279**, 627–645.

Ceplecha Z. (1987). "Geometric, dynamic, orbital and photometric data on meteoroids from photographic fireball networks". *Bull. Astron. Inst. Cz.*, **38**, 222–234.

Espartero F. A. and Madiedo J. M. (2016). "The Northern ω-Scorpiid Meteoroid Stream: Orbits and Emission Spectra". *Earth, Moon, and Planets*, **118**, 81–89.

Jenniskens P., Nénon Q., Albers J., Gural P. S., Haberman B., Holman D., Morales R., Grigsby B. J., Samuels D. and Johannink C. (2016). "The established meteor showers as observed by CAMS". *Icarus*, **266**, 331–354.

Madiedo J. M., Trigo-Rodríguez J. M., Lyytinen E., Dergham J., Pujols P., Ortiz J. L. and Cabrera J. (2013). "On the activity of the γ-Ursae Minorids meteoroid stream in 2010 and 2011". *Monthly Notices of the Royal Astronomical Society*, **431**, 1678–1685.

Madiedo J. M. (2014). "Robotic systems for the determination of the composition of solar system materials by means of fireball spectroscopy". *Earth, Planets & Space*, **66**, 70.

Madiedo J. M., Ortiz J. L., Trigo-Rodríguez J. M., Dergham J. and Castro-Tirado A.J. (2014). "Analysis of bright Taurid fireballs and their ability to produce meteorites". *Icarus*, **231**, 356–364.

Madiedo J. M. (2015a). "Spectroscopy of a κ-Cygnid fireball afterglow". *Planetary and Space Science*, **118**, 90–94.

Madiedo J. M. (2015b). "The ρ-Geminid meteoroid stream: orbits, spectroscopic data and implications for its parent body". *Monthly Notices of the Royal Astronomical Society*, **448**, 2135–2140.

Madiedo J. M., Ortiz J. L., Organero F., Ana-Hernández L., Fonseca F., Morales N. and Cabrera-Caño J. (2015a). "Analysis of Moon impact flashes detected during the 2012 and 2013 Perseids". *Astronomy and Astrophysics*, **577**, A118.

Madiedo J. M., Ortiz J. L., Morales N. and Cabrera-Caño J. (2015b). "MIDAS: Software for the detection and analysis of lunar impact flashes". *Planetary and Space Science*, **111**, 105–115.

Madiedo J. M., Espartero F., Castro-Tirado A. J., Pastor S., and De los Reyes J. A. (2016). "An Earth-grazing fireball from the Daytime ζ-Perseid shower observed over Spain on 2012 June 10". *Monthly Notices of the Royal Astronomical Society*, **460**, 917–922.

Madiedo J. M. (2017). "Automated systems for the analysis of meteor spectra: The SMART Project". *Planetary and Space Science*, **143**, 238–244.

Madiedo J. M., Ortiz J. L. and Morales N. (2018). "The first observations to determine the temperature of a lunar impact flash and its evolution". *Monthly Notices of the Royal Astronomical Society*, **480**, 5010–5016.

Madiedo J. M., Ortiz J. L., Morales N. and Santos-Sanz P. (2019a). "Multiwavelength observations of a bright impact flash during the 2019 January total lunar eclipse". *Monthly Notices of the Royal Astronomical Society*, **486**, 3380–3387.

Madiedo J. M., Ortiz J. L., Yanagisawa M., Aceituno J. and Aceituno F. (2019b). "Impact flashes of meteoroids on the Moon". *Meteoroids: Sources of Meteors on Earth and Beyond*, Ryabova G. O., Asher D. J., and Campbell-Brown M. D. (eds.), Cambridge, UK. Cambridge University Press, ISBN 9781108426718, 2019, p. 136–158.

Madiedo J. M., Ortiz J. L., Santos-Sanz P., Aceituno J. and de Guindos E. (2021). "Bright fireballs recorded during January 2021 in the framework of the Southwestern Europe Meteor Network". *eMetN*, **6**, 247–254.

Molau S. and Rendtel J. (2009). "A Comprehensive List of Meteor Showers Obtained from 10 Years of Observations with the IMO Video Meteor

Network". *WGN, Journal of the International Meteor Organization*, **37**, 98–121.

Ortiz J. L., Madiedo J. M., Morales N., Santos-Sanz P. and Aceituno F. J. (2015). "Lunar impact flashes from Geminids: analysis of luminous efficiencies and the flux of large meteoroids on Earth". *Monthly Notices of the Royal Astronomical Society*, **454**, 344–352.

Segon D., Andreic Z., Korlevic K., Novoselnik F., Vida D. and Skokic I. (2013). "8 new showers from Croatian Meteor Network data". *WGN, Journal of the International Meteor Organization*, **41**, 70–74.

Beta Tucanids (BTU #108) meteor outburst in 2021

P. Jenniskens

SETI Institute, 189 Bernardo Ave, Mountain View, CA 94043, USA
pjenniskens@seti.org

Last year's surprise activity from the beta Tucanids meteor shower in the southern hemisphere was repeated this year on March 12 and 13, 2021. The beta Tucanids displayed strong activity in CAMS low-light video data in the period between March 12 10^h and March 13 06^h UTC. The possible parent body is asteroid-looking object 2006 CS. This shower has been confused with the nearby delta Mensids. In 2020, the nearby activity that continued for two weeks after the outburst of beta Tucanids were the delta Mensids. In 2020, the delta Mensids were active until March 26, with good detections on March 20–22.

1 Introduction

In 2020, the beta Tucanids (BTU#108) showed strong activity in SAAMER southern hemisphere radar data, peaking on March 12 at 9^h30^m UTC (Janches et al., 2020a). There were also larger particles: CAMS triangulated a handful of beta Tucanids during this event (Janches et al., 2020a). Janches et al. (2020b) identified a possible source for this activity: now asteroid-looking object 2006 CS (asteroid 248590). The asteroid moves in a Jupiter-family comet orbit with Tisserand parameter T_J = 2.44. Jupiter-family comets have T_J values between 2 and 3.

From the beginning, the outburst was thought to be part of the delta Mensids (DME#130), but I later found that the radiants from this outburst were slightly different from those of the delta Mensid shower (*Table 1*). The delta Mensids (DME#130) were first detected by visual observers in the southern hemisphere and received their shower number in Jenniskens (2006). The shower was confirmed from low-light video observations by the CAMS New Zealand network (Jenniskens et al., 2018).

In 2020, the delta Mensids were well detected in the period March 20–22 (see CAMS website[13] for dates of 2020 March 20 to 22), and it is interesting to check if that activity is annual and will return this year on those days.

2 The 2021 activity

In 2021, the Southern hemisphere "Cameras for Allsky Meteor Surveillance" (CAMS) networks again detected the beta Tucanid meteor shower (IAU#108) in the brief interval between March 12 10^h and 13 06^h UTC, 2021, corresponding to solar longitudes 351.77–352.57 degrees (equinox J2000.0). 29 meteors were triangulated. These radiants can be seen on the CAMS data visualization website[13] for the date of 2021 March 13 (*Figure 1*).

The 29 beta Tucanid meteors were detected by CAMS Namibia (T. Hanke, E. Fahl, and R. van Wyk, with the H.E.S.S. Collaboration), CAMS Chile (S. Heathcote and T. Abbott, AURA/Cerro Tololo; and E. Jehin, University of Liege), CAMS Australia (M. Towner, Curtin University, with support of L. Toms and C. Redford), CAMS New Zealand (J. Baggaley, University of Canterbury; and N. Frost, Mount John Observatory, with support from I. Crumpton and C. and L. Duncan), and CAMS South Africa (T. Cooper, Astronomical Society of Southern Africa; and P. Mey, South African Radio Astronomy Observatory).

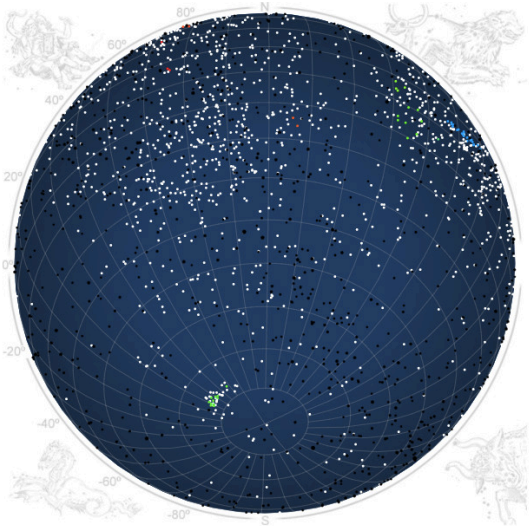

Figure 1 – The beta Tucanids and nearby delta Mensids registered by CAMS during 2021 between March 12 10^h and 13 06^h UTC.

The radiant and orbit data obtained in 2021 are compared to older data in *Table 1*. The results are in good agreement with 2020 results from CAMS data (cf. Janches et al., 2020a).

[13] http://cams.seti.org/FDL/

Table 1 – Median orbital elements for the delta Mensids (IAU#130) and beta Tucanids (IAU#108) (equinox J2000.0), comparing data published in 2006 (Jenniskens, 2006) and 2018 (Jenniskens et al., 2018) with CAMS data for 2020 and 2021.

	2006	2018	2020	2021
Shower	130	130	108	108
$\lambda_\odot$ (°)	356.7	358.4	352.40 ± 0.08	352.26 ± 0.05
α_g (°)	58	75.6	61.4 ± 3.8	62.2 ± 4.9
δ_g (°)	–80	–78.9	–76.7 ± 0.7	–77.4 ± 1.1
v_g km/s	33	34.8	31.0 ± 2.4	30.9 ± 1.6
a a.u.	3.2	7.01	3.4	3.0
q a.u.	0.982	0.992	0.976 ± 0.005	0.977 ± 0.004
e	–	0.859	0.700 ± 0.030	0.679 ± 0.094
ω (°)	345.6	352.8	342.9 ± 2.3	343.8 ± 2.5
Ω (°)	177.1	178.4	172.40 ± 0.08	172.26 ± 0.22
i (°)	56.1	56.5	50.8 ± 1.1	51.1 ± 2.0
N	–	18	5	29

The beta Tucanids shower peaked at solar longitude 352.26 ± 0.05 degrees with a full-width-at-half-maximum of about 0.5 degrees in solar longitude. In 2020, the shower peaked at solar longitude 352.40 ± 0.08 degrees (cf. Janches et al., 2020a) and continued to be detected until March 26.

Outside this interval, the rate of detections was only around 1 meteor per day from what appears to be the delta Mensids, instead. Based on 2020 observations, that annual delta Mensids shower is ongoing and indeed more shower members were triangulated in the recent days immediately following March 13.

CAMS detected the delta Mensid shower particularly well March 20–22, 2020. Those dates fall over a weekend this year, and during a first quarter Moon. If this activity repeats this year, then southern hemisphere meteor observers may have a chance to see some meteors from this high southern declination shower after midnight, weather permitting.

References

Janches D., Bruzzone J. S., Weryk R. J., Hormaechea J. L., Brunini C., Wiegert P., Jenniskens P. (2020a). "Delta Mensid meteor shower 2020". CBET 4772. D. W. E. Green (ed.), IAU Central Bureau for Astronomical Telegrams. 1 pp.

Janches D., Bruzzone J. S., Weryk R. J., Hormaechea J. L., Wiegert P., Brunini C. (2020b). "Observations of an unexpected meteor shower outburst at high ecliptic southern latitude and its potential origin". *Astrophysical Journal Letters*, **895**, L25–31.

Jenniskens P. (2006). Meteor Showers and their Parent Comets, ISBN 0521853494. Cambridge, UK: Cambridge University Press, 2006. page 701.

Jenniskens P., Baggaley J., Crumpton I., Aldous P., Pokorny P., Janches D., Gural P. S., Samuels D., Albers J., Howell A., Johannink C., Breukers M., Odeh M., Moskovitz N., Collison J. and Ganjuag S. (2018). "A survey of southern hemisphere meteor showers". *Planetary Space Science*, **154**, 21–29.

Narrow shower of zeta Pavonids (ZPA, #853)

P. Jenniskens

SETI Institute, 189 Bernardo Ave, Mountain View, CA 94043, USA
pjenniskens@seti.org

On March 22, 2021, CAMS networks again detected the zeta Pavonid meteor shower (ZPA, #853), now demonstrating that it has an unusually short duration. The full-width-at-half-maximum duration is only 0.46 degrees in solar longitude. The peak was at median solar longitude 1.41 degrees in 2021, 1.25 degrees in 2020 and 1.15 degrees in 2016 (equinox J2000.0). The short duration of the shower and the long-period orbital elements of the meteoroids suggest they originated from a long-period comet that passed close to Earth's orbit in the past.

1 Introduction

Short lived activity of the zeta Pavonids (ZPA, IAU shower number 853) was recorded by CAMS networks in 2021 (*Figure 1*). Because such brief showers can give approximate orbital elements of a yet-to-be-discovered potentially hazardous long-period comet, a CBET was published (Jenniskens, 2021). The shower was first detected in 2016, when CAMS New Zealand triangulated 5 meteors with this radiant (Jenniskens et al., 2018). Weather prevented observations in 2017–2019.

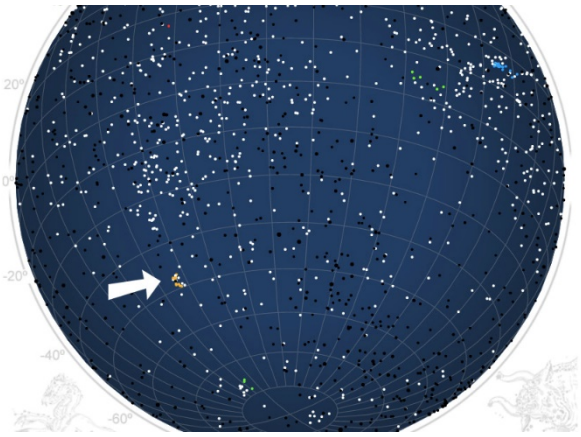

Figure 1 – Zeta Pavonid radiants recorded by CAMS networks on March 22, 2021 (cf. CAMS website[14]).

2 CAMS networks

CAMS networks in the southern hemisphere were expanded in mid-2019, so that a more continuous monitoring of southern hemisphere meteor showers has become possible since. In 2021, six zeta Pavonids were triangulated by CAMS Namibia (T. Hanke, E. Fahl, and R. van Wyk, involved with the H.E.S.S. Collaboration), six by CAMS Chile (S. Heathcote and T. Abbott, AURA/Cerro Tololo, and E. Jehin, University of Liege), three by CAMS Australia (M. Towner, Curtin University, with support of Linda Toms and Carol Redford), and two by CAMS South Africa (T. Cooper, Astronomical Society of Southern Africa, and P. Mey, South African Radio Astronomy Observatory). No zeta Pavonids were triangulated the night before or after.

3 Results

The shower was detected between 2021 March 21, 19^h, and March 22, 11^h UTC, corresponding to solar longitudes 1.11 to 1.73 degrees (equinox J2000.0). Based on the median value and dispersion of the solar longitude of 17 triangulated meteors, the shower's activity profile had a full-width-at-half-maximum duration of only 0.46 degrees centered on 1.41 deg solar longitude. This is one of the first meteor showers to peak in the new Solar Longitude year.

Table 1 – Median orbital elements for the zeta Pavonids (equinox J2000.0), comparing data observed in 2016 (Jenniskens et al., 2018) with CAMS data for 2020 and 2021. Error bars are 1-sigma dispersions in the observed elements and include measurement error.

	2016	2020	2021
λ_O (°)	1.15 ± 0.10	1.25 ± 0.15	1.41 ± 0.20
α_g (°)	277.8 ± 1.5	279.0 ± 3.3	279.5 ± 1.8
δ_g (°)	–71.8 ± 0.7	–71.3 ± 0.5	–71.1 ± 1.0
v_g km/s	55.1 ± 1.2	56.2 ± 2.0	55.6 ± 1.6
a a.u.	25.5	–	∞ (†)
q a.u.	0.994 ± 0.001	0.993 ± 0.003	0.993 ± 0.002
e	0.961 ± 0.079	1.054 ± 0.161	1.0
ω (°)	354.1 ± 0.8	353.5 ± 2.8	353.6 ± 1.7
Ω (°)	181.1 ± 0.1	181.3 ± 0.2	181.4 ± 0.2
i (°)	99.2 ± 1.6	100.2 ± 1.6	99.6 ± 0.5
N	5	10	17

Note: (†) Parabolic orbit that is a best match to the observations.

Orbital elements are those of a long-period comet with semi-major axis close to the parabolic limit. The median orbit is slightly hyperbolic, but spread over bound and unbound orbits, with orbital elements a strong function of the measured entry speed. The orbit becomes parabolic for an entry speed of v_g = 55.6 km/s. The best-fit parabolic orbit

[14] http://cams.seti.org/FDL/

is compared with the previously known orbit from 2016 in *Table 1*. There is no known parent body.

It is unclear at present if the activity itself is unusual or returns annually. The shower was also detected by the same networks in 2020, when 10 meteors were triangulated centered on 1.25 degrees solar longitude. In addition, one meteor occurred in the night before the peak, one meteor in the night after in 2020. In 2016, the 5 observed meteors centered on 1.15 degrees solar longitude (Jenniskens et al., 2018). Planetary perturbations are expected to move the peak activity slightly from year to year.

4 Discussion

The duration of the shower is interesting, because it is wider than that of the 1-revolution dust trail encounters with dust from comet Kiess, for example, but narrower than most known annual long-period comet showers like that of the April Lyrids (Jenniskens, 2006).

The long orbital period of the meteoroids suggests this meteoroid stream might have originated from a new comet that fragmented during a past return to the inner solar system. The meteoroids may have completed more than one orbit or we are passing the center of the stream at a large miss-distance. If so, this shower should be monitored for possible meteor outbursts from passing the 1-revolution dust trail. If there is a 1-revolution dust trail on top of this activity, then the comet parent body might still exist and return to the inner solar system on an orbit that passes close enough to Earth's orbit to intersect. Such outbursts are expected to happen only once or twice every 60 years.

References

Jenniskens P. (2006) Meteor Showers and their parent comets. Cambridge University Press, Cambridge, U.K., 790 pp.

Jenniskens P., Baggaley J., Crumpton I., Aldous P., Pokorny P., Janches D., Gural P. S., Samuels D., Albers J., Howell A., Johannink C., Breukers M., Odeh M., Moskovitz N., Collison J. and Ganju S. (2018). "A survey of southern hemisphere meteor showers". *Planetary Space Science*, **154**, 21–29.

Jenniskens p. (2021). "Zeta Pavonid meteors 2021". CBET 4951, issued 2021 March 28, D. W. E. Green (ed.) Central Bureau for Astronomical Telegrams.

A note on the likely non-reality of the September pi Orionids (POR,#430)

John Greaves

cpmjg@tutanota.com

A comment is made about the September π Orionids (POR#430) suggesting that this shower is likely to be spurious because the evidence for its detection in 2012 is considered insufficient.

In Greaves (2012) a September shower in Orion was suggested. This is now formally catalogued as the September π Orionids, code POR shower number 430.

In retrospect the existence of this shower's radiant roughly 90 degrees West of the Solar position and slightly below the Ecliptic during its peak activity in tandem with its highly inclined retrograde orbit and consequent high geocentric velocity places it amongst the region of the mid-September realm of the Southern Apex. Consequently, the shower is either a false detection delineated by unrecognized Apex meteors or at best barely distinguishable from said, thus just as unproven. Accordingly, there is no real evidence for the shower 430 POR existing as a discrete shower.

Ironically, and possibly somewhat prophetically, at the time of submission the author's suggested code of POR and the name π4 Orionids for this shower was suggested to the then relevant naming committee which then modified it to the current name and changed the code to SPO. The referee of the paper, the well-known and experienced (late) Wayne T Halley, very correctly took umbrage to this, and in an important contribution pointed out that SPO had long been utilized as the abbreviation for sporadic meteors, at least amongst amateurs. Accordingly, based on his advice, the abbreviation was changed from SPO to the current one. The ironic aspect being that in the end the orbits used to define this "shower" were in fact likely sporadic ones, and therefore are SPO!

References

Greaves J. (2012). "Four Meteor Showers from the SonotaCo Network Japan". *WGN, Journal of the International Meteor Organization*, **40**, 16–23.

February alpha Corvid (FAC#1101) meteors

P. Jenniskens

SETI Institute, 189 Bernardo Ave, Mountain View, CA 94043, USA
pjenniskens@seti.org

Low-light video observations show a compact but weakly active meteor shower with a radiant situated in the constellation of Corvus around February 16 in recent years. This newly identified shower has been listed in the IAU Working List of Meteor Showers as the February alpha Corvids (FAC #1101). The meteoroid stream responsible is in the orbit of an unknown long-period comet that passed close to Earth's orbit in a prior return to the inner solar system.

1 Introduction

A weak but unusually compact meteor shower (*Figure 1*) was added to the IAU Working List of Meteor Showers[15], now called the February alpha Corvids, and given the code FAC and the number 1101 (Jenniskens, 2021). The shower is significant because it marks the orbit of an unknown long-period comet that passed close to Earth's orbit in a prior return. If part of the nucleus survived when the stream was created, it might now be a potentially hazardous comet when it returns to the inner solar system.

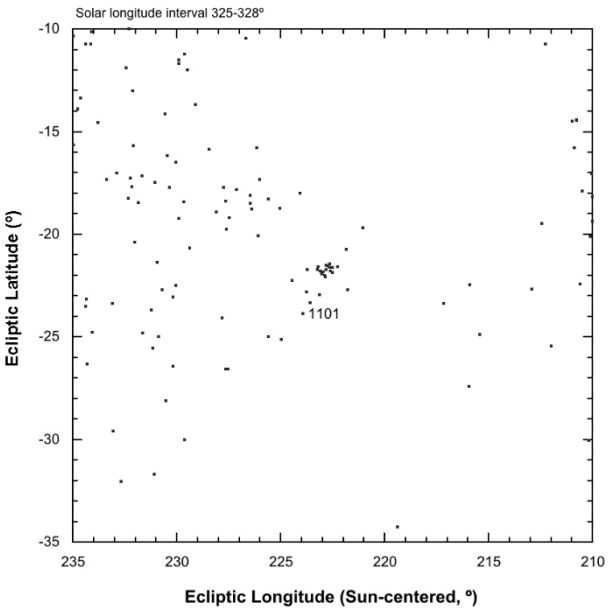

Figure 1 – The compact February alpha Corvid radiant.

2 2021 observations

On 2021 February 16, two southern-hemisphere "Cameras for Allsky Meteor Surveillance" (CAMS)[16] networks detected and triangulated three meteors from this shower: CAMS Australia (M. Towner, Curtin University, with support of L. Toms and C. Redford) and CAMS New Zealand (J. Baggaley, University of Christchurch, with support from N. Frost, I. Crumpton, and L. and C. Duncan). The radiant was found to be located at R.A. = 180.36 ± 0.13°, Decl. = –23.81 ± 0.15° (equinox J2000.0) with geocentric velocities of 54.2 ± 1.0 km/s during the solar longitude interval 327.33 – 327.53° (equinox J2000.0). Another two February alpha Corvids were detected outside this interval during February 14–19 (Jenniskens, 2021).

3 Earlier observations

This radiant was only recognized when data were compared to those from prior years. In 2020, seven meteors were triangulated by CAMS Florida (A. Howell) and CAMS California from the same radiant at R.A. = 179.72 ± 0.33°, Decl. = –23.65 ± 0.31°, with geocentric velocity 55.9 ± 1.3 km/s during the solar longitude interval 326.7–327.6° for the date of 2020 February 16. Orbital elements cover both bound and unbound orbits due to uncertainties in the measured velocities. The median orbit of all available CAMS data is slightly hyperbolic (*Table 1*). A geocentric velocity of $v_g = 54.73 \pm 0.02$ km/s results in a parabolic orbit with corresponding orbital elements $q = 0.236 \pm 0.002$ AU, $e = 1.0$, $i = 102.29 \pm 0.08°$, $\omega = 121.5 \pm 0.3°$, and $\Omega = 146.8 \pm 1.1°$ (equinox J2000.0).

4 An independent search

Because the radiant is so compact, this weak shower can be recognized also in other low-light video data back to 2011. Using the parabolic orbit above, Paul Roggemans searched in a dataset with 191393 orbits collected by the Global Meteor Network[17] and a dataset with 630402 UFO-software orbits (EDMOND[18] and SonotaCo). This search resulted in 20 similar orbits registered during the time interval $\lambda_\odot$ [318.8°, 331.6°] or February 7–20 from a Sun-centered radiant in geocentric ecliptic coordinates at λ_g–$\lambda_\odot$ [221.7°, 226.9°] and β_g [–23.9°, –18.1°] within a geocentric velocity range v_g = [51.6 km/s, 57.6 km/s]. Omitting 4 outliers the mean orbits for UFO software and for Global Meteor Network orbits were calculated using the method described

[15] http://pallas.astro.amu.edu.pl/~jopek/MDC2007/
[16] http://cams.seti.org/FDL/
[17] https://globalmeteornetwork.org/
[18] https://www.meteornews.net/edmond/

by Jopek et al. (2006). The results are compared in *Table 1* and are in good agreement with the CAMS data.

Table 1 – Median orbital elements (equinox J2000.0) and 1-sigma dispersions measured by CAMS compared with the mean values obtained from UFO software orbits and Global Meteor Network (GMN) orbits (the latter two courtesy of Paul Roggemans).

	CAMS	UFO-Orbit	GMN
$\lambda_\odot$ (°)	326.8	324.4	324.8
α_g (°)	179.8 ± 1.2	178.7	182.3
δ_g (°)	–23.6 ± 0.5	–23.1	–22.0
v_g (km/s)	55.0 ± 1.1	54.5	55.4
λ-$\lambda_\odot$ (°)	222.8 ± 0.3	223.9	226.3
β (°)	–21.7 ± 0.2	–21.4	–19.3
a (AU)	–	10.0	6.2
q (AU)	0.241 ± 0.011	0.229	0.224
e	1.009 ± 0.022	0.977	0.964
ω (°)	120.5 ± 2.6	123.3	124.8
Ω (°)	147.0 ± 1.2	144.1	146.0
i (°)	102.7 ± 1.5	104.7	111.6
Π (°)	268.1 ± 3.3	267.4	270.7
Q (AU)	–	19.7	12.2
T_j	–0.34	0.37	0.62
P (y)	–	31.5	15.5
N	15	10	6

References

Jenniskens P. (2021). “February alpha Corvid meteors”. CBET 4954 edited by Daniel W. E. Green, published 2021 April 7.

Jopek T. J., Rudawska R. and Pretka-Ziomek H. (2006). “Calculation of the mean orbit of a meteoroid stream”. *Monthly Notices of the Royal Astronomical Society*, **371**, 1367–1372.

Gamma Draconid (GAD#1106) meteor shower

Denis Vida[1] **and Damir Šegon**[2]

[1]**Department of Earth Sciences, University of Western Ontario, London, Ontario, N6A 5B7, Canada**
denis.vida@gmail.com

[2]**Astronomical Society Istra Pula, Park Monte Zaro 2, HR-52100 Pula, Croatia**

A new shower has been detected by the Global Meteor Network during the time range in solar longitude 14.0–15.5 degrees with a radiant at R.A. = 275.68 deg, Decl. = +53.86 deg, within a circle with the standard deviation of ± 0.9 deg (equinox J2000.0). The shower has been listed as number 1106 in the IAU Working List of Meteor Showers and named the gamma Draconids (GAD).

1 Introduction

The Global Meteor Network was created in 2018 and is still in full expansion. Since its start, more than 200000 accurate video meteor orbits have been collected. The goal of the GMN is to monitor meteor shower activity, activity enhancements, outbursts, new meteor shower appearances, and aid with meteorite recovery.

In its first years of existence GMN already confirmed some outbursts and enhanced shower activities (Roggemans, 2019; 2021; Roggemans et al., 2020a; 2020b; 2020c; Vida et al., 2018; Vida and Eschman, 2020). The better the coverage of the GMN becomes, the better the chances to detect new showers or unusual activity.

Here we report an outburst of a previously unknown meteor shower with a radiant in Draco. 12 meteors were observed by the Global Meteor Network[19] on 2021 April 3–5. The shower was independently observed by cameras in 8 different countries.

2 New shower parameters

The meteors (ranging in magnitude from +2.5 to –3.0) had a median radiant near gamma Draconis (equinox J2000.0). All meteors appeared during the solar longitude interval 14.0–15.5 degrees, with no obvious peak in that interval. The shower is now listed as number 1106 in the IAU Working List of Meteor Showers[20] and named the gamma Draconids (GAD). The meteor shower parameters and mean orbital elements are listed in *Table 1*.

The shower was seen by Global Meteor Network cameras in 8 countries, here are the station codes for each observed meteor:

- HR0001, HR000T (Croatia);
- RU000C, RU000F (Russia);
- HR000T, HR001D (Croatia);
- HR000U, SI0001 (Croatia, Slovenia);
- US0001, US0004, US0007, US000A, US000D, US000K, US000L, US000R (USA);
- ES0005, ES000E (Spain);
- DE0002, DE0009 (Germany);
- HR000K, HR000N (Croatia);
- FR000F, NL0003 (France, the Netherlands);
- HR000M, HR001G (Croatia);
- USL002, USL006, USL00L (USA);
- US0006, US000J, US000L (USA).

Table 1 – Mean parameters and orbital elements (equinox J2000.0) computed using the method of Jopek et al. 2006.

	Mean value
$\lambda_\odot$ (°)	15.04
α_g (°)	275.68 ± 0.9
δ_g (°)	+53.86 ± 0.9
v_g (km/s)	35.98 ± 1.8
λ-$\lambda_\odot$ (°)	270.47
β (°)	+76.94
a (AU)	8.3
q (AU)	0.998 ± 0.00032
e	0.880 ± 0.110
ω (°)	178.316 ± 1.11
Ω (°)	14.85 ± 0.529
i (°)	57.965 ± 1.955
Π (°)	193.17 ± 1.2
Q (AU)	15.6
T_j	1.26
P (y)	24.0
N	12

[19] https://globalmeteornetwork.org/data/ for the dates of 2021 April 3–5.

[20] https://www.ta3.sk/IAUC22DB/MDC2007/Roje/pojedynczy_obiekt.php?kodstrumienia=01106&colecimy=&kodmin=00001&kodmax=01106&sortowanie=

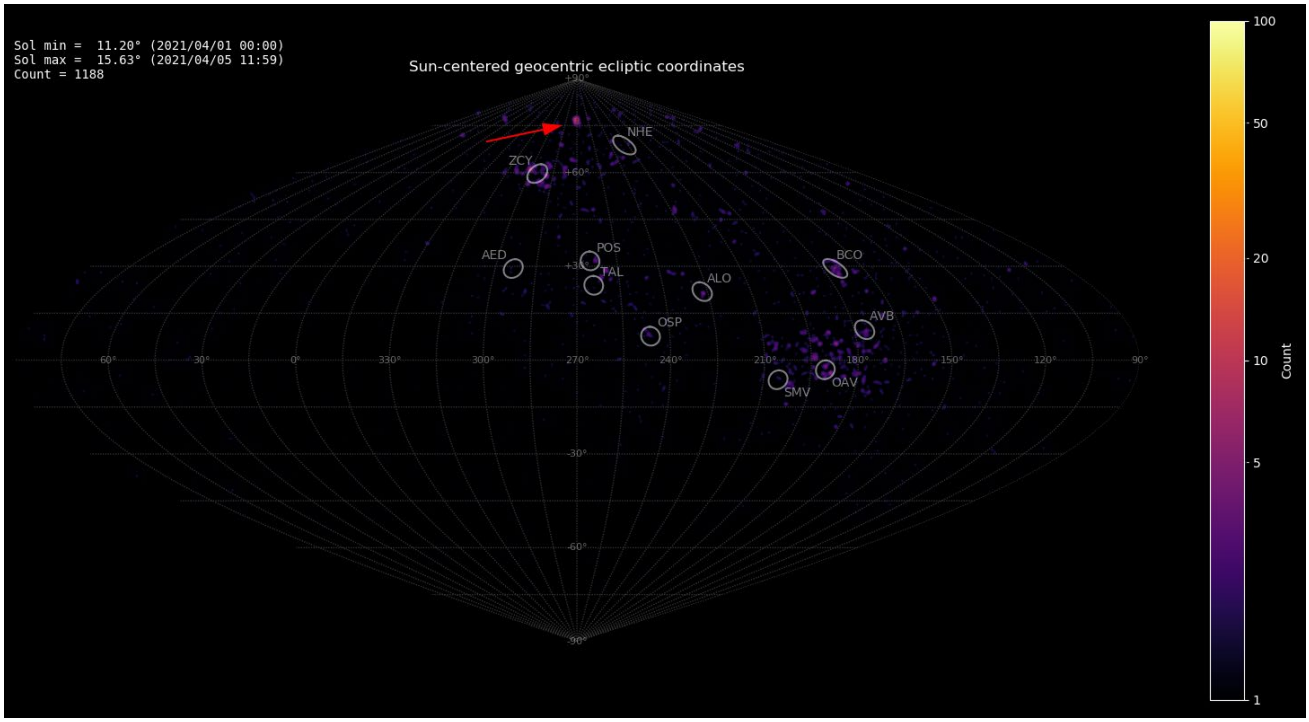

Figure 1 – The Sun-centered geocentric ecliptic coordinates for the time bin $11.2° < \lambda_O < 15.63°$. The new shower is indicated with a red arrow.

Table 2 – The results of the parent body search with the top 5 matched sorted on the Southworth and Hawkins discrimination criterion D_{SH} (Southworth and Hawkins, 1963).

Name	q	e	i	ω	Ω	D_{SH}
C/1953 T1 (Abell)	0.97	1.001	53.23	194.382	3.031	0.273
C/1918 L1 (Reid)	1.102	1	69.71	194.906	18.838	0.401
2009 FA	1.159	0.557	42.1	200.6	3.2	0.514
C/1845 D1 (de Vico)	1.255	1	56.4	205.452	349.281	0.515
2020 WT3	0.679	0.55	58.7	167.1	33	0.533

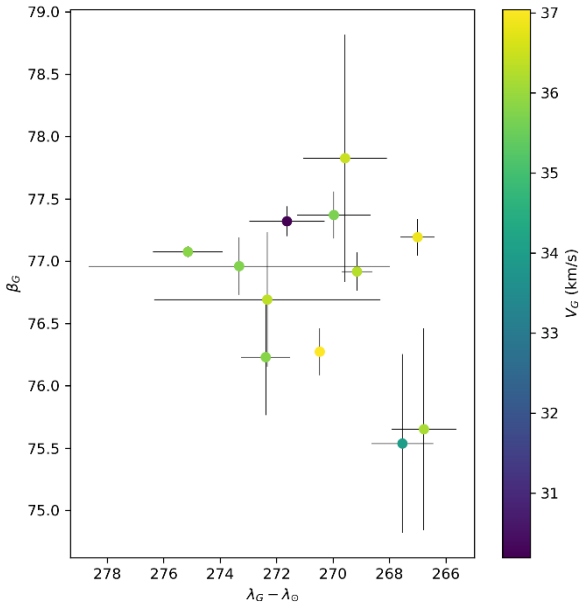

Figure 2 – The plot of the radiant in Sun-centered geocentric ecliptic coordinates.

Figure 1 shows the Sun-centered geocentric ecliptic coordinates for the time bin $11.2° < \lambda_O < 15.63°$. *Figure 2* shows the detailed plot of the radiant in Sun-centered geocentric ecliptic coordinates.

The parent body search didn't return any viable candidates. The best matches are listed in *Table 2* but none of them is likely to be the parent body. The Tisserand value relative to Jupiter with a value of 1.26 indicates that the orbit is a prograde Halley-type comet orbit. The parent body may still remain to be discovered.

Acknowledgment

The Global Meteor Network[21] is released under the CC BY 4.0 license[22]. The authors thank all the volunteers who contribute to the Global Meteor Network.

References

Jopek T. J., Rudawska R. and Pretka-Ziomek H. (2006). "Calculation of the mean orbit of a meteoroid

[21] https://globalmeteornetwork.org/data/

[22] https://creativecommons.org/licenses/by/4.0/

stream". *Monthly Notices of the Royal Astronomical Society*, **371**, 1367–1372.

Roggemans P. (2019). "June epsilon Ophiuchids (JEO#459), 2019 outburst and an impactor?". *eMeteorNews*, **4**, 201–206.

Roggemans P., Howell J.A. and Gulon T. (2020a). "Alpha Monocerotids (AMO#246) outburst 2019". *eMeteorNews*, **5**, 13–18.

Roggemans P., Johannink C. and Sekiguchi T. (2020b). "Phi Serpentids (PSR#839) activity enhancement". *eMeteorNews*, **5**, 178–185.

Roggemans P., Johannink C. and Sekiguchi T. (2020c). "h Virginids (HVI#343) activity enhancement in 2020". *eMeteorNews*, **5**, 233–244.

Roggemans P. (2021). "Global Meteor Network and the 2020 Ursid return". *eMeteorNews*, **6**, 15–18.

Southworth R. R. and Hawkins G. S. (1963). "Statistics of meteor streams". *Smithson. Contrib. Astrophys.*, **7**, 261–286.

Vida D., Merlak A. and Šegon D. (2018). "2018 Draconids as seen by a low-cost RPI based meteor camera". *eMeteorNews*, **3**, 298–299.

Vida D. and Eschman P. (2020). "2019 Camelopardalid (CAM#451) outburst as seen by Global Meteor Network stations in New Mexico". *eMeteorNews*, **5**, 30–32.

Is DLM (#0032) a mystical meteor shower?

Ivan Sergei

Mira Str.40-2, 222307, Molodechno Belarus
seriv76@tut.by

The reason for the study of the DLM (#0032) and COM (#0020) meteor showers was a contradiction between the name of the meteor shower from the CAMS video networks and CMOR radar.

1 Introduction

Studying the distribution of meteor radiant sources from the CAMS video networks and the Canadian orbital radar CMOR, I paid attention to the fact that different meteoroid streams had radiants at the same position at the sky. Thus, CAMS has the COM radiant in the constellation of Leo Minor, while CMOR detected a radiant for the meteor shower DLM. For example, the Orionids have a radiant at the date of maximum in Orion, the Perseids in Perseus, the Geminids in Gemini, so why the Coma Berenicids (COM) have their radiant in the constellation of Leo, while it should be in the constellation of Coma Berenices. The DLM radiant on the date of maximum is in the constellation Leo, the COM radiant on the date of maximum almost in Coma Berenices (at the junction of the constellations Coma Berenices and Leo). This is logical and correct. Can the radiant of different meteoroid streams be at the same position at the same time? It is possible if it is an optical superposition of two different showers with significantly different geocentric velocities v_g. This study provides evidence that this is not the case – COM and DLM are two different showers, albeit with similar geocentric velocities.

2 CAMS data

I have studied the distribution of meteor radiants in 2019 and 2020 from the CAMS video networks between December 16 and 21 (Jenniskens et al., 2011;2018). The radiant distribution map shows very clearly a meteor shower with coordinates for December 19, 2020 at R.A. = 160° and Decl. = +31°, identified as COM (#0020). This is a wrong identification! Could the radiant of a meteor shower in the constellation of Leo Minor be a radiant of the Coma Berenicid meteor shower? It is logic to suppose that the radiant of the Coma Berenicid meteor shower is in the constellation of Coma Berenices or at the junction of adjacent constellations, and given that it is an ecliptic shower, it is likely that the radiant is in the vicinity of the constellation Leo. *Figures 2 and 3* show the location the Coma Berenicid radiant from December 16 to 21, 2020. We should understand that this is actually the location of the December Leonis Minorids (DLM#0032) radiant. not the Coma Berenicids (COM#0020)!

I did a search for a probable COM radiant at the junction of the constellations Leo and Coma Berenices and I found no distinct radiant. This indicates that the radiant of the shower is very diffuse and dispersed in space and is being detected by the video networks as part of the sporadic background.

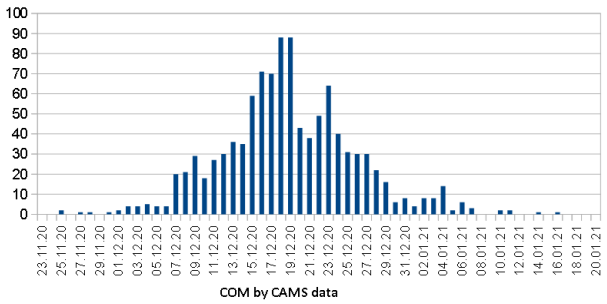

Figure 1 – Activity of COM in 2020 according to CAMS.

Figure 1 is a graph of the COM meteor shower activity for the year 2020. Activity is the total number of all meteors of the shower, according to all video networks. You have to understand that this is actually the activity of the meteor shower DLM, not COM. The maximum activity occurred in the interval December 18–19, 2020.

3 CMOR data

The CMOR radar data (Jones et al., 2005) detects more often a DLM radiant than a COM radiant. In some cases, for example, on December 21, 2019, the radar detected and identified a COM and DLM radiant simultaneously. This is a direct evidence for the existence of two meteor showers. CMOR radar data shows a diffuse blurred structure of the COM shower radiant, i.e. this shower is more difficult for radar detection than the DLM, and this may indicate the dispersion of this shower, which will eventually lead to its disappearance.

The radar correctly shows the location of the COM and DLM radiants. Some difference with the reference data can be explained by the fact that the radar has access to much fainter meteoroids than the video methods or visual method, from which the reference of this shower was calculated.

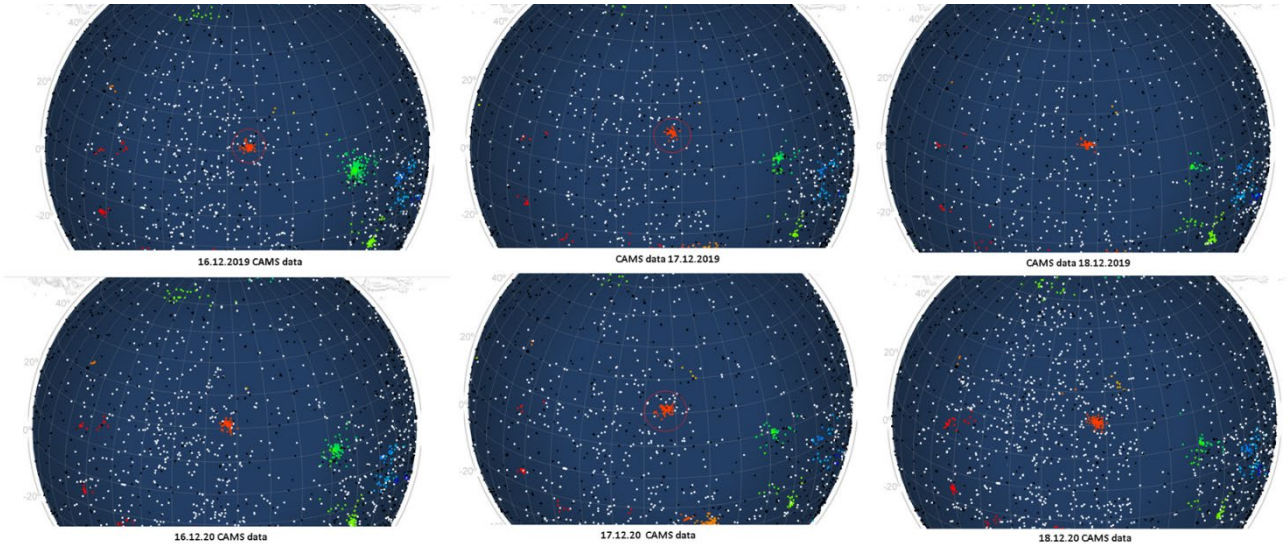

Figure 2 – Radiant position of the COM meteor shower in Sun centered ecliptic coordinates by CAMS data 2020–2021.

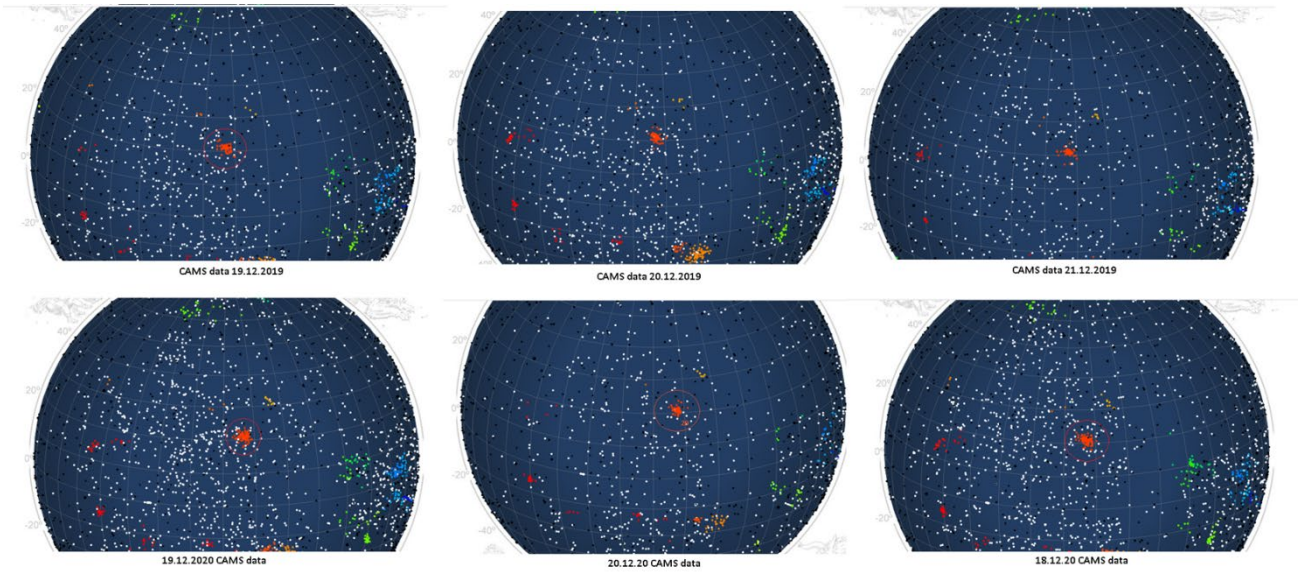

Figure 3 – Radiant position of the COM meteor shower in Sun centered ecliptic coordinates by CAMS data 2020–2021..

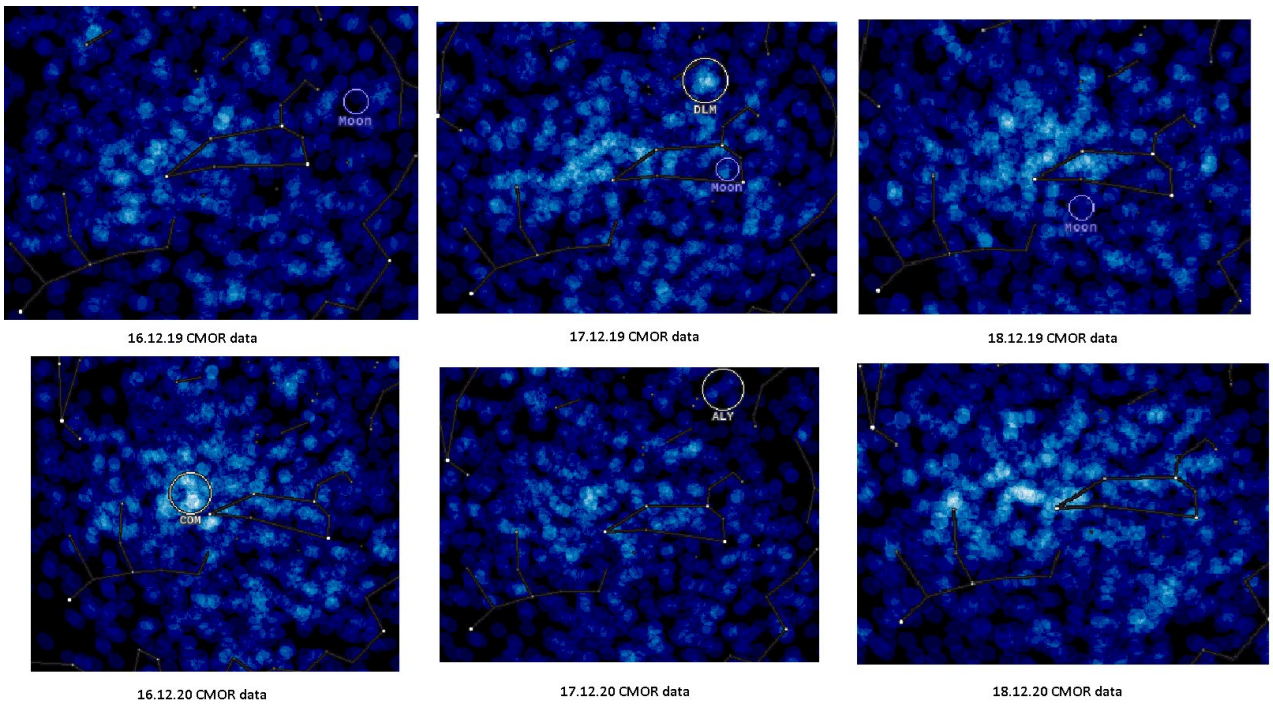

Figure 4 – Radiant position for COM and DLM according to CMOR data 16–18 December 2019–2020.

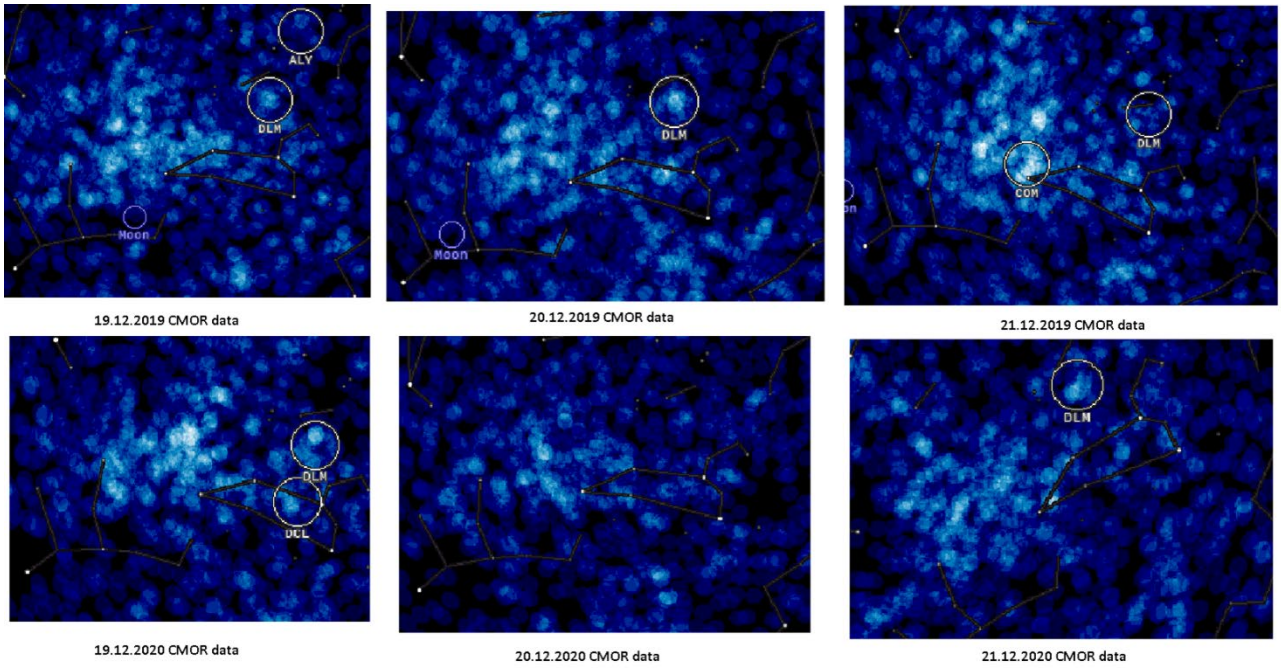

Figure 5 – Radiant position for COM and DLM according to CMOR data 19–21 December 2019–2020.

4 IMO data

The IMO data (VMDB) does not contain any observations of the COM meteor shower. IMO consists of fairly experienced observers, so there is no reason not to trust the IMO visual data. According to the IMO meteor calendar, COM is active December 12–23. One can suppose that few observers observe at this time, because of the unfavorable weather conditions, as the COM radiant culminates after midnight, however VMDB has GEM observations for each year, hence COM observations should be present. This may indicate that the shower is not actually detected visually.

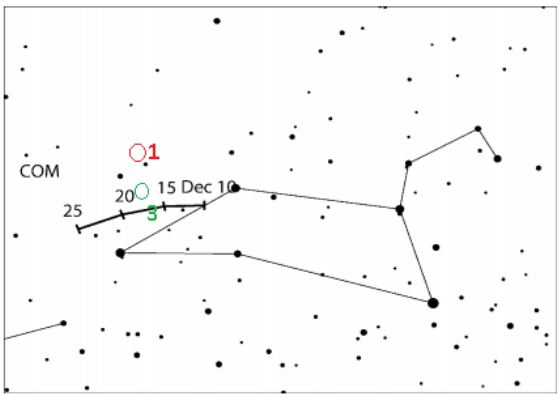

Figure 6 – Radiant drift COM by IMO Meteor Shower Calendar.

The IMO data (VMDB) contains observations of the DLM meteor shower over the entire history of the IMO. On the IMO website you can see graphs of activity changes of this shower as well as tabular data. The IMO meteor calendar gives information about the COM meteor shower, there is a radiant drift table, but no observations of this shower! So maybe in fact the mystical shower is COM and not DLM?

Curiously, the earlier editions of the calendar show the location of the radiant about 8 degrees further south than the later versions, as well as different peak dates. For example, the 2005 maximum is on December 19, R.A. = 175° Decl. = +25°, while the 2019 maximum is on December 16, R.A. = 175°, Decl. = +18°. The inconsistency in the location of the radiants may confirm the idea of a strong dispersion of the meteoroid stream in space.

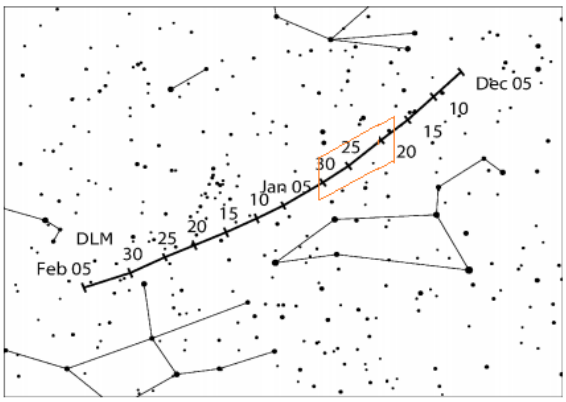

Figure 7 – Radiant drift DLM by IMO Meteor Shower Calendar.

Molau and Rendtel (2009), based on IMO video network data in their paper conclude: “The conclusion from our analysis is clear: there are two showers. We find COM (#0020) for 260°–271° (December 12–23) and the other, slightly stronger DLM (#0032) in the period 253°–315° (December 5 – February 4).” The IMO VMDB database contains observations of the DLM since 1989. It is quite possible that this is a confirmation of the existence of this meteor shower.

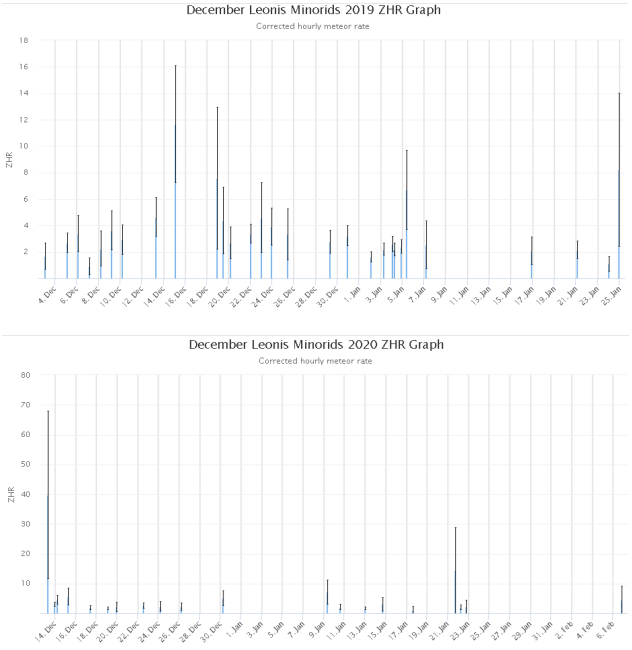

Figure 8 – Activity DLM from visual IMO data 2019–2020.

5 IAU MDC data

The IAU MDC data contains information about two meteor showers at once. This is incorrect. *Figure 9* shows the IAU MDC data. There are two pairs of records. I have highlighted them in red (Jenniskens, 2006) and in green (Molau and Rendtel, 2009). The same shower cannot have two radiants at an angular distance of about 10 degrees.

After the "DE" column in *Figure 9*, the correct identification of the meteor showers is marked. In the IAU MDC, the DLM shower is listed as a removed shower. This is incorrect! The DLM is consistently active and is well detected by CAMS video networks. The COM shower is not detected by CAMS video networks, but that doesn't mean it can be inactive and should be put in removed showers.

In 2016 Jenniskens gives $\Delta\delta = -0.39°$. In the 2006 paper, he gives the coordinates of the radiant $\lambda_\odot = 274°$, R.A. = 175.2°, Decl. = +22.2°, and a second radiant with $\lambda_\odot = 262.2°$ R.A. = 156.1°, Decl. = +32.7°. If these are the same meteor shower, then $\Delta\delta = -0.87°$, which contradicts the $\Delta\delta = -0.39°$ determined by Jenniskens in 2016. Hence, the researcher in 2006 gives information in the IAU MDC about two meteor showers! *Figure 6* shows the locations of the radiants from the IAU MDC Table numbers 1 and 3. The most likely classification of the radiant is COM. *Figure 7* shows in light red the location of the other 7 radiant in the IAU MDC records. The most likely classification of the radiants is DLM. Entry number 1 in the IUA MDC table (Jenniskens, 2006) gives the radiant for $\lambda_\odot = 274°$ (December 26), a radiant closer to the calculated COM radiant, and quite far from the calculated DLM radiant, therefore this entry is shown in the table with a question mark.

Comission F1 Division F, IAU

~~COM~~ ~~Comae Berenicids~~ **Single Shower - Status - Established** Next

S. Lon	RA [deg] J2000	DE		dRA	dDE	VG [km/s]	a [AU]	q [AU]	e	Peri	Node [deg] J2000	Incl	N	OT	Referer
274 1	175.2	22.2	COM?			63.7	14.4	0.541		265.0	283.3	139.4	00004		1. Jenniskens, 2006
265.7	159.7	31.6	DLM	0.79	-0.32	63.0	14.4	0.541		265.0	283.3	139.4	00652	T	2. SonotaCo, 2009
264 3	174.5	18.2	COM	0.65	-0.08	67.7							00435	T	3. Molau and Rendtel, 2009
275.9	168.8	27.2	DLM			67.0		0.611	1.152	253.0	275.9	137.3	00008	T	4. Rudawska and Jenniskens, 2014
277.4	169.5	26.6	DLM			63.06		0.536	0.955	266.1	277.4	135.3	00062	T	5. Kornos et al., 2014
262.2	156.1	32.7	DLM			62.3	11.9	0.554		265.6	262.2	133.8	00006		6. Jenniskens, 2006
261.7	163.7	39.7				64	3.76	0.81		249	261.7	138	00009	R	7. Kashcheyev and Lebedinets, 1967
268	161.5	30.5	DLM	0.86	-0.43	64.0							03181	T	8. Molau and Rendtel, 2009
274.0	167.0	28.0	DLM	0.96	-0.39	63.3	8.58	0.557	0.962	263.5	272.2	135.3	00497	T	9. Jenniskens et al., 2016, Icarus, 26

Previously named December Leonis Minords

Figure 9 – Data for COM, DLM in IAU MDC data.

6 Conclusion

CAMS video networks have blindly taken the situation as true from the current IAU MDC data, which is incorrect. IMO and CMOR did not use IAU MDC data, so their data is correct. In the IAU MDC table, the "COM" record includes two showers COM and DLM. It is necessary to separate these entries into two showers separately, COM and DLM. The current entry is incorrect. There are 6 cases with DLM data in this record and 2 cases with COM records. Undoubtedly realistically there are two meteor showers COM and DLM. COM consists of smaller particles (a diffuse and dispersed shower), so it is virtually undetectable by CAMS video networks, but well-detected by CMOR radar, which has access to much smaller particles. DLM consists of larger particles (it is an annual meteoroid stream with more or less constant weak activity), so it is well detected by CAMS video networks, and it is also clearly visible on CMOR radar maps. We can also conclude that the dust in the COM shower is not distributed very evenly over the orbit, and in some years it becomes within reach for the video observing method (Molau and Rendtel, 2009). A definitive conclusion about these meteoroid streams can be drawn from the latest orbit data from CAMS video network observations and from the most recent radar (orbit) data. Unfortunately, I do not have access to such data and my conclusions reflect my personal point of view. My conclusions are confirmed by Masahiro Koseki (Koseki, 2021), who conducted an analysis of orbits.

Acknowledgment

I thank Paul Roggemans and Jürgen Rendtel for the recommendations and advice on this article.

References

Jenniskens P. (2006). Meteor showers and their parent comets. Cambridge, UK: Cambridge University Press.

Jenniskens P., Gural P.S., Dynneson L., Grigsby B.J., Newman K.E., Borden M., Koop M. and Holman D. (2011). "CAMS: Cameras for All-sky Meteor Surveillance to establish minor meteor showers". *Icarus*, **216**, 40–61.

Jenniskens P., Baggaley J., Crumpton I., Aldous P., Pokorny P., Janches D., Gural P. S., Samuels D., Albers J., Howell A., Johannink C., Breukers M., Odeh M., Moskovitz N., Collison J. and Ganjuag S. (2018). "A survey of southern hemisphere meteor showers". *Planetary Space Science*, **154**, 21–29.

Jones J., Brown P., Ellis K. J., Webster A. R., Campbell-Brown M., Krzemenski Z., and Weryk R. J. (2005). "The Canadian Meteor Orbit Radar: system overview and preliminary results". *Planetary and Space Science*, **53**, 413–421.

Koseki M. (2021). "The actiivity of meteor showers recorded by SonotaCo Net video observations 2007-2018". *eMetN*, **6**, page 218.

Molau S., Rendtel J. (2009). "Comprehensive List of Meteor Showers Obtained from 10 Years of Observations with the IMO Video Meteor Network". *WGN, Journal of the International Meteor Organization*, **37**, 98–121.

Rendtel J. (2020). "Meteor Shower Calendar". IMO.

December 2020 report CAMS BeNeLux

Paul Roggemans

Pijnboomstraat 25, 2800 Mechelen, Belgium
paul.roggemans@gmail.com

A summary of the activity of the CAMS BeNeLux network during the month of December 2020 is presented. 8150 multiple station meteors were registered. The weather was very unfavorable; December 2020 was the worst month of December in the CAMS BeNeLux history. 24 nights allowed to collect some orbits with 8 nights with more than 100 orbits and 7 nights without any orbit. In total 2693 orbits were added to the CAMS BeNeLux database.

1 Introduction

December might be the most interesting month of the year meteor wise. Meteor rates remain at a high level with several very active minor showers during this month. The Geminids are one of the most active annual showers of the year and the Ursids sometimes contribute with unexpected enhanced activity. This rich activity comes with the long winter nights of over 14 hours dark sky in the BeNeLux area. Could we be lucky with the weather in 2020?

2 December 2020 statistics

CAMS BeNeLux collected 8150 multi-station meteors in December 2020 (against 12329 in December 2019 and 13220 in December 2018). Indeed, this number suggests the weather circumstances were not favorable at all this year. Most of the rich Geminid nights were missed and December 2020 was characterized by mainly cloudy nights. The final number of orbits reached a total of 2693 orbits, still an impressive number when taking the poor weather circumstances into account. This is the lowest number of orbits for the month of December since 2015, far below the totals of 4124 orbits of December 2019 and 4908 orbits of December 2018 when CAMS BeNeLux had its best December month ever.

This month counted only 8 nights with more than 100 orbits (13 in 2019) and 7 nights remained without any orbits (3 in 2019). Best night of December 2020 was 18–19 with 495 orbits. The nice score in orbits in December 2018 was thanks to a lucky coincidence that some of the very few clear nights happened during the best Geminid activity nights. In December 2019 the Geminids were missed but the weather was more favorable in general.

The statistics of December 2020 are compared in *Figure 1* and *Table 1* with the same month in previous years since the start of CAMS BeNeLux in 2012. In 9 years, 206 December nights allowed to obtain orbits with a grand total of 22320 orbits collected during December during all these years together.

While December 2019 had a maximum of 82 cameras operational on some nights, 72.8 on average, December 2020 had 86 cameras at best and 72.4 on average. Not everyone has the possibility to operate cameras every night, however experience learns it is highly recommended to try to keep as many cameras as possible operational all nights.

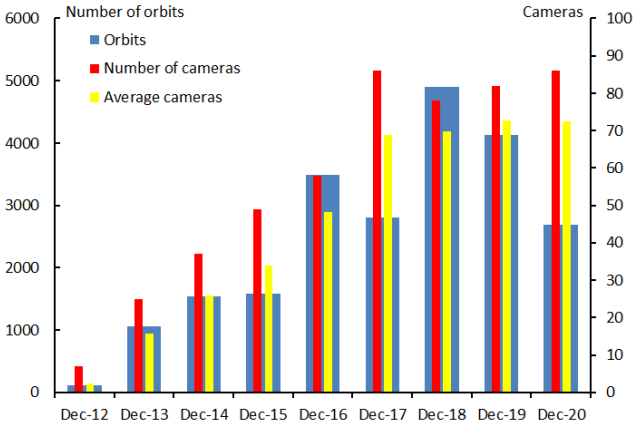

Figure 1 – Comparing December 2020 to previous months of December in the CAMS BeNeLux history. The blue bars represent the number of orbits, the red bars the maximum number of cameras running in a single night and the yellow bar the average number of cameras running per night.

Table 1 – December 2020 compared to previous months of December.

Year	Nights	Orbits	Stations	Max. Cams	Min. Cams	Avg. Cams
2012	12	117	6	7	-	2.4
2013	23	1053	10	25	-	15.7
2014	19	1540	14	37	-	25.8
2015	27	1589	15	49	8	33.8
2016	25	3492	21	58	25	48.3
2017	25	2804	22	86	49	68.9
2018	23	4908	21	78	52	69.8
2019	28	4124	21	82	64	72.8
2020	24	2693	24	86	56	72.4
Total	206	22320				

Although the lower total number of orbits is mainly due to bad weather, there were many nights that camera operators in the northern part of the BeNeLux network didn't start their cameras, assuming the sky would remain overcast,

while the southern part of the network functioned 7/7 with AutoCams and registered meteors during unexpected clear periods. A substantial part of the orbits obtained by CAMS BeNeLux were obtained during often mainly cloudy nights with unforeseen clear periods. Best practice is to keep cameras operational 7/7 as nobody can foresee if a cloudy night will actually remain 100% overcast. For this purpose, the RMS cameras are ideal since these function totally automated. A new RMS camera started contributing to the CAMS BeNeLux network from 4–5 December 2020 installed at Dwingeloo, Netherlands, by *Tammo Jan Dijkema*.

3 Conclusion

December 2020 brought the lowest score in terms of orbits since 2015 when less cameras and stations participated in the network. It is difficult to compare with earlier December results as no AutoCams existed before 2015 and significant less cameras were available. December 2020 may have been the very worst December month in the CAMS BeNeLux history.

Acknowledgment

This report is based on the online data taken from the CAMS website[23]. First of all, thanks to Martin Breukers for collecting all the data and running Coincidence to obtain the trajectories and orbits during this month. Many thanks to all participants in the CAMS BeNeLux network for their dedicated efforts. The CAMS BeNeLux team was operated by the following volunteers during the month of December 2020:

Felix Bettonvil (Utrecht, Netherlands, CAMS 376 and 377), *Jean-Marie Biets* (Wilderen, Belgium, CAMS 379, 380, 381 and 382), *Martin Breukers* (Hengelo, Netherlands, CAMS 320, 321, 322, 323, 324, 325, 326 and 327), *Guiseppe Canonaco* (Genk, RMS 3815), *Bart Dessoy* (Zoersel, Belgium, CAMS 397, 398, 804, 805 and 806), *Tammo Jan Dijkema* (Dwingeloo, Netherlands, RMS 3199), *Jean-Paul Dumoulin, Dominique Guiot and Christian Walin* (Grapfontaine, Belgium, CAMS 814 and 815, RMS 003814), *Uwe Glässner* (Langenfeld, Germany, RMS 3800), *Luc Gobin* (Mechelen, Belgium, CAMS 3890, 3891, 3892 and 3893), *Tioga Gulon* (Nancy, France, CAMS 3900 and 3901), *Robert Haas* (Alphen aan de Rijn, Netherlands, CAMS 3160, 3161, 3162, 3163, 3164, 3165, 3166 and 3167), *Robert Haas* (Texel, Netherlands, CAMS 810, 811, 812 and 813), *Robert Haas / Edwin van Dijk* (Burlage, Germany, CAMS 801, 802, 821 and 822), *Kees Habraken* (Kattendijke, Netherlands, RMS 000378), *Klaas Jobse* (Oostkapelle, Netherlands, CAMS 3030, 3031, 3032, 3033, 3034, 3035, 3036 and 3037), *Carl Johannink* (Gronau, Germany, CAMS 311, 314, 317, 318, 3000, 3001, 3002, 3003, 3004 and 3005), *Hervé Lamy* (Dourbes, Belgium, CAMS 394 and 395), *Hervé Lamy* (Humain Belgium, CAMS 816), *Hervé Lamy* (Ukkel, Belgium, CAMS 393), *Koen Miskotte* (Ermelo, Netherlands, CAMS 351, 352, 353 and 354), *Tim Polfliet* (Gent, Belgium, CAMS 396), *Steve Rau* (Zillebeke, Belgium, CAMS 3850 and 3852), *Paul and Adriana Roggemans* (Mechelen, Belgium, CAMS 383, 384, 388, 389, 399 and 809, RMS 003830 and 003831), *Hans Schremmer* (Niederkruechten, Germany, CAMS 803) and *Erwin van Ballegoij* (Heesch, Netherlands, CAMS 347 and 348).

[23] http://cams.seti.org/FDL/

Annual report 2020 CAMS BeNeLux

Paul Roggemans

Pijnboomstraat 25, 2800 Mechelen, Belgium
paul.roggemans@gmail.com

A summary of the activity of the CAMS BeNeLux network during the year 2020 is presented. The year 2020 brought unusual good weather for astronomical observations with many clear nights during the period from March until September. 45743 orbits could be computed during 325 different nights which corresponds to 89% of all 366 nights in 2020. The months January, February, October and December 2020 were rather poor months while January, March, April, May and September had the best scores ever for these months.

1 Introduction

The first CAMS network started in October 2010 in California and celebrated its tenth anniversary in 2020. CAMS BeNeLux was the first CAMS network outside the USA and had its first orbits in the night of 14–15 March 2012. Meanwhile we are almost 9 years later and the CAMS BeNeLux network exceeded by far all expectations. Meanwhile other networks are on their decline or stopped working and some new players entered into the field.

In CAMS BeNeLux all the cameras, optics, computers and other required equipment are bought and financed by the participants themselves. Operating cameras for the CAMS network also requires some time on a regular basis to confirm meteors, remove false detections and report the data. The commitment in such project requires a strong motivation which is crucial to maintain these efforts.

Until 2017 CAMS BeNeLux expanded fast in number of cameras while in recent years the total number of cameras did not change much. Some CAMS stations quit; few others joined the network. The total volume of the atmosphere covered by CAMS BeNeLux cameras gradually increased. Past two years the classic Watec H2 Ultimate cameras got less popular and most of the recent cameras were all RMS which deliver data to both CAMS and Global Meteor Network. The use of RMS cameras for the CAMS BeNeLux network has the advantage that these are fully automated and functioning 7 nights on 7.

2 CAMS BeNeLux 2020 statistics

The year 2020 started very promising with a lucky Quadrantid night 3–4 January and a record number of 660 orbits in a single January night. Apart from that very successful night most of the month brought unfavorable winter weather. With a total of 2075 orbits, slightly better than the previous January record of 2058 orbits in 2017, the year started with a new record for this month. The poor weather and mostly stormy overcast sky of the last 10 nights of January continued throughout February. The situation of 2018 and 2019 with exceptional clear February nights did not happen in 2020 and the month ended with a modest 1215 orbits, far less than the 3485 orbits in 2019 or the 4147 orbits in 2018.

Very poor weather dominated most nights until half March 2020 when a major and long-lasting weather improvement resulted in a splendid second half of March. With 3026 orbits, March 2020 was another record month with more than twice the number of orbits that had been recorded during any previous month of March. The general stable favorable weather maintained during most of April with as highlights the outburst of the phi Serpentids (PSR#839) on April 15 (Roggemans et al., 2020) an excellent coverage of the 2020 Lyrids and an enhanced activity of the h Virginids (HVI#343) during the week following the Lyrid maximum (Roggemans et al., 2020). April 2020 ended with a splendid record number of 4128 orbits, beating the previous record of April 2019 when 2538 orbits were collected.

The last few nights of April and the first of May, the long period with good weather seemed to come to an end, but after a few less good nights the weather improved again and most nights in May obtained nice numbers of orbits. May 2020 became the third month in a row with a record number of orbits, after March and April. With a total of 3226 orbits May 2020 exceeded by far the previous record of 2426 orbits obtained in May 2018. Another particular record for May 2020, CAMS BeNeLux had on average 90.5 cameras running this month, with a maximum of 93 and a minimum of 70, an absolute record for the network. The long-lasting favorable weather period came to an end in early June and clouds dominated the sky until 18 June when a week of clear and partial clear nights allowed to register plenty of orbits. June 2020 ended with 1834 orbits, far less than the 2457 orbits of the record year 2019 for this month, but still good for a second place.

July 2020 started with very variable weather and apart from some partial clear nights, it took until the end of July before some nice clear nights allowed to harvest large numbers of orbits. 30–31 July had as many as 542 orbits on a single July night, an absolute record for this month. However, the weather in July 2020 wasn't good enough to improve the record for the month as a whole. With 3823 orbits July 2020 was the third best month of July after July 2018 with 4098

orbits and the best ever month of July in 2019 with 4139 orbits.

August counted many favorable nights for video meteor work. With 720 orbits, 12–13 August was the absolute top night of 2020, but still far less than the best August nights of 2019 when 13–14 had 1175 orbits and 11-12 had 870 orbits. The absolute August record night remains 12–13 August 2017 when 1555 obits were registered, also 13–14 August 2017 with 750 and 12–13 August 2016 with 830 orbits was better than the best August 2020 night while only 54 cameras at 20 stations were available in 2016 against 90 cameras at 24 stations in August 2020.

Clear skies dominated the first three weeks of September and resulted in another record with 6132 orbits as the best September month ever, compared to the 5606 orbits of the previous best September month in 2018. The night 18–19 September 2020 with 514 orbits in a single night was the best September night ever for the network. One highlight in September were the chi Cygnids (CCY#757) which had been found in 2015 (Jenniskens, 2015; Roggemans et al., 2016; Koukal et al., 2016) and for which some early activity had been detected in late August 2020 (Jenniskens, 2020). Unfortunately, no details were communicated about this shower for the 2020 CAMS BeNeLux data.

Table 1 – Statistics for each month of 2020.Total numbers of nights (*N*) with orbits, number of orbits, number of camera stations (*S*), maximum of cameras available (M_x), minimum of cameras available (M_i), average number of cameras (M_m), total number of meteors and percentage of multiple station meteors.

M	N	Orbits	S	M_x	M_i	M_m	Meteors	%
Jan	23	2075	21	83	64	72.9	12997	47%
Feb	24	1215	22	84	62	73.1	7665	46%
Mar	27	3026	25	93	66	81.7	17983	57%
Apr	29	4128	25	94	76	89.4	24465	62%
May	29	3226	24	93	70	90.5	18592	62%
Jun	27	1834	24	93	60	83.1	–	–
Jul	28	3823	24	90	59	79.1	–	–
Aug	31	8845	24	90	59	80.6	–	–
Sep	26	6132	24	90	52	76.2	–	–
Oct	29	3305	23	90	52	70.9	20135	45%
Nov	28	5441	23	88	57	72.6	–	–
Dec	24	2693	24	86	56	72.4	–	–
	325	45743						

Last week of September 2020 the weather turned into the worst possible scenario and remained rather unstable without any complete clear night until begin of November. With a total of 3305 orbits, 2020 brought the poorest month of October since 2015. Most of the rich Orionid activity was missed once again, another year without luck for this shower. November didn't bring completely clear nights, but at least the many partial clear nights allowed to collect many orbits. November 2020 ended with 5441 orbits, the second-best month of November after November 2018 when 6916 orbits were collected. December started with totally overcast nights, most of the Geminid activity was missed and the predicted enhanced Ursid activity remained hidden behind the clouds. With a total of 2693 orbits, December 2020 became the poorest month of December since 2015. Taking into account the larger surface of the atmosphere covered and the higher number of cameras, December 2020 was probably the worst December month in the CAMS BeNeLux history. Question is if this time of the year would ever bring a month with favorable weather for meteor work?

An overview of the monthly statistics for CAMS BeNeLux is presented in *Table 1*. February and December 2020 were the worst months of 2020. Except for January, June and October all other months were rather exceptionally good.

Good or bad weather determine the success of a camera network, but of course the hardware needs to be available. After a strong build-up of the network in 2017 we had a drop in the number of cameras in 2018 to about 80% of what was available before and the number was kept down throughout 2019 due to technical problems. This is visible in *Figure 1*, as a drop in the maximum (green line) and the average number (red line) of cameras available each month since 2018. The situation finally improved a lot in the first half of 2020 when less technical problems occurred and a few new cameras were added to the network. Unfortunately, since the summer of 2020 we see again a decline in the number of available cameras. No technical issues, but after operating cameras for years some participants seem to lose the motivation to maintain these efforts. Once cameras quit registering meteors, it is not always easy to resume participation in the network. For instance, the 4 cameras at Terschelling, Netherlands, remain unavailable for about two years now, apart from a short period end of March to begin of April when two of the four cameras could be used.

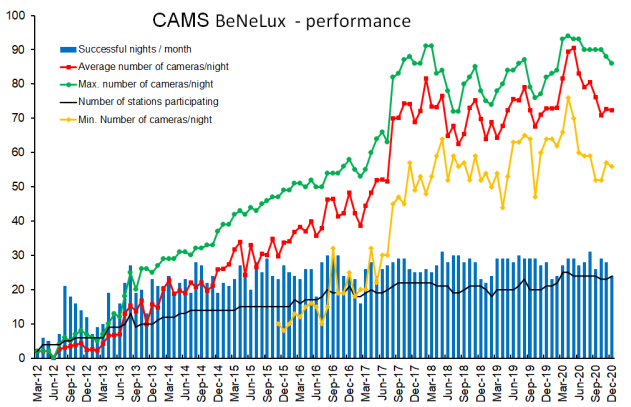

Figure 1 – Cams BeNeLux performance at a glimpse. The blue bars represent the number of nights with orbits for each month. The black line is the number of operational Cams stations, the green line the maximum number of operational cameras, the red line the average number of operational cameras and the yellow line the minimum number of operational cameras.

One particular phenomenon in 2019 were the so-called "Zebrids", meteor trails with irregular interruptions caused by dropped frames during the capture of the appearance of the meteor. "Zebrids" make the measurement of the time

duration of the meteor and its velocity corrupted. The CAMS trajectory and orbit solving app Coincidence rejects such meteors because of the erroneous velocity measurement. This problem seems solved since some operators switched from EzCap116 to a Sensoray card, or reinstalled their CAMS PC or just reinstalled the older version of FTP_CaptureDonglesAndDetect.exe.

Some new cameras were added to the CAMS BeNeLux network in 2020 at geometric strategic positions for the existing CAMS stations (see also *Figure 2*):

- CAMS 3800 became operational on 5–6 February 2020. This is an RMS camera with a 6 mm lens installed at Langenfeld, Germany and owned by *Uwe Glässner*. The advantage of the RMS camera is that data reduction can be done remotely. The confirmation for CAMS for this camera is done from Mechelen in Belgium. The camera is pointed over the north of the Netherlands, a direction for which Langenfeld provides a geometric strategic position to combine with multiple other cameras pointed in the northern part of CAMS BeNeLux;
- CAMS 3000, 3001 and 3002 are three new Watecs H2 Ultimate pointed at high elevation by *Carl Johannink* in Gronau, Germany, active since 12–13 March 2020;
- CAMS 378 got operational 21–22 March. This is another RMS (NL0009) with a 36mm lens installed at Kattendijke, Netherlands and owned by *Kees Habraken*. The camera is pointed north and covers a large part of the Netherlands, North Sea and part of Germany;
- CAMS 3198 is another RMS (NL000A) camera with a 6 mm lens installed in Dwingeloo, Netherlands, by *Tammo Jan Dijkema*. This camera started 4–5 December 2020.

Figure 2 – Location of all the active CAMS BeNeLux stations and cameras during 2020.

3 2020 compared to previous years

In total 45743 orbits were collected in 2020, good for a second-best year after 2018 when as many as 49627 orbits were collected. *Figure* 3 compares the data from year to year and *Table 2* lists the numeric values. 2020 did slightly better than 2019 when 42749 orbits were added to the dataset. From *Table 2* we learn that 2020 brought slightly less favorable weather than previous two years. The average number of 27.1 nights with orbits was slightly less good than in 2019 with 27.8 and 2018 with 27.5. Also, the total number of nights that produced one or more orbits was less than previous two years with 325 nights in 2020 against 333 in 2019 and 330 in 2018. These numbers are actually huge when considering the often-cloudy atmosphere over the BeNeLux region. The number of complete clear nights is much lower and it would make a substantial difference if our cameras wouldn't be operated 7 nights on 7.

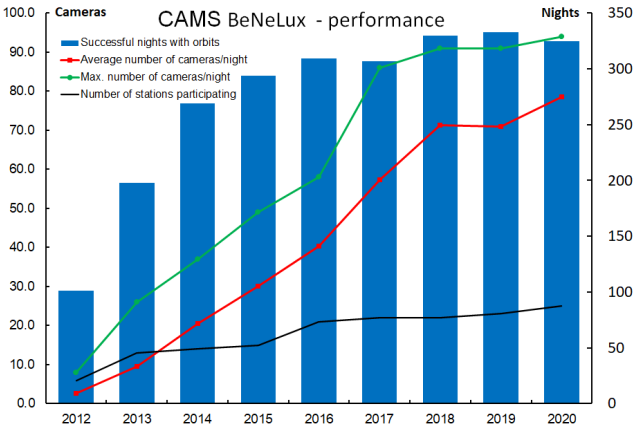

Figure 3 – The performance of the CAMS BeNeLux network from year to year. The blue bars represent the total number of nights during which orbits were obtained. The black line is the number of CAMS stations, the green line the maximum number of cameras available and the red line the average number of cameras available.

Table 2 – Total numbers per year: average number of nights with orbits per month (D_m), orbits, average number of cameras per month (C_m), maximum number of operational cameras, number of operational stations and total number of nights with orbits.

Year	D_m	Orbits	C_m	Cameras	Stations	Nights
2012	10.1	1079	2.6	8	6	101
2013	16.5	5684	9.5	26	13	198
2014	22.4	11288	20.6	37	14	269
2015	24.5	17259	30.1	49	15	294
2016	25.8	25187	40.3	58	21	309
2017	25.6	35591	57.2	86	22	307
2018	27.5	49627	71.3	91	22	330
2019	27.8	42749	70.9	91	23	333
2020	27.1	45743	78.5	94	25	325
		234204				2466

With less favorable weather 2020 ended with more orbits. The explanation why is obvious in *Table 2* with the highest number of cameras on average capturing meteors, the highest number of cameras ever available and the highest minimum number of cameras capturing on average per month (not shown) are the reasons why more orbits could be harvested despite slightly less favorable weather. The use of AutoCAMS for the Watecs and of course the new RMS cameras made the difference!

The expansion of the network covering a larger surface than few years ago offered better chances for local clear sky in some regions while other parts of the network remained 100% cloudy. Amateurs who operate their cameras only during predicted clear sky are missing all the unforeseen periods with clear sky. For that reason, all meteor camera networks in the world keep their cameras recording, regardless the weather. CAMS BeNeLux is the only video camera meteor network where several stations remain inactive when the weather looks unfavorable.

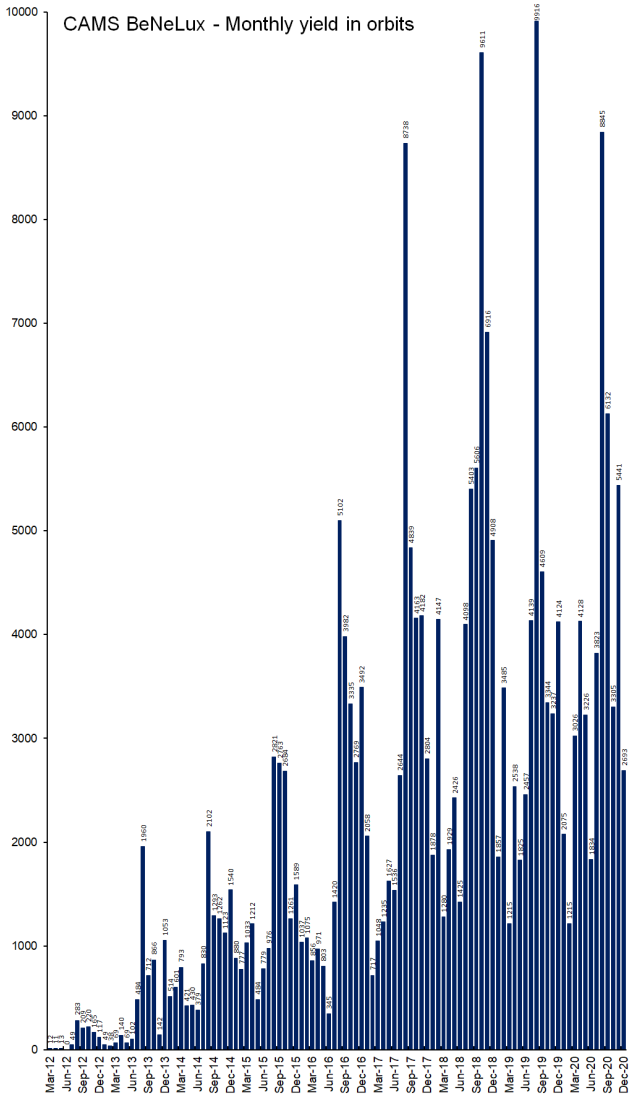

Figure 4 – The total number of orbits collected per month. August 2019 has the record with 9921 orbits in a single month.

Figure 4 shows the number of orbits registered per month, apart from the peaks, 2020 did very well. The graph shows the fluctuations from month to month. Good or bad luck with some major showers, favorable or unfavorable weather and the fact that some participants every now and then cannot contribute to the network altogether explain the lows and the highs. Some months it may look like clear skies will never return, but even in the worst periods, orbits can be obtained.

Looking at the accumulated number of orbits over the years in *Figure 5*, we see how CAMS BeNeLux took off after 2016 when AutoCAMS made it easy to run cameras 7 on 7 and the network got at full strength in 2017. The graph mentions the totals at the end of each year. 2020 ended with an accumulated total of 234204 orbits collected by CAMS BeNeLux. Ten years ago, nobody would ever have expected this to happen. A project like CAMS BeNeLux isn't a short-term project. The purpose is to keep it going as long as possible, keeping everyone motivated.

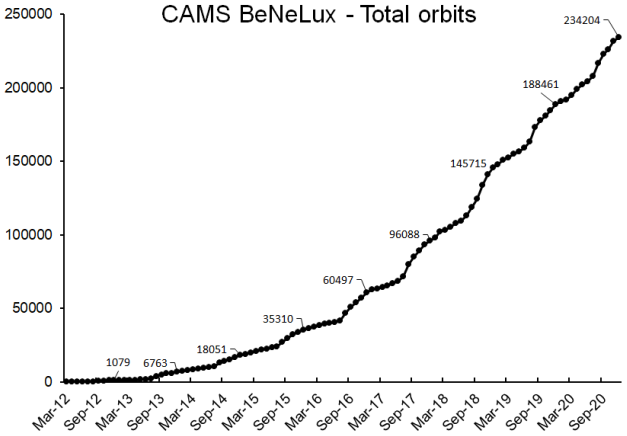

Figure 5 – The evolution of the number of orbits collected by the CAMS BeNeLux network.

Ten years ago, at the start of the CAMS project, the purpose of the project was to collect at least a hundred orbits for each calendar date to detect unknown minor showers caused by weak dust trails. This initial target proved to be too modest as meanwhile the BeNeLux Cams network alone almost accomplished this purpose. CAMS proved much more successful than ever expected. In 2020 all the CAMS networks together on average collected more than 1000 orbits per day!

Figure 6 shows the total number of orbits collected per calendar date since 2012 by CAMS BeNeLux alone, until end of 2019 (top) and until end of 2020 (bottom). End 2020 only 8 nights were left with less than 100 orbits with 23–24 January as the most miserable night since 2013 with as few as 5 orbits collected during all these years together. January seems to be the most challenging month for the weather. Also, the night 21-22 December remained poorly covered, no luck with the Ursids so far for CAMS BeNeLux.

End 2020 we had 177 nights with more than 500 orbits, 69 nights had more than 1000 orbits accumulated. The influence of the major meteor showers is reflected in the numbers of orbits: the Quadrantids 3–4 January, Lyrids 22–23 April, the delta Aquariids South end of July, most of the Perseid activity period with as best night 12–13 August

TOTAL	01-02	02-03	03-04	04-05	05-06	06-07	07-08	08-09	09-10	10-11	11-12	12-13	13-14	14-15	15-16	16-17	17-18	18-19	19-20	20-21	21-22	22-23	23-24	24-25	25-26	26-27	27-28	28-29	29-30	30-31	31-01	
January	99	400	716	312	386	204	438	358	149	172	75	21	212	171	159	203	414	434	667	818	506	132	5	69	198	234	55	214	206	126	120	8273
February	77	247	343	140	352	395	184	226	32	173	210	648	708	458	920	376	549	197	109	304	365	476	698	818	488	522	595	150	80			10840
March	55	114	183	198	159	124	271	232	194	231	356	346	240	216	153	181	182	246	145	194	164	181	145	325	218	198	200	227	248	155	227	6308
April	224	79	178	183	203	244	152	261	213	321	222	276	287	169	260	255	456	451	733	643	514	661	387	96	115	223	155	253	101	138		8453
May	308	127	334	372	440	319	276	456	179	369	240	335	320	439	248	91	207	75	171	247	189	152	249	244	279	220	63	251	33	143	301	7677
June	222	86	158	171	201	268	74	177	244	198	168	222	260	174	247	301	268	276	121	270	338	252	168	110	253	314	334	361	459	328		7023
July	417	548	516	218	504	384	332	559	281	268	274	365	317	540	299	411	633	565	412	509	415	599	652	459	518	208	470	458	722	872	915	14640
August	978	801	898	867	1668	1738	965	1028	1110	1553	1760	4252	2636	955	1425	510	799	1036	732	750	917	1312	814	954	1106	683	808	822	700	764	989	36330
September	1121	951	458	393	613	369	692	657	1301	645	535	492	928	1073	542	868	1043	787	871	854	957	570	920	1111	700	1237	728	1142	802	653		24013
October	530	738	411	1102	936	271	621	1865	872	997	905	864	1194	1113	1106	468	646	937	883	925	471	656	234	123	417	722	1558	435	1197	1230	1058	25485
November	790	943	806	380	660	1026	1132	334	441	576	391	375	1051	633	536	1349	995	680	672	339	341	736	466	788	494	220	623	837	734	447		19795
December	375	599	1035	1157	432	236	752	364	1160	775	1233	2188	2038	991	397	457	117	342	456	567	24	177	167	184	297	346	690	631	838	324	278	19627
																																188464
0 orbits:		0																														
>0 orbits:		366																														
>100 orbits		347																														
>500 orbits:		143																														
>1000 orbits:		38																														

TOTAL	01-02	02-03	03-04	04-05	05-06	06-07	07-08	08-09	09-10	10-11	11-12	12-13	13-14	14-15	15-16	16-17	17-18	18-19	19-20	20-21	21-22	22-23	23-24	24-25	25-26	26-27	27-28	28-29	29-30	30-31	31-01	
January	111	400	1376	315	403	306	439	358	149	213	106	56	212	239	447	314	586	630	841	866	538	135	5	69	203	238	55	244	247	127	120	10348
February	107	248	382	239	427	526	222	234	32	183	261	697	708	464	920	410	613	228	109	461	433	476	718	857	491	546	741	153	169			12055
March	114	235	208	198	159	158	280	242	194	231	357	422	302	231	267	277	333	334	167	283	380	464	345	581	354	402	347	307	422	310	428	9332
April	322	94	293	367	373	337	229	359	399	485	414	308	324	337	441	405	538	494	957	960	978	1030	521	156	297	401	225	268	101	172		12585
May	345	246	334	510	600	473	347	549	260	369	387	415	451	609	397	225	332	174	273	372	248	153	345	253	414	310	219	395	190	283	425	10903
June	334	140	160	178	224	279	85	177	272	200	251	240	282	180	279	327	268	375	241	426	418	432	346	291	450	322	334	485	532	329		8857
July	500	615	539	218	607	472	335	564	292	471	467	522	404	547	299	415	815	730	421	805	702	848	667	539	518	316	550	656	1128	1414	1087	18463
August	1299	1125	1176	1250	2128	2202	1536	1184	1563	2120	2294	4972	3049	1083	1701	717	1252	1538	755	756	1114	1472	884	1181	1163	865	845	1134	942	771	1099	45170
September	1281	988	458	399	855	759	875	744	1533	887	806	731	1346	1355	862	1111	1449	1301	1266	1299	1390	877	1041	1215	701	1237	730	1142	854	653		30145
October	686	741	475	1157	941	300	648	1882	1019	1212	1066	915	1594	1119	1127	539	783	988	979	925	845	1117	413	124	560	936	1613	548	1197	1274	1067	28790
November	790	1307	1261	822	930	1596	1503	549	610	586	406	986	1076	783	798	1353	1067	813	903	522	343	933	559	946	611	267	691	888	890	447		25236
December	375	599	1037	1376	590	237	805	403	1206	1015	1234	2262	2048	991	569	458	544	837	515	812	24	177	183	421	342	346	782	648	859	324	301	22320
																																234204
0 orbits:		0																														
>0 orbits:		366																														
>100 orbits		358																														
>500 orbits:		177																														
>1000 orbits:		69																														

Figure 6 – Day-by-day tally of the cumulated number of orbits per day collected by CAMS-BeNeLux. Top: the overview up to 31 December 2019, bottom: the situation on 31 December 2020.

with 4252 orbits for the Perseid maximum night. September proves to be a most rewarding meteor month although no major shower is active during this month. The 1882 orbits for 08–09 October were mainly due to the Draconid outburst in 2018. Past 9 years no really favorable circumstances occurred during the rich Orionid activity in October. Sooner or later our network should be lucky with this one! Of course, the Geminids provided large numbers of orbits, but a clear night for the Geminid maximum would change the numbers by a lot. From this overview it is very obvious how rich the meteor activity is in the second half of the year compared to the first half of the year.

4 Should we use more RMS cameras?

In 2019 the first RMS cameras were used to provide extra coverage to the CAMS BeNeLux network. Looking in *Table 3* we see that the top 5 of best performing cameras are all 5 RMS cameras. The main reason is the larger FoV combined with a very good resolution:

- RMS 36mm 47 × 88°, 3.9 arcmin/pix;
- RMS 6mm 30 × 54°, 2.5 arcmin/pix;
- RMS 8mm 22 × 41°, 1.9 arcmin/pix;
- Watec 12mm 22 × 30°, 2.6 arcmin/pix (PAL);
- Watec 12mm 22 × 30°, 2.8 arcmin/pix (NTSC).

The RMS with 8mm lens comes closest to the classic CAMS configuration with the 1.2/12mm lens. The small FoV proves ideal in light polluted areas. For darker areas the RMS 6mm is the best compromise with significant larger FoV and comparable in resolution to the CAMS standard optics. The RMS 36mm can be used only at very dark skies but is less accurate for the many short meteor trails registered and therefore not recommended to be used within the CAMS network. The RMS doesn't need AutoCAMS and functions 7 nights on 7, apart from some occasional technical issues. Financially the RMS is absolute more attractive, bought plug&play, 450 euro for the camera + Rpi computer against 600 euro for a Watec with optics without the required CAMS PC.

The most important advantage of the RMS is its calibration system. The classic CAMS system uses a single calibration for the entire night while the RMS system recalibrates for each single detection. The resolution of 2 to 4 arcmin/px isn't the only parameter to look at. During the night the plate center of a CAMS camera, if it is well fixed, wanders around the reference and may deviate 10, 12 or more arcminutes just because of the expansion, contraction of the camera support (arm, wall, mount, …) due to variations in temperature. The classic CAMS approach ignores this completely but the RMS system recalibrates for each individual detection. This is an absolute superior approach compared to the use of a single calibration for a whole night.

Table 3 – Selection of 20 cameras with the highest scores in orbits during the year 2020.

Camera	Total orbits	Nights active	Nights with orbits
003814 RMS Grapfontaine (B)	7430	361	239
000378 RMS Kattendijke (Nl)	4613	253	196
003815 RMS Genk (B)	4191	360	225
003830 RMS Mechelen (B)	3509	354	229
003800 RMS Langenfeld (D)	3078	295	200
000384 Watec Mechelen (B)	2793	366	261
000399 Watec Mechelen (B)	2633	365	257
000816 Watec Humain (B)	2607	354	231
003831 RMS Mechelen (B)	2559	361	230
003005 Watec Gronau (D)	2418	214	166
003003 Watec Gronau (D)	2404	207	159
000394 Watec Dourbes (B)	2381	366	238
000388 Watec Mechelen (B)	2330	366	242
000395 Watec Dourbes (B)	2305	366	238
003891 Watec Mechelen (B)	2276	343	227
000353 Watec Ermelo (Nl)	2271	193	169
003004 Watec Gronau (D)	2256	216	166
000814 Watec Grapfontaine (B)	2244	363	216
000379 Watec Wilderen (B)	2211	366	233
003035 Watec Oostkapelle (Nl)	2140	216	203

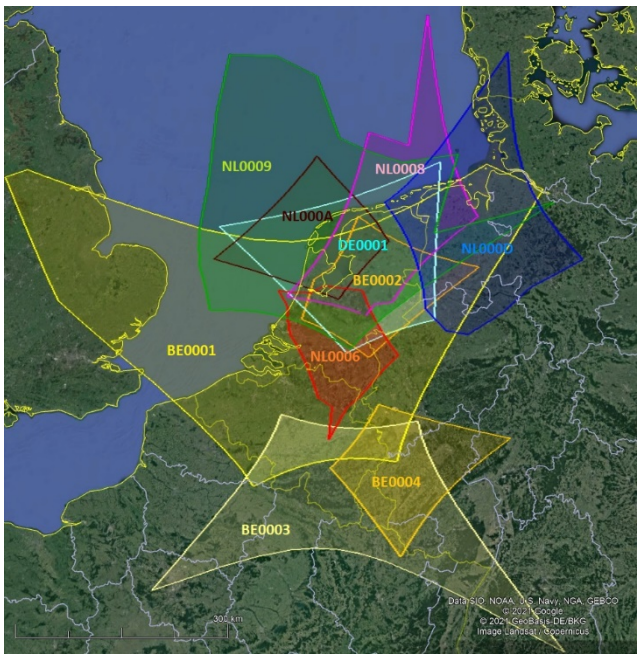

Figure 7 – Fields of View (FoV) of the RMS cameras that contributed to the CAMS BeNeLux network in 2020.

The Watec cameras are old technology, the required framegrabbers become expensive and difficult to purchase. The many Watec cameras used in CAMS BeNeLux are definitely not yet to be replaced, but it would be wise to rather buy RMS cameras for any future extensions. With the budget required for two CAMS configured Watecs, three RMS cameras can be bought as plug & play or the components to build 6 homemade RMS cameras can be ordered for anyone handy. Another advantage is that the RMS uploads its data to the Global Meteor Network where the multi-station results are publicly shared while the CAMS data remains under embargo unavailable to anyone.

5 CAMS BeNeLux in the world

CAMS is a global project in which different networks around the world participate all using the same CAMS software.

Altogether the CAMS networks collected about 418000 orbits in 2020 (against 364000 in 2019), the largest number of orbits in a single year and about as many orbits what CAMS collected from its start in October 2010 until end 2016. The different CAMS networks had the following numbers of orbits (raw data):

- CAMS Arkansas 14389 (13630 in 2019);
- CAMS Australia 31240 (37837 in 2019, 7 months);
- CAMS BeNeLux 45743 (42749 in 2019);
- CAMS California 42281 (69924 in 2019);
- CAMS Chile 66556 (51700 in 2019);
- EXOSS Brazil 399 (342 in 2019);
- CAMS Florida 30303 (24944 in 2019);
- LOCAMS Arizona 44858 (49748 in 2019);
- CAMS Namibia 98581 (18875 in 2019, 4 months);
- CAMS New Zealand 21561 (23806 in 2019);
- CAMS Northern California 5413 (4582 in 2019);
- CAMS South Africa 13006 (9640 in 2019, 6 months);
- UAZ-CN 24003 (16085 in 2019);
- CAMS MA 992 (0 in 2019);
- CAMS Texas 960 (new network);
- Total 2020 ~418000 orbits (~364000 in 2019);

CAMS BeNeLux contributed almost 11% of the total score for 2020. Since the start of the CAMS project more than 1500000 video meteor orbits have been collected of which 234204 orbits by CAMS BeNeLux. This is currently the largest collection of optical orbits worldwide and the project is expected to be continued for more years to come.

Acknowledgment

Many thanks to all participants in the CAMS BeNeLux network for their dedicated efforts. Thanks to *Martin Breukers* and *Carl Johannink* for collecting the data, computing the trajectories and orbits and transferring the CAMS BeNeLux data to the CAMS headquarters. These statistics are based on the data published on the CAMS website[24]. In 2020, the CAMS BeNeLux team was operated by the following volunteers:

Hans Betlem (Leiden, Netherlands, CAMS 371, 372 and 373), *Felix Bettonvil* (Utrecht, Netherlands, CAMS 376 and

[24] http://cams.seti.org/FDL/index-BeNeLux.html

377), *Jean-Marie Biets* (Wilderen, Belgium, CAMS 379, 380, 381 and 382), *Martin Breukers* (Hengelo, Netherlands, CAMS 320, 321, 322, 323, 324, 325, 326, 327, RMS 328 and 329), *Guiseppe Canonaco* (Genk, Belgium, RMS 3815), *Bart Dessoy* (Zoersel, Belgium, CAMS 397, 398, 804, 805, 806 and 888), *Tammo Jan Dijkema* (Dwingeloo, Netherlands, RMS 3198), *Jean-Paul Dumoulin, Dominique Guiot and Christian Wanlin* (Grapfontaine, Belgium, CAMS 814 and 815, RMS 003814), *Uwe Glässner* (Langenfeld, Germany, RMS 3800), *Luc Gobin* (Mechelen, Belgium, CAMS 3890, 3891, 3892 and 3893), *Tioga Gulon* (Nancy, France, CAMS 3900 and 3901), *Robert Haas* (Alphen aan de Rijn, Netherlands, CAMS 3160, 3161, 3162, 3163, 3164, 3165, 3166 and 3167), *Robert Haas / Edwin van Dijk* (Burlage, Germany, CAMS 801, 802, 821 and 822) , *Robert Haas* (Texel, Netherlands, CAMS 810, 811, 812 and 813), *Klaas Jobse* (Oostkapelle, Netherlands, CAMS 3030, 3031, 3032, 3033, 3034, 3035, 3036 and 3037), *Carl Johannink* (Gronau, Germany, CAMS 311, 312, 314, 317, 318, 3000, 3001, 3002, 3003, 3004 and 3005), *Hervé Lamy* (Ukkel, Belgium, CAMS 393), *Hervé Lamy* (Dourbes, Belgium, CAMS 394 and 395), *Hervé Lamy* (Humain, Belgium, CAMS 816), *Koen Miskotte* (Ermelo, Netherlands, CAMS 351, 352, 353 and 354), *Jos Nijland* (Terschelling, Netherlands, CAMS 841 and 842), *Tim Polfliet* (Gent, Belgium, CAMS 396), *Steve Rau* (Zillebeke, Belgium, CAMS 3850 and 3852), *Adriana en Paul Roggemans* (Mechelen, Belgium, CAMS 383, 384, 388, 389, 399 and 809, RMS 003830 and 003831), *Hans Schremmer* (Niederkruechten, Germany, CAMS 803) and *Erwin van Ballegoij* (Heesch, Netherlands, CAMS 347 and 348).

References

Jenniskens P. (2015). “New Chi Cygnids meteor shower”. CBET 4144. IAU Central Bureau for Astronomical Telegrams. D. W. E. Green (ed.), 1pp.

Jenniskens P. (2020). “Possible upcoming return of the chi Cygnids in September 2020”. *eMetN*, **5**, 287–289.

Koukal J., Srba J., Toth J. (2016). “Confirmation of the chi Cygnids (CCY, IAU#757)”. *WGN, Journal of the IMO*, **44**, 5–9.

Roggemans P., Johannink C., Breukers M. (2016). “Status of the CAMS-BeNeLux network”. In: Roggemans, A.; Roggemans, P., editors, Proceedings of the International Meteor Conference, Egmond, the Netherlands, 2-5 June 2016. IMO, pages 254–260.

Roggemans P., Johannink C., Sekiguchi T. (2020a). “Phi Serpentids (PSR#839) activity enhancement”. *eMetN*, **5**, 178–185.

Roggemans P., Johannink C., Sekiguchi T. (2020b). “h Virginids (HVI#343) activity enhancement in 2020”. *eMetN*, **5**, 233–244.

January 2021 report CAMS BeNeLux

Paul Roggemans

Pijnboomstraat 25, 2800 Mechelen, Belgium
paul.roggemans@gmail.com

A summary of the activity of the CAMS BeNeLux network during the month of January 2021 is presented. January 2021 was a typical winter month with mostly unfavorable weather circumstances. 2725 multi-station meteors were recorded, good for 991 orbits. January 2021 was the poorest month of January since 2015 in spite of a record number of cameras available.

1 Introduction

January tends to be one of the worst months for astronomy in the BeNeLux with mostly overcast sky. During the 8 past years the CAMS BeNeLux network did not have any single month of January with favorable weather circumstances. It looks like January is the most difficult month for the weather circumstances, a pity as the nights are very long for the BeNeLux area while the meteor activity is still at a fairly good level. Would 2021 bring us finally better luck for January?

2 January 2021 statistics

The new year 2021 started like 2020 ended, with cloudy sky and little or no chance to do astronomical observations. The best we got were nights with some clear spans. As many as 9 nights ended without any single orbit. Also, the Quadrantid maximum night was completely missed this year.

CAMS BeNeLux captured only 2725 multi-station meteors (6045 in 2020, 5124 in 2019), good for 991 orbits (2075 in 2020, 1857 in 2019), the worst month of January since 2015. Only three nights had more than 100 orbits, the best night 8–9 January had 188 orbits. In 2020 the Quadrantid night 3–4 January alone had as many as 660 orbits.

At best 92 operational cameras were active during some nights in January 2021 (83 in 2020). On average 73.7 cameras were capturing per night. Thanks to AutoCAMS and the meanwhile significant number of RMS cameras, the surveillance of the BeNeLux sky was guaranteed with a minimum of 64 active cameras on all nights, same number as last year. On 22 nights orbits have been collected. The long winter nights may often start with an overcast sky looking hopeless to get anything like clear sky, but nights with up to 14 hours of dark sky often prove to have time spans with unpredicted clear sky. Casual observers often remain unaware of such clear periods while the AutoCAMS and RMS users get happily surprised when confirming unexpected meteors. A substantial part of the January 2021 orbits comes from this permanent alertness provided by AutoCAMS and RMS.

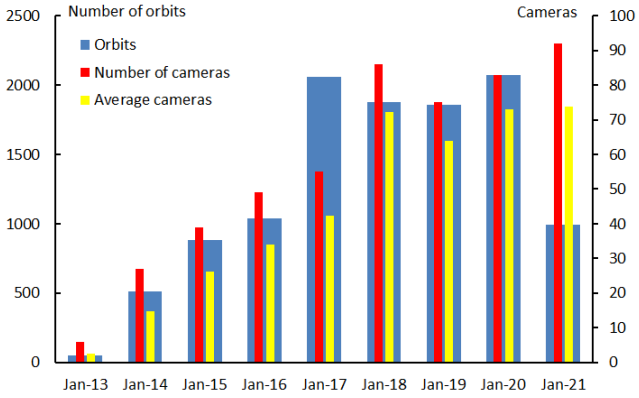

Figure 1 – Comparing January 2021 to previous months of January in the CAMS BeNeLux history. The blue bars represent the number of orbits, the red bars the maximum number of cameras running in a single night and the yellow bars the average number of cameras running per night.

Table 1 – January 2021 compared to previous months of January.

Year	Nights	Orbits	Stations	Max. Cams	Min. Cams	Avg. Cams
2013	7	49	6	6	-	2.6
2014	21	514	11	27	-	14.8
2015	22	880	14	39	-	26.1
2016	25	1037	15	49	10	34.0
2017	23	2058	18	55	18	42.3
2018	25	1878	22	86	53	72.0
2019	22	1857	20	75	54	64.0
2020	23	2075	21	83	64	72.9
2021	22	991	26	92	64	73.7
Tot.	190	11339				

Figure 1 and *Table 1* show the evolution compared to the previous months of January. Remarkable many cameras in the northern part of the BeNeLux network remained inactive during several nights while the southern part remained fully operational. Poor weather is the main cause for the low number of orbits, but of course with many of the cameras kept switched off several nights the chances for multi-station events for the remaining active cameras get much reduced.

3 Conclusion

The team members spent a lot of efforts to get some results out of mostly cloudy nights. Despite several extra RMS cameras compared to last year, the larger camera capacity couldn't compensate the unfavorable weather circumstances.

Acknowledgment

This report has been based on the CAMS BeNeLux data listed on the CAMS website[25]. Many thanks to all participants in the CAMS BeNeLux network for their dedicated efforts. Thanks to *Carl Johannink* for coordinating the network data. The CAMS BeNeLux team is operated by the following volunteers:

Hans Betlem (Leiden, Netherlands, CAMS 3071, 3702 and 3073), *Felix Bettonvil* (Utrecht, Netherlands, CAMS 376 and 377), *Jean-Marie Biets* (Wilderen, Belgium, CAMS 379, 380, 381 and 382), *Martin Breukers* (Hengelo, Netherlands, CAMS 320, 321, 322, 323, 324, 325, 326 and 327), *Guiseppe Canonaco* (Genk, RMS 3815), *Pierre de Ponthiere* (Lesve, Belgium, RMS 3816), *Bart Dessoy* (Zoersel, Belgium, CAMS 397, 398, 804, 805, 806), *Tammo Jan Dijkema* (Dwingeloo, Netherlands, RMS 3198, 3199), *Jean-Paul Dumoulin, Dominique Guiot and Christian Walin* (Grapfontaine, Belgium, CAMS 814 and 815, RMS 003814), *Uwe Glässner* (Langenfeld, Germany, RMS 3800), *Luc Gobin* (Mechelen, Belgium, CAMS 3890, 3891, 3892 and 3893), *Tioga Gulon* (Nancy, France, CAMS 3900 and 3901), *Robert Haas* (Alphen aan de Rijn, Netherlands, CAMS 3160, 3161, 3162, 3163, 3164, 3165, 3166 and 3167), *Robert Haas* (Texel, Netherlands, CAMS 810, 811, 812 and 813), *Robert Haas / Edwin van Dijk* (Burlage, Germany, CAMS 801, 802, 821 and 822), *Kees Habraken* (Kattendijke, Netherlands, RMS 000378), *Klaas Jobse* (Oostkapelle, Netherlands, CAMS 3030, 3031, 3032, 3033, 3034, 3035, 3036 and 3037), *Carl Johannink* (Gronau, Germany, CAMS 311, 314, 317, 318, 3000, 3001, 3002, 3003, 3004 and 3005), *Hervé Lamy* (Dourbes, Belgium, CAMS 394 and 395), *Hervé Lamy* (Humain Belgium, CAMS 816), *Hervé Lamy* (Ukkel, Belgium, CAMS 393), *Koen Miskotte* (Ermelo, Netherlands, CAMS 351, 352, 353 and 354), *Tim Polfliet* (Gent, Belgium, CAMS 396), *Steve Rau* (Zillebeke, Belgium, CAMS 3850 and 3852), *Paul and Adriana Roggemans* (Mechelen, Belgium, CAMS 383, 384, 388, 389, 399 and 809, RMS 003830 and 003831), *Hans Schremmer* (Niederkruechten, Germany, CAMS 803) and *Erwin van Ballegoij* (Heesch, Netherlands, CAMS 347 and 348).

[25] http://cams.seti.org/FDL/

Automated feature extraction from Radio Meteor Spectrograms

Paul Mohan

Pine Hill Observatory, 46157 Galway, Novi, MI 48374, USA
pine_hill@illinoisalumni.org

This article examines the utility of applying image analysis methods to time-frequency spectrograms of RF meteor scatter. The constrained scatter-receiver geometry and associated Doppler behavior lends itself to efficient image processing approaches for extracting individual meteor scatter events from the raw, noise contaminated spectrogram. Classical segmentation and 'blob' analysis can be applied to derive metrics associated with event rates, Doppler 'center of mass' and proxies for scatter return energy. A baseline feature extraction approach is described and applied to sample data collected at the Pine Hill Observatory (PHO) site in SE Michigan. Preliminary results presented here are hoped to encourage collaboration to explore potential correlations between spectrogram derived metrics and other more established measures used by the meteor observation community.

1 Introduction

Time-frequency spectrograms are an established tool supporting radio meteor observation, showing the dynamic time-dependent aspects of the scatter signal's spectral structure[26]. Real-time implementations find widespread use in audio analysis and are equally useful when applied to the down converted RF baseband signal from a meteor scatter receiver. Representative discussion and application of meteor observation using spectrograms are provided by Martinez (1988), Sanderson (2000), Bourdillon et al. (2005), Mohan (2003), and Verbelen (2020) to name a few. *Figure 1* is an example of a meteor scatter spectrogram collected at PHO using illumination originating from the 55.154MHz video carrier of Canadian TV CHBX (46°35'39.84" N, 84°21'0.00" W)[27] located 465km from our receiver site. The spectrogram's horizontal axis spans 30 minutes (starting 9 January 2021; 16^h00^m UTC) and the vertical frequency axis spans 120Hz. The illumination carrier is centered on ~960Hz and vertical displacement of the scatter signals represent ± Doppler induced frequency shifts. Spectrograms typically use Fast Fourier Transforms with block lengths from 8192 to 32768 samples and sample rates from 8K to 48K samples/sec. As in all frequency domain analyses, there is a tradeoff between frequency and time resolution, with an improvement in one degrading the other. The amplitude components displayed in the spectrogram are generally scaled to logarithmic power (dB) and can be color mapped using one of several common look-up tables. Several analysis programs are available providing spectrogram tools; Spectrum Lab[28], Spectran[29] and R_Meteor[30] to name a few. It is upon these spectrogram 'images' that we investigate the application of image processing algorithms to enable extraction of scatter response metrics. Beyond event counting, we can define and quantify other metrics such as received scatter energy and Doppler 'center of mass'.

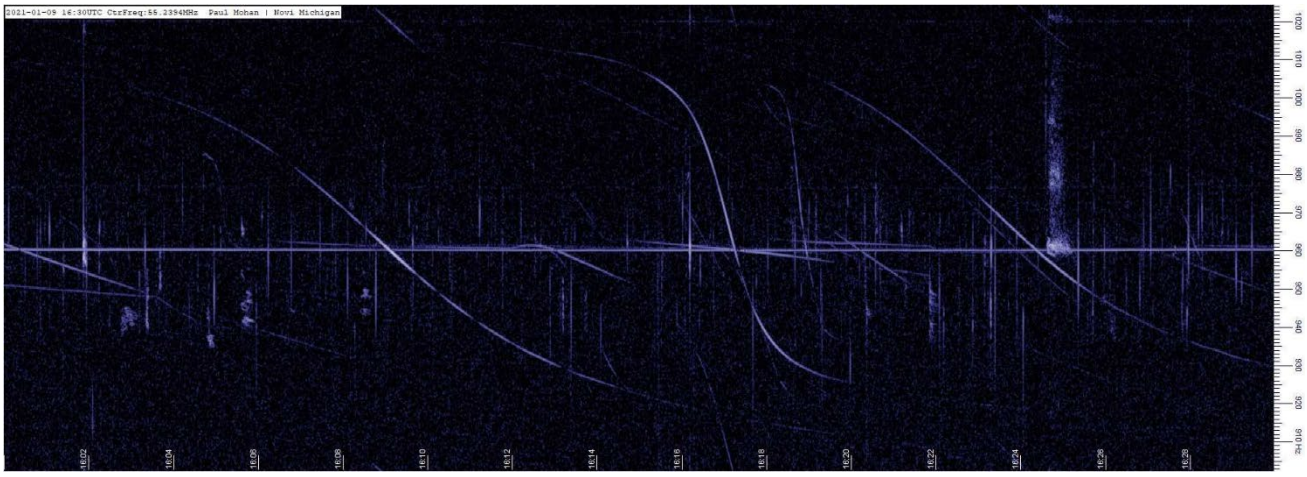

Figure 1 – Time-frequency spectrogram from a 30 minute interval of moderate meteor activity observed at PHO.

[26] https://brams.aeronomy.be/spectrograms
[27] https://fccdata.org/?lang=en&cantv=CHBX-TV
[28] http://www.qsl.net/dl4yhf/spectra1.html
[29] https://www.i2phd.org/spectran.html
[30] https://www.coaa.co.uk/r_meteor.htm

There are several ongoing efforts in the radio meteor community seeking to exploit spectrograms and automatically extract potentially new and useful information. BRAMS[31] is employing a neural network approach using training data manually extracted via crowd sourcing using spectrograms from continuous data collections by their network.

2 Approach

The functional flow of an algorithm developed at PHO for extracting meteor scatter metrics from their associated spectrograms is illustrated in *Figure 2*. Each of the algorithm steps is a standalone function generally available in image processing libraries with their foundational theory outlined in numerous texts such as Rosenfeld et al. (1976). While some of our algorithms internal parameter settings are driven by the particular collection system and signal characteristics at PHO, it is anticipated the basic structure of the algorithm is adaptable to other collection sites. Implementation of the processor was done using ImageJ[32], an open source and highly capable frame work / toolset for rapid prototyping of image analysis algorithms. *Figure 3* shows the ImageJ processing script that executes the algorithm. It processes a typical spectrogram in 1 to 2 seconds on an i5 Core PC w/ 8GB RAM. Summary descriptions of the high-level processing steps follow.

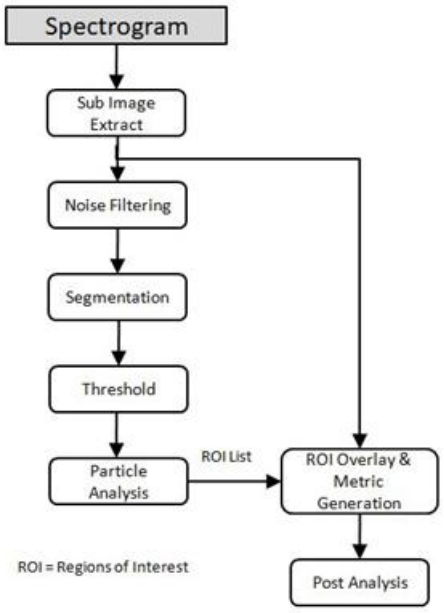

Figure 2 – Functional processing flow of PHO algorithm for automated feature extraction.

Sub-image extract

The raw spectrogram available to the processing chain generally contains other reference information not needed by the processor (e.g., axis labels, headers). Further, for the illumination source used by PHO, the transmitted video carrier contains 60 Hz frame rate harmonics which can cause vertically offset replications of strong scatter returns. The extraction of a fixed size sub-image, vertically centered on the zero-Doppler offset frequency, serves to ensure that only the desired window of the image is passed on for processing

Noise filtering

RF noise sources and reflections from aircrafts occasionally pollute the meteor scatter spectrogram. While these are visually suppressed by the human observer, they must be removed to prevent false alarms within the downstream Segmentation stage. The approach chosen here is based on grayscale morphology, with Dougherty (1992) providing an introduction to its theoretical basis. In our algorithm, we apply a vertical structuring element in what is termed an 'Opening' operation, which is erosion followed by dilation. This approach was driven by the relatively consistent structure of the Doppler signature of the desired scatter events which are strongly vertically oriented in the frequency dimension. In contrast, the Doppler signatures from aircrafts are primarily horizontally oriented and extend over much longer time (horizontal) scales. These same features also apply to other forms of radio interference that produce horizontal signatures in the spectrogram. The Opening operation retains vertically oriented connected pixel groups within the spectrogram, and eliminates the remainder. It therefore also efficiently removes the salt and pepper contributions of random background noise.

Segmentation

Following extraction of appropriate vertical segments by the filtering stage, segmentation consolidates connected regions into single objects based on criteria of 1) minimum # of connected points in region and 2) amplitude threshold for inclusion in a region. In whole, this module serves to consolidate the associated vertical segments that make up the structures of interest in the spectrogram. This is particularly necessary for time-extended over dense trail returns that occupy larger areas within the spectrogram.

Thresholding

This step is simply a conversion from a grayscale image delivered by the segmentation stage into a binary image required by the Particle Analysis module to follow.

Particle analysis

With the individual scatter regions built and isolated by segmentation, Particle Analysis then catalogs each region with a numerical identity and a bounding region descriptor that is placed into a region of interest (ROI) table. This list of regions is the key data set that defines the overlay map used in the following step.

ROI overlay & metric generation

The ROI table generated in the previous step generates a region map that is overlaid back onto the raw sub-image extracted above. *Figure 4* shows the output from this processing stage using the spectrogram of *Figure 1* as input. Registration of the extracted regions (yellow outlines) with the original scatter traces is generally quite good, with the exception of the occasional false alarm. Within each

[31] https://brams.aeronomy.be/zoo/

[32] https://imagej.nih.gov/ij/

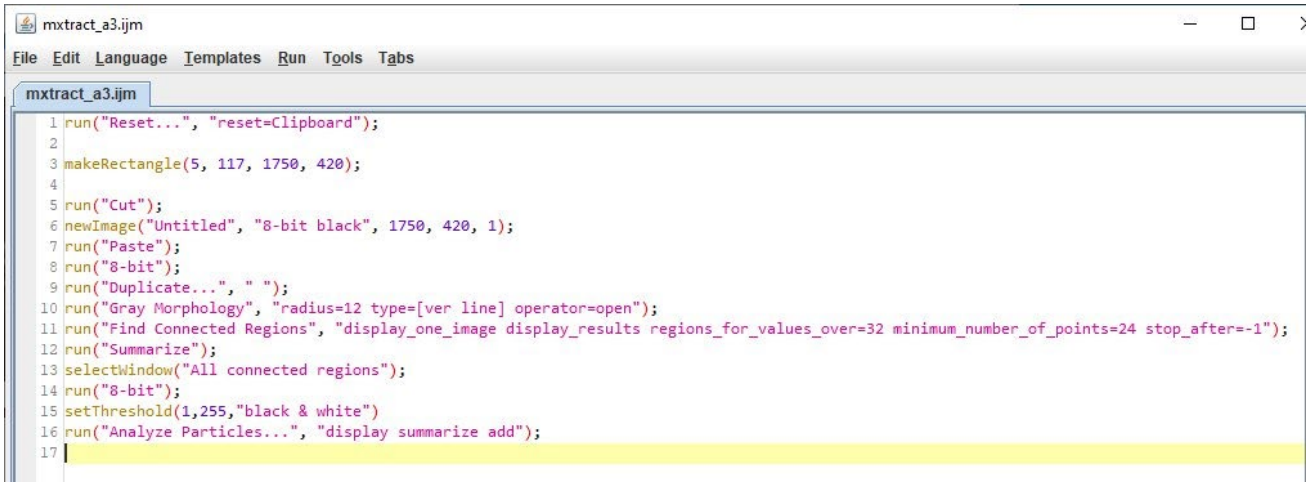

Figure 3 – Image J processing script for automated extraction of scatter events.

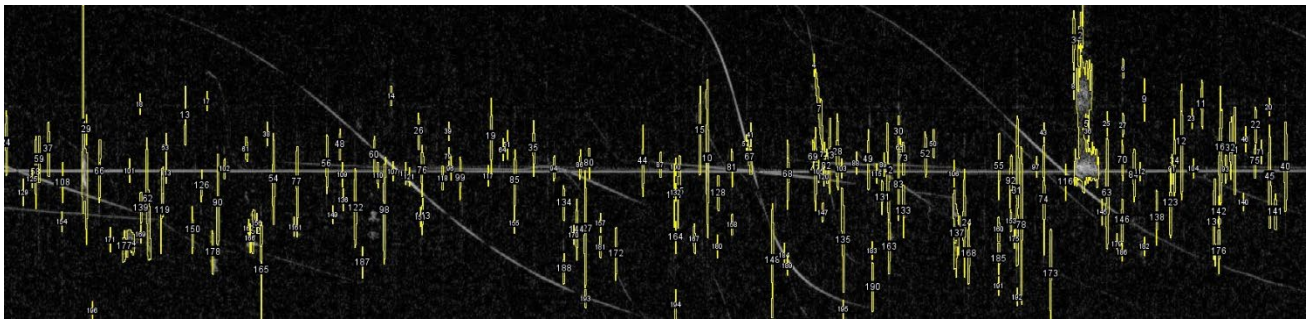

Figure 4 – Extracted and labeled scatter events overlaid onto the spectrogram of Figure 1.

Table 1 – Sample of region metrics associated with scatter events labeled in Figure 4.

Region	Area	Mean	StdDev	X	Y	XM	YM	BX	BY	Width	Height
1	1112	77.44	42.18	107.49	187.51	107.58	197.32	104	0	8	320
2	306	58.04	28.25	1446.59	43.39	1446.6	43.13	1443	0	7	82
3	180	45.98	15.66	1437.4	44.9	1437.39	43.11	1436	7	3	80
4	30	44.1	25.1	1088.5	80	1088.5	76.75	1088	65	1	30
5	2970	79.37	41.15	1452.53	167.18	1452.33	174.23	1438	67	33	184
6	50	50.6	19.66	1503.98	84.48	1503.95	82.92	1503	71	2	26
7	383	64.13	29.51	1095.51	139.08	1095.63	140.4	1090	85	10	109
8	36	43.25	10.94	1437.5	108	1437.5	106.97	1437	90	1	36
9	57	40.96	14.48	1532.5	126.5	1532.5	122.85	1532	98	1	57
10	619	80.26	41.11	944.97	200.93	945.03	204.58	943	99	4	212
11	152	53.49	27.37	1609.72	131.12	1609.85	126.75	1608	100	3	65
12	394	54.35	23.03	1582.41	186.79	1582.47	189.58	1581	105	3	155
13	105	43.56	16.96	243.25	153.81	243.32	153.76	242	108	2	79
14	52	40.19	9.93	520	121	520.06	120.77	519	108	2	26
15	214	58.85	25.17	935.05	172.38	935.03	176.88	934	108	2	119

overlaid region we can access the raw spectrogram data within it to measure specific metrics such as mean value, area, centroid, center of mass, among others. *Table 1* provides an example of metrics generated for each overlay region. Here, *X* and *Y* are the image coordinates of the region centroid, *XM*, *YM* are coordinates of the center of mass and Width, Height are the dimensions of the region bounding box.

Post analysis

Based on the ROI data extracted for each scatter event, various derivative analyses can be performed using tools like MatLab, Excel or MathCAD. Determining the appropriate interpretation and use of the data is subject to some considered thought accounting for the underlying scatter phenomenology and particular influences of the data acquisition chain. Some candidate analysis exhibits are

presented below, recognizing they are placeholders as more data is analyzed.

3 Strawman analysis exhibits

Access to data extracted for each scatter event presents several options for further analysis. Initial application of the extraction algorithm has motivated several data reduction examples described below.

Received scatter energy

A metric representative of the scattered RF energy received per event can be considered based on the following:

a) The spectrogram provides a measure of signal power (dB) mapped to 8-bits for display (e.g., 256 gray levels). The mean pixel amplitude within a given region is a proxy for power spectral density in units joules/(sec×Hz).
b) The area of a given scatter ROI (in pixels) represents the product of frequency × time (Hz×sec)
c) The product of (a) × (b) yields units of joules scaled by some constant *k*.

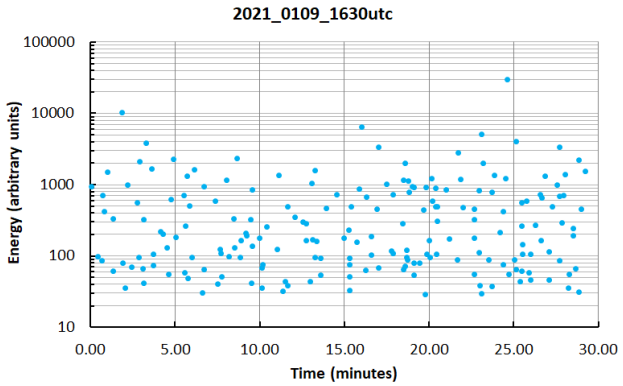

Figure 5 – Plot of received scatter energy (arbitrary units) versus time over the 30 min. interval of Figure 1.

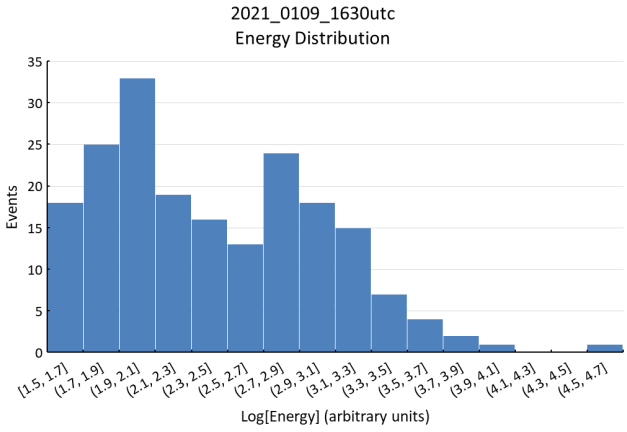

Figure 6 – Distribution of received scatter energy (arbitrary units) over the 30 minute interval of Figure 5.

Applying this approach to the events extracted from *Figure 1* yields the plot of *Figure 5* showing the proxy for returned scatter energy versus time (30-minute interval). The abrupt cutoff on the low end of the energy scale is believed due to the limiting SNR of the receiver chain as well as effects of threshold settings currently used within the processing algorithm. *Figure 6* shows the distribution of energy associated with the data of *Figure 5*. The presence of a double peak invites further investigation.

Event Doppler

The vertical displacement of the individual scatter returns in the spectrogram are a direct measure of relative motion induced Doppler shift. The zero Doppler reference line is centered on ~960 Hz and is the direct path signal (not scattered) from the illumination source. For each event region, the vertical pixel displacement (frequency offset) of its spectral 'center of mass' can be measured. *Figure 7* shows a plot of Doppler versus time for the event regions indicated in *Figure 4*. A linear regression line shows the trend of Doppler frequency over time. Note that in the collection geometry available to PHO, the meteor trail segments being detected via reflection are nearly perpendicular to the horizontal line of sight to both the transmitter and receiver, in a configuration analyzed by Richardson (1999). Therefore, the radial motion of the scatter trail with respect to transmitter and receiver is relatively low, inducing only small Doppler frequency shifts (tens of Hz).

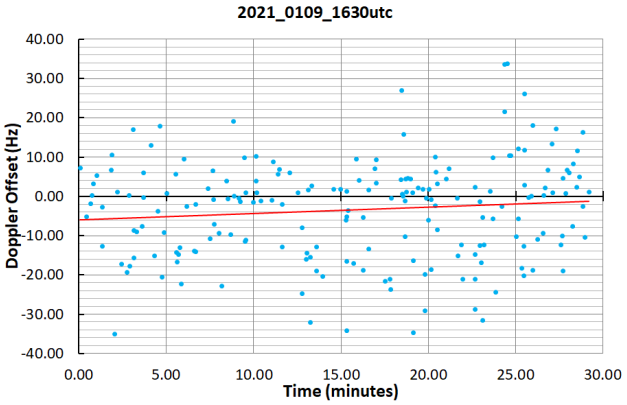

Figure 7 – Scatter event Doppler versus time.

Mean power vs. time-bandwidth product

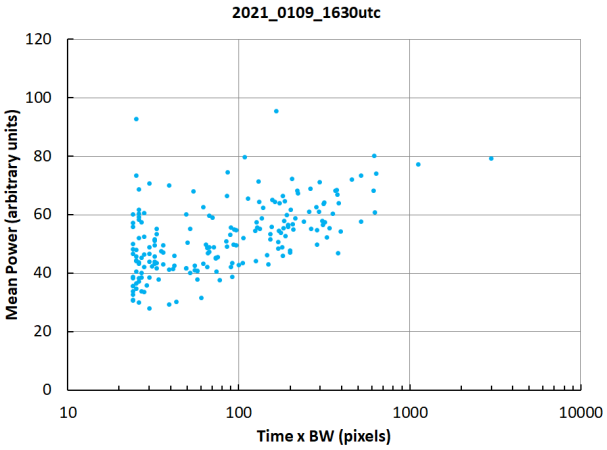

Figure 8 – Mean event power versus the time-bandwidth product (pixel area) over the 30 min. interval of Figure 1.

A scatter plot of mean event received power versus the time-bandwidth product (pixel area) is illustrated in *Figure 8*. It reveals a trend (consistent in other spectrograms

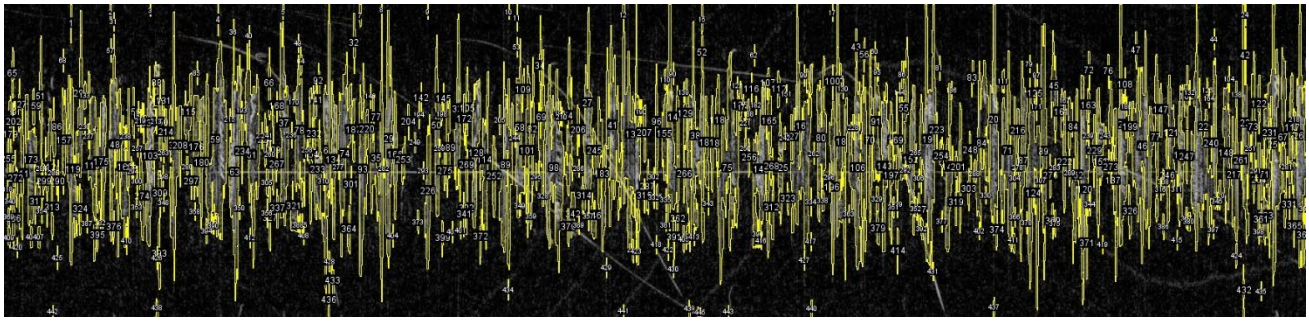

Figure 9 – Awaiting further analysis , a continum of detections from the peak of the 2021 Quadrantid meteor shower.

processed by PHO) that the larger the time-bandwidth product of an event, the greater the mean power. This would indicate that longer persisting events generally present a larger radar cross sections as well, versus a lower cross section that persists longer. The prominent clustering 'wall' observed at (time × bandwidth) values 25–28 is believed to be a lower bound imposed by the length of the structuring element used by the morphology filter (currently radius = 12 pixels), as well as the limiting frequency and time resolution currently in use. Reducing this effect is a future objective.

4 Comments and next directions

We have introduced examples of analysis templates and data extraction from event regions in meteor scatter spectrograms. A very limited set of spectrogram samples have been evaluated to date. Therefore, no general conclusions are promoted at this point. Moving forward, feedback from the broader meteor observation community would improve the value of these tools and methods. We anticipate that relationships could be drawn between the spectrogram derived metrics and those originating from other meteor analysis techniques. We further look forward to reporting results from spectrograms collected at PHO during the recent Quadrantid meteor shower. Preliminary processing shows solid detection performance despite dense populations of scatter events (~500 detections/30min during peak) as *Figure 9* illustrates. Data reduction and analysis over extended time intervals is necessary to identify trends in behavior; for example, the anticipated bi-polar Doppler profile as the shower radiant rotates across the field of view.

Algorithm Performance: Preliminary measurements of two key metrics of the event detection process, probability of detection (*Pd*) and false alarm rate (*Pfa*), yield values of *Pd* = 96%; Pfa = 5.6%. These are based on a limited set of data and clearly need to be better assessed across a larger volume of spectrograms over varying environmental conditions and meteor activity levels. This is planned to be accomplished in the coming months.

We note that it is expected that different sets of threshold parameters within the algorithm could optimize detection/false alarm rates for a given class of meteor activity (i.e., sporadic events, meteor showers). Further, it is clear that the particulars of a specific data collection site and signal chain, (i.e., effective signal gain, time/frequency resolution, display intensity mapping, to name a few) will influence selection of algorithm parameters.

It is evident that on occasion aircrafts within the field of view which passing close to nadir produce reflections with relatively high Doppler slopes. This spectrogram signature mimics the vertical structure of meteor returns and false alarms are observed. Improvements in the filtering stage are needed to minimize these effects.

References

Bourdillon A., Haldoupis C., Hanuise C., Roux Y., Menard J. (2005). "Long duration meteor echoes characterized by Doppler spectrum bifurcation". *Geophysical Research Letters*, **32**. (5), L05805 (4 p.).

Dougherty E. (1992). An Introduction to Morphological Image Processing. SPIE Optical Engineering Press.

Martinez P. (1998). "Using Doppler DSP to study HF propagation". *RadCom*, May 1998.

Mohan P. (2003). "Leonids 2002 high-resolution dynamic Doppler spectra using CW bistatic radar". 2003 Leonid MAC Workshop, Poster session.

Richardson J. (1999). "The meteor meniscus: Meteor distance versus meteor zenith angle". *Meteor Trails, Journal of the AMS*, (No. 4).

Rosenfeld A., Kak A. (1976). Digital Picture Processing. Academic Press.

Rueden C. T., Schindelin J., Hiner M. C. (2017). ImageJ2 ImageJ for the next generation of scientific image data. BMC Bioinformatics 18:529, PMID 29187165, doi:10.1186/s12859-017-1934-z (on Google Scholar).

Sanderson T. (2000). "Echoes from the Leonids". *RadCom*, March 2000.

Verbelen F. (2020). "Radio meteors August 2020". *eMetN*, **6**, 73–80.

Radio meteors February 2021

Felix Verbelen

Vereniging voor Sterrenkunde & Volkssterrenwacht MIRA, Grimbergen, Belgium
felix.verbelen@skynet.be

An overview of the radio observations during February 2021 is given.

1 Introduction

The graphs show both the daily totals (*Figure 1 and 2*) and the hourly numbers (*Figure 3 and 4*) of "all" reflections counted automatically, and of manually counted "overdense" reflections, overdense reflections longer than 10 seconds and longer than 1 minute, as observed here at Kampenhout (BE) on the frequency of our VVS-beacon (49.99 MHz) during the month of February 2021.

The hourly numbers, for echoes shorter than 1 minute, are weighted averages derived from:

$$N(h) = \frac{n(h-1)}{4} + \frac{n(h)}{2} + \frac{n(h+1)}{4}$$

Local interference and unidentified noise were quite strong at times, but no lightning activity was detected.

This month there were no eye-catching showers and overall meteor activity was low and declining over the month, but the activity of a few minor showers was clearly noticeable.

Only 5 reflections of more than 1 minute were observed here during this month.

A selection of striking or strong reflections is attached (*Figures 5, 6, 7, 8, 9, 10, 11 and 12*).

If you are interested in the actual figures, or in plots showing the observations as related to the solar longitude (J2000) rather than to the calendar date. I can send you the underlying Excel files and/or plots, please send me an e-mail.

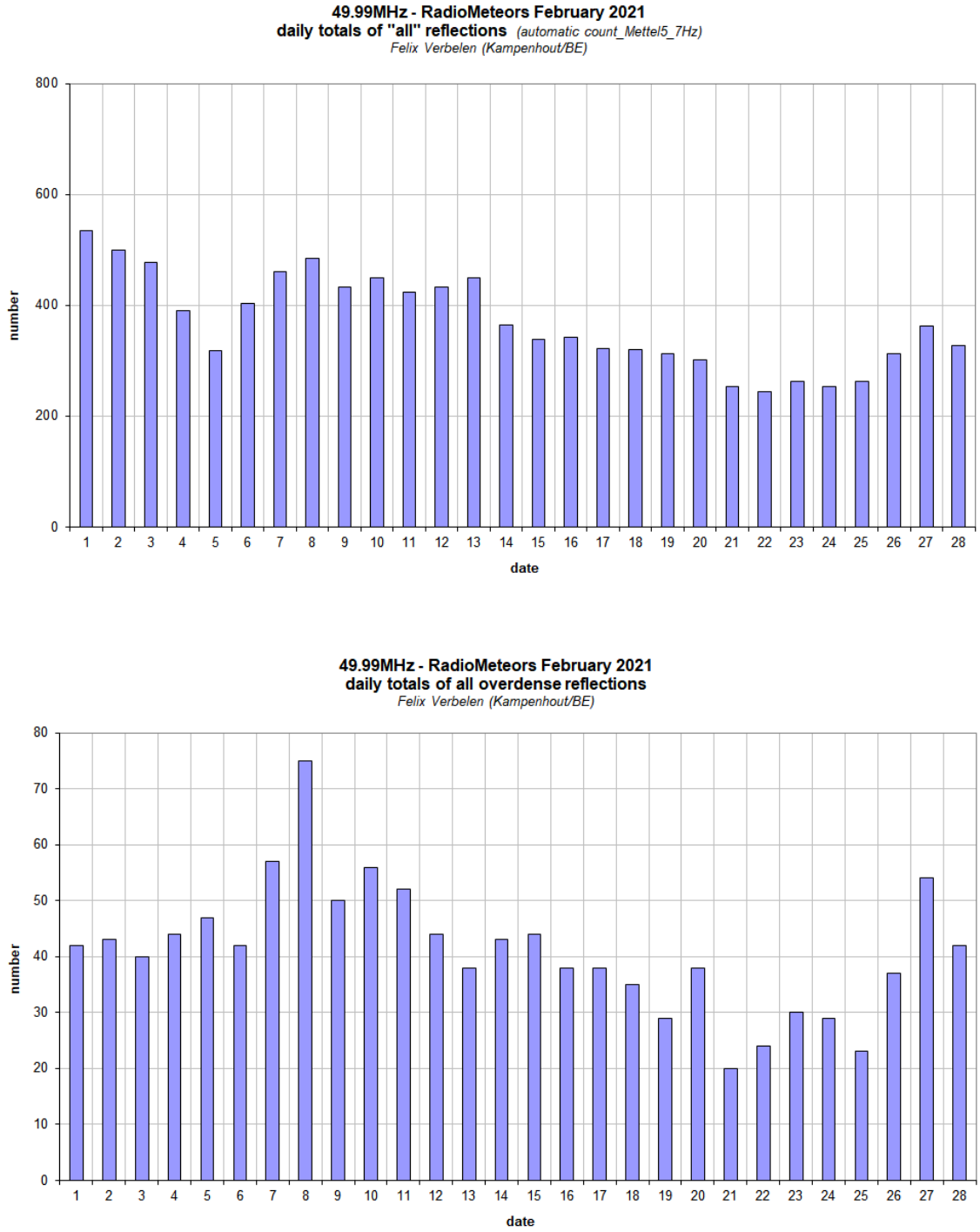

Figure 1 – The daily totals of "all" reflections counted automatically, and of manually counted "overdense" reflections, as observed here at Kampenhout (BE) on the frequency of our VVS-beacon (49.99 MHz) during February 2021.

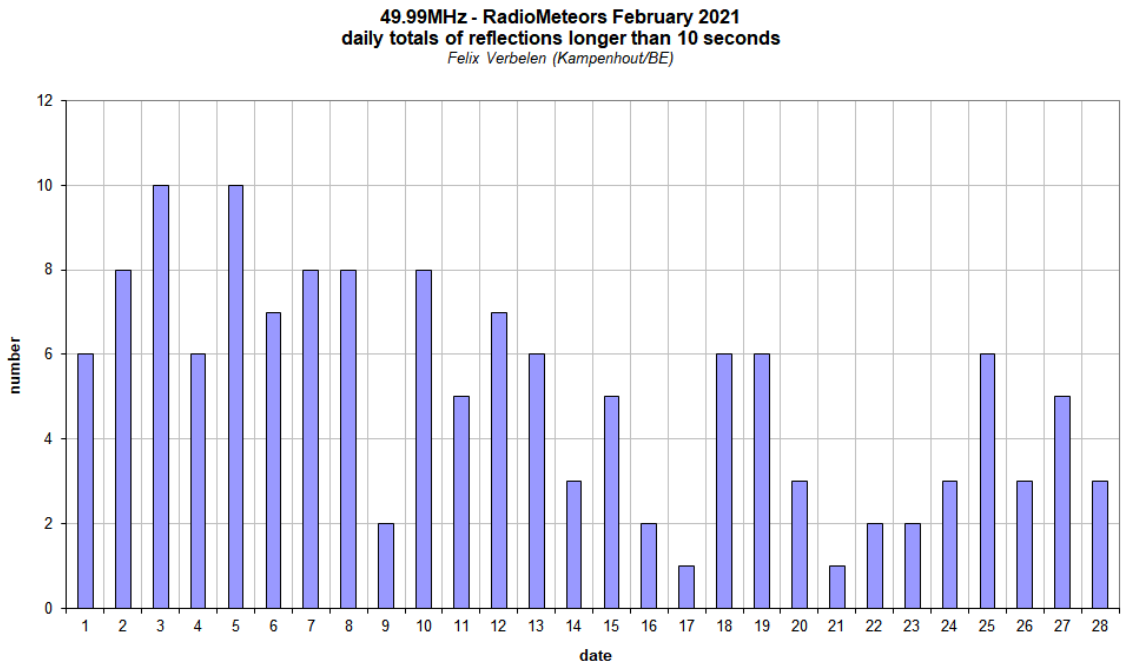

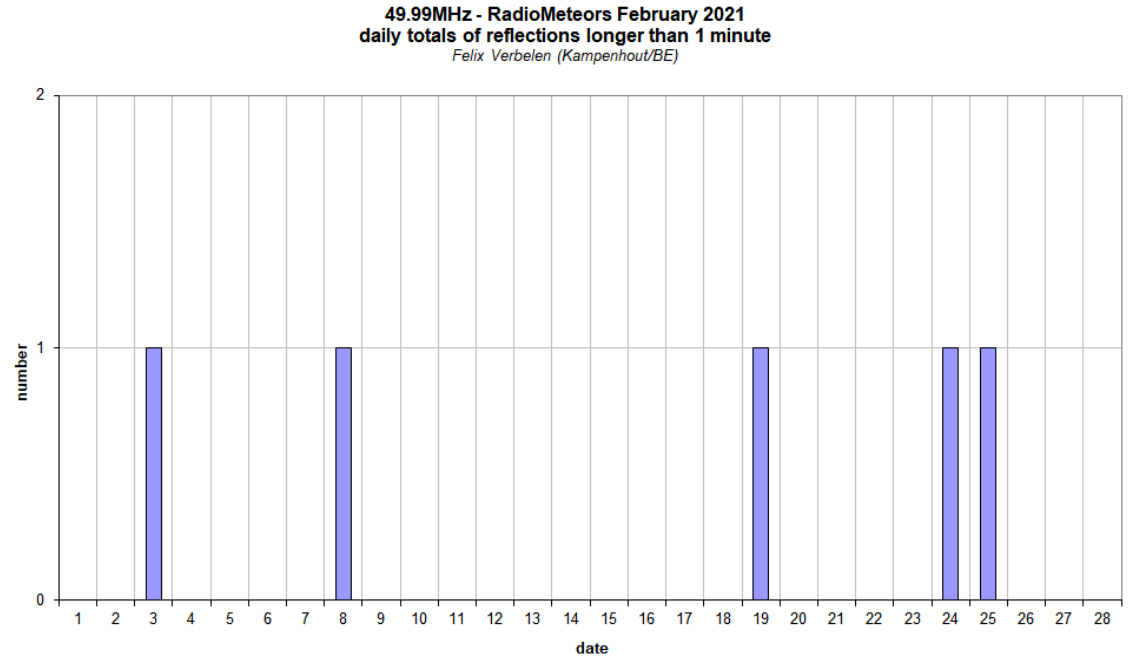

Figure 2 – The daily totals of overdense reflections longer than 10 seconds and longer than 1 minute, as observed here at Kampenhout (BE) on the frequency of our VVS-beacon (49.99 MHz) during February 2021.

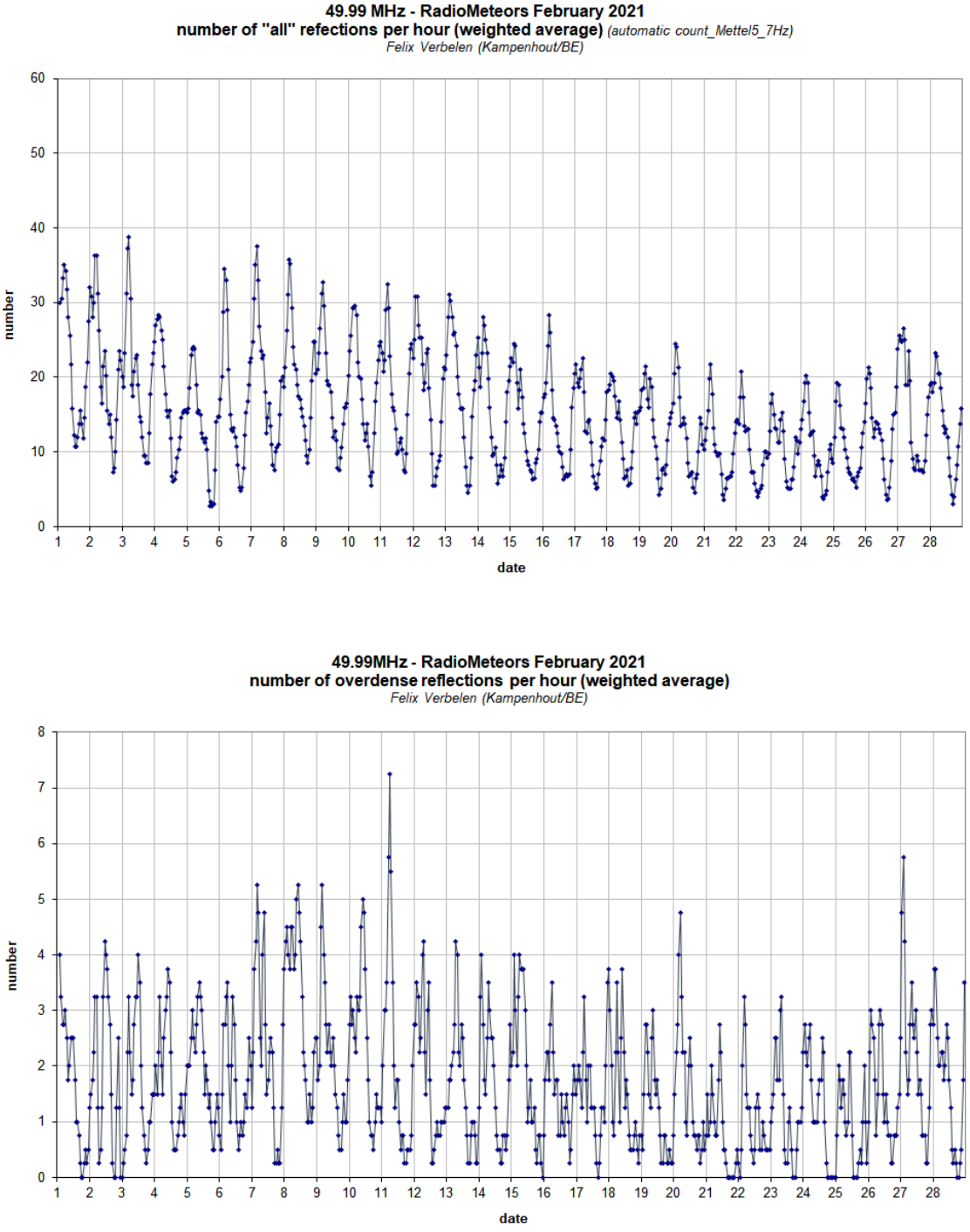

Figure 3 – The hourly numbers of "all" reflections counted automatically, and of manually counted "overdense" reflections, as observed here at Kampenhout (BE) on the frequency of our VVS-beacon (49.99 MHz) during February 2021.

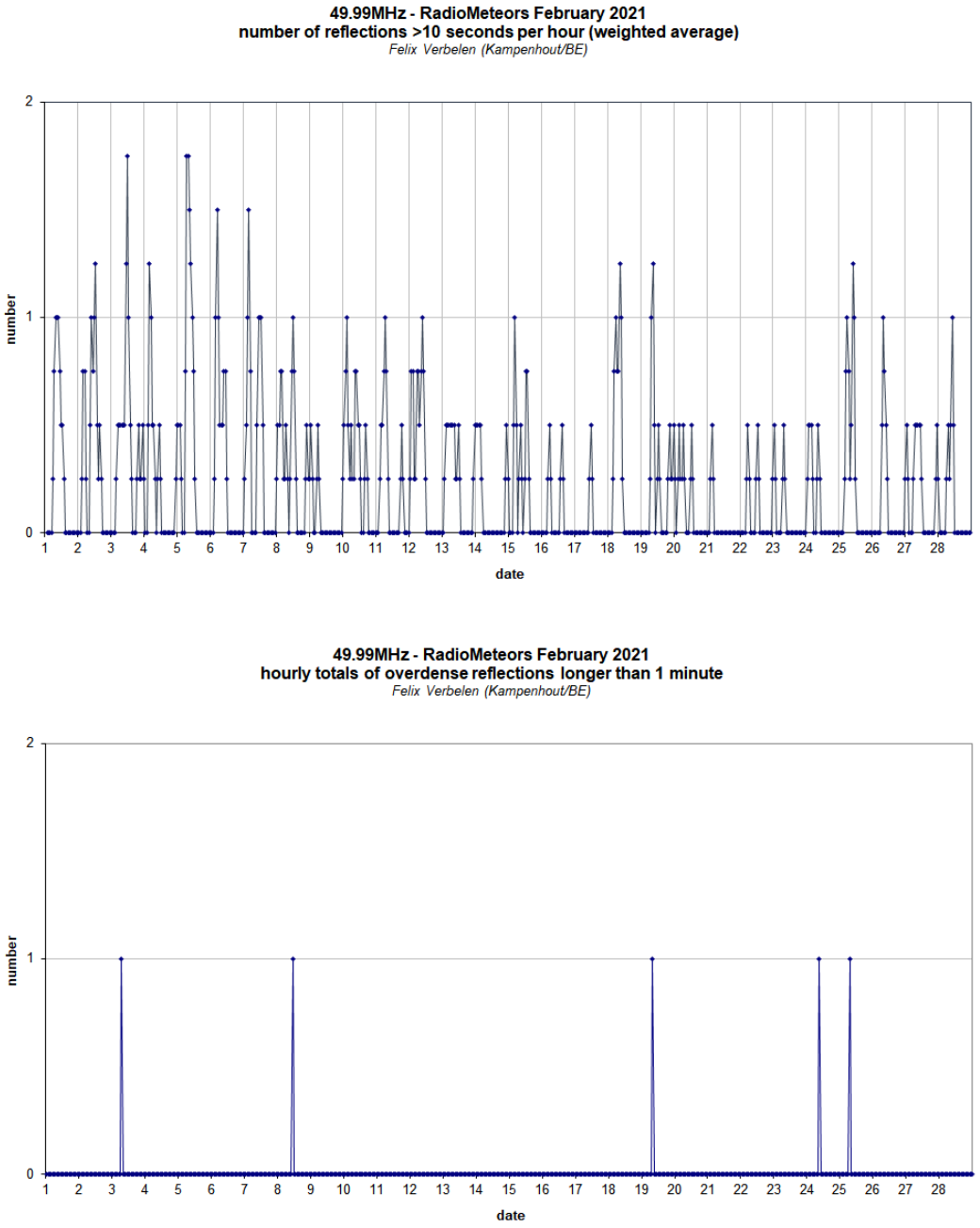

Figure 4 – The hourly numbers of overdense reflections longer than 10 seconds and longer than 1 minute, as observed here at Kampenhout (BE) on the frequency of our VVS-beacon (49.99 MHz) during February 2021.

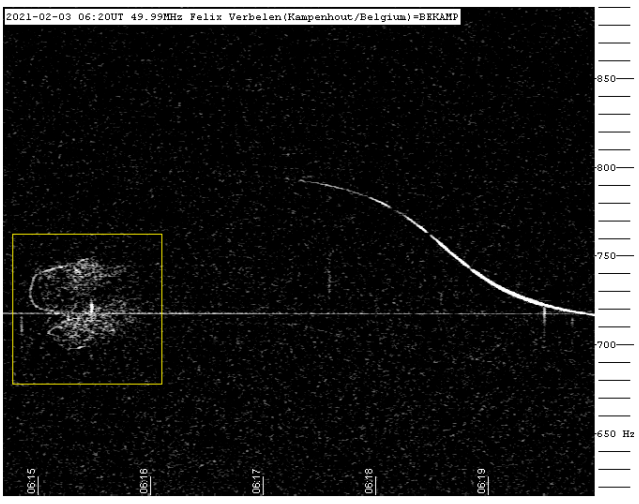

Figure 5 – Meteor reflection 03 February 2021, 06^h20^m UT.

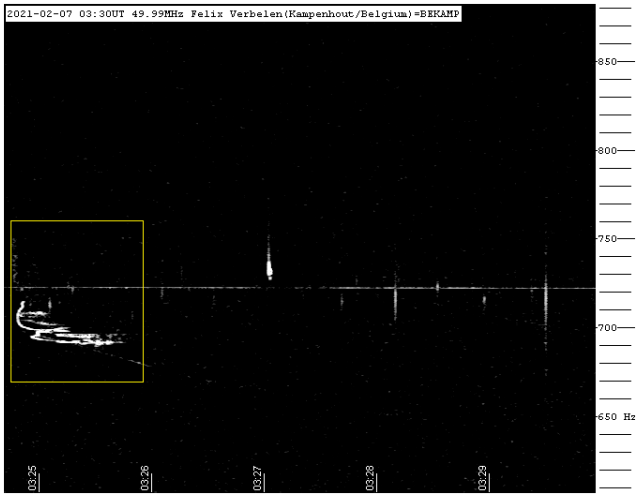

Figure 6 – Meteor reflection 07 February 2021, 03^h30^m UT.

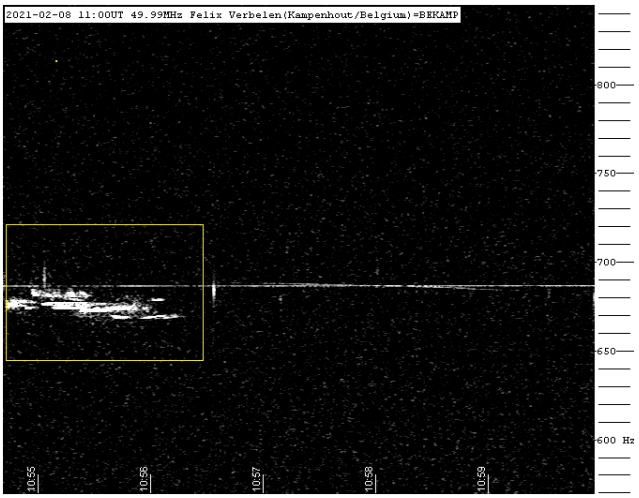

Figure 7 – Meteor reflection 08 February 2021, 11^h00^m UT.

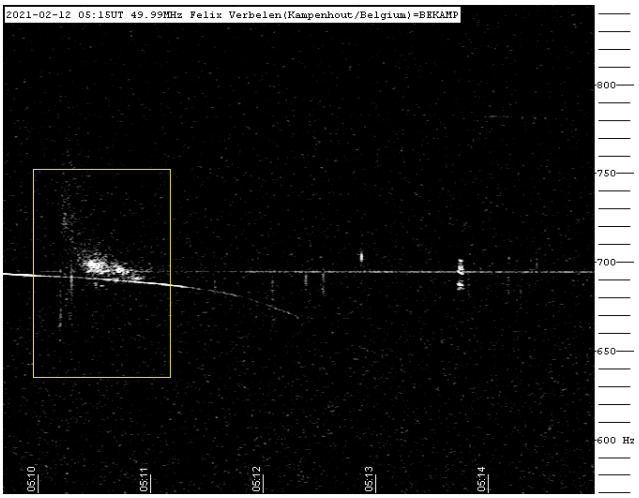

Figure 8 – Meteor reflection 12 February 2021, 05^h15^m UT.

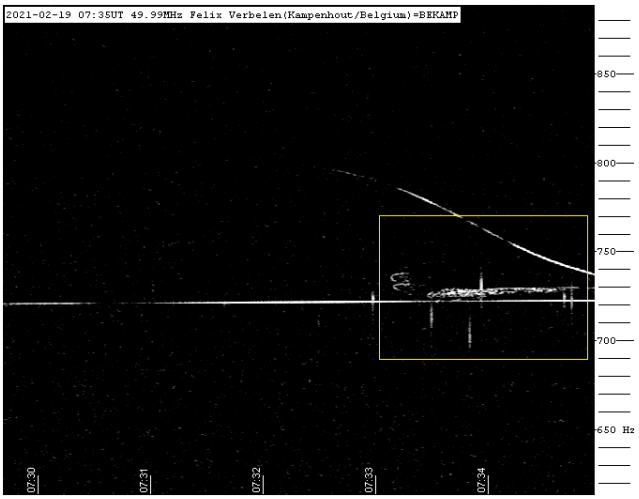

Figure 9 – Meteor reflection 19 February 2021, 07^h35^m UT.

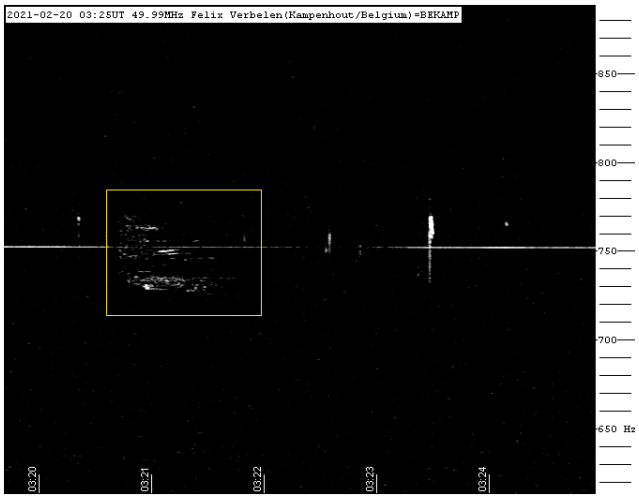

Figure 10 – Meteor reflection 20 February 2021, 03^h25^m UT.

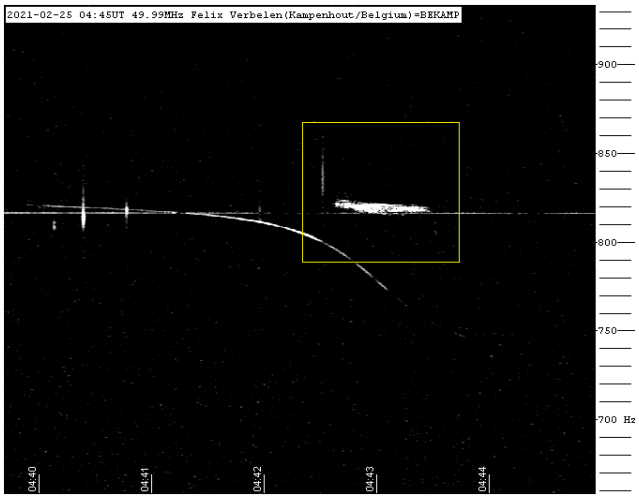

Figure 11 – Meteor reflection 25 February 2021, 04^h45^m UT.

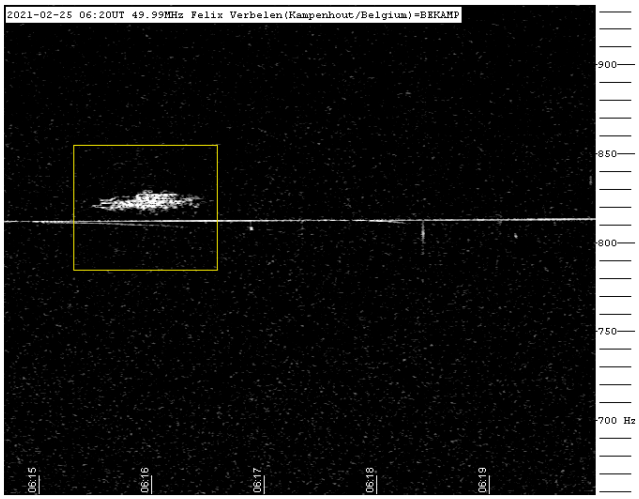

Figure 12 – Meteor reflection 25 February 2021, 06^h20^m UT.

Radio meteors March 2021

Felix Verbelen

Vereniging voor Sterrenkunde & Volkssterrenwacht MIRA, Grimbergen, Belgium
felix.verbelen@skynet.be

An overview of the radio observations during March 2021 is given.

1 Introduction

The graphs show both the daily totals (*Figure 1 and 2*) and the hourly numbers (*Figure 3 and 4*) of "all" reflections counted automatically, and of manually counted "overdense" reflections, overdense reflections longer than 10 seconds and longer than 1 minute, as observed here at Kampenhout (BE) on the frequency of our VVS-beacon (49.99 MHz) during the month of March 2021.

The hourly numbers, for echoes shorter than 1 minute, are weighted averages derived from:

$$N(h) = \frac{n(h-1)}{4} + \frac{n(h)}{2} + \frac{n(h+1)}{4}$$

Local interference and unidentified noise remained fairly low for most of the month, except for March 30th and 31st, when very strong unidentified noise often made counting of underdense and short overdense reflections impossible. As a result, data are left out for these categories of reflections from 2021 March 30, 09^h00^m till 2021 March 31, 15^h00^m UT.

Only on March 12th and 13th, moderate lightning activity was detected.

As expected, the overall shower activity remained low, with no real eye-catchers, but with some interesting minor meteor showers, as shown by the graphs of reflections longer than 10 seconds. During this month 5 reflections lasting more than 1 minute were observed. A selection of striking or strong reflections is attached. (*Figures 5 to 10*)

If you are interested in the actual figures, or in plots showing the observations as related to the solar longitude (J2000) rather than to the calendar date. I can send you the underlying Excel files and/or plots, please send me an e-mail.

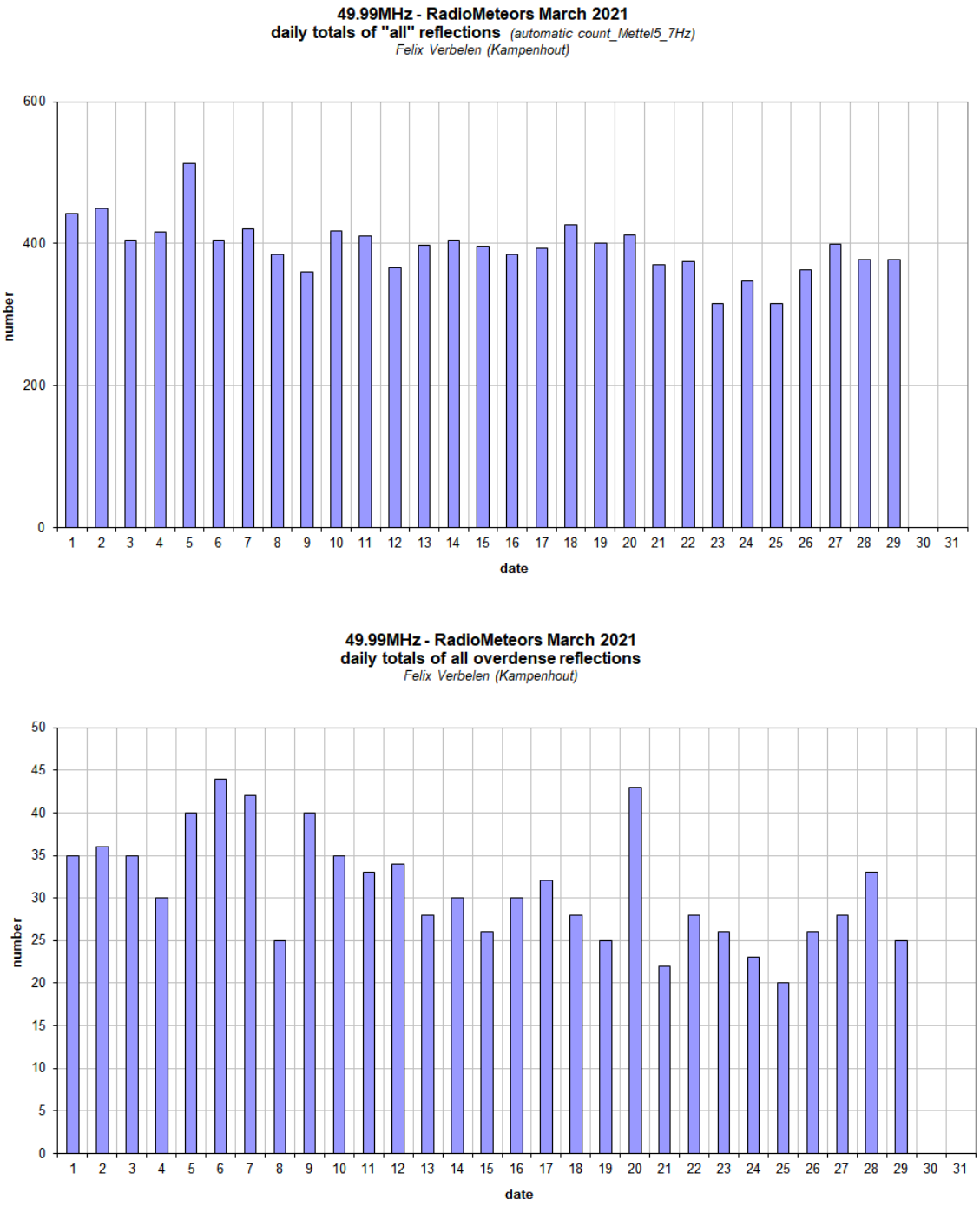

Figure 1 – The daily totals of "all" reflections counted automatically, and of manually counted "overdense" reflections, as observed here at Kampenhout (BE) on the frequency of our VVS-beacon (49.99 MHz) during March 2021.

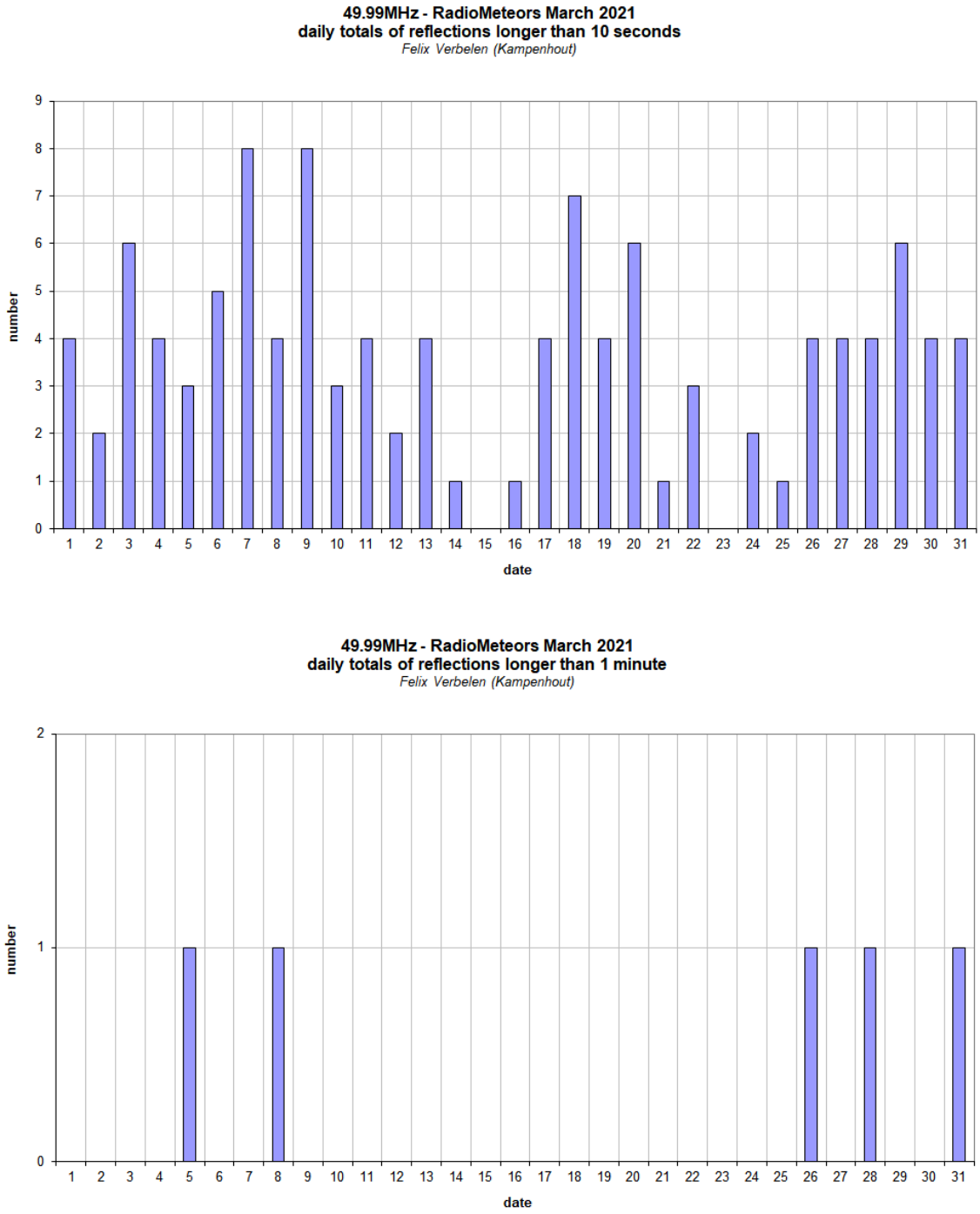

Figure 2 – The daily totals of overdense reflections longer than 10 seconds and longer than 1 minute, as observed here at Kampenhout (BE) on the frequency of our VVS-beacon (49.99 MHz) during March 2021.

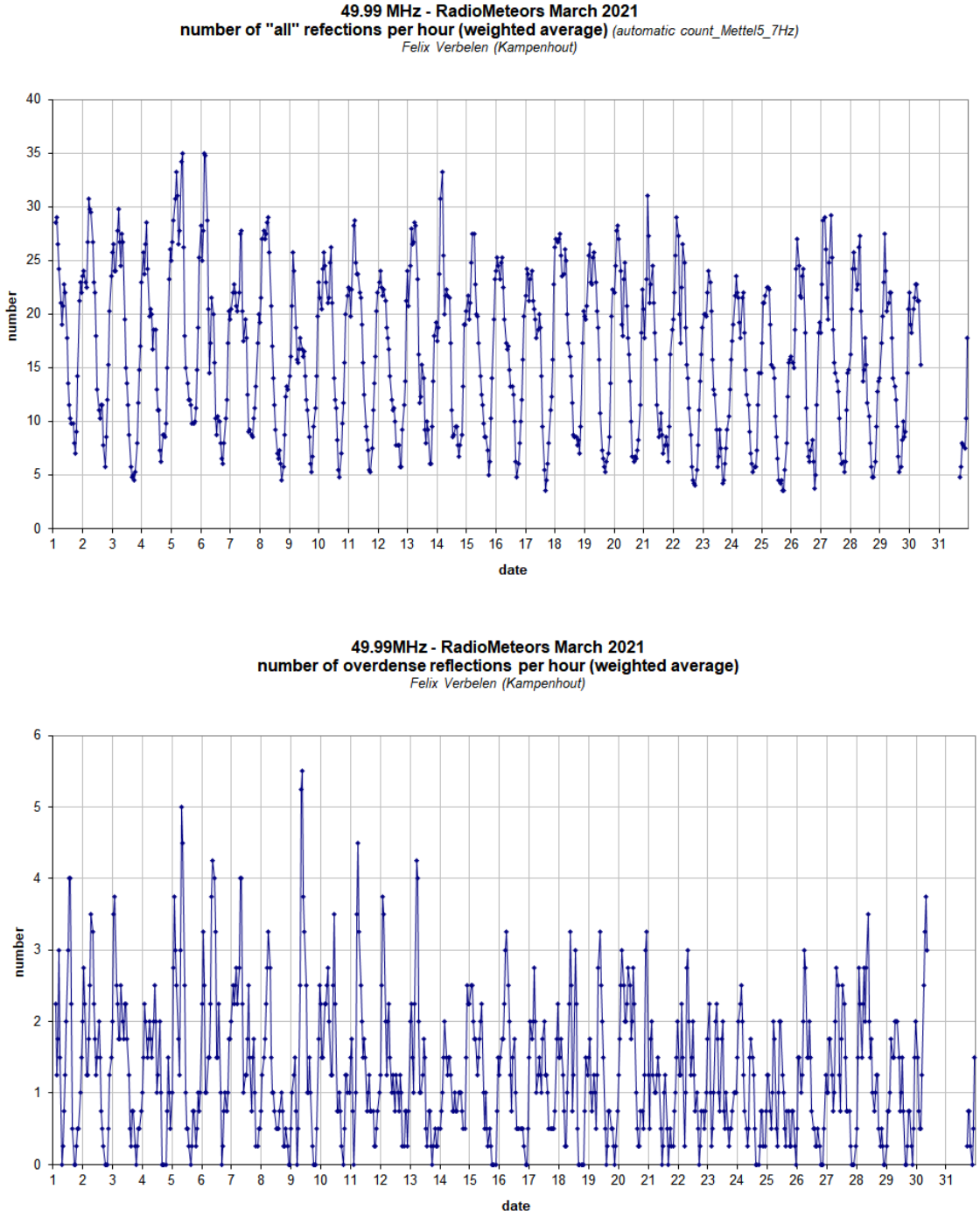

Figure 3 – The hourly numbers of "all" reflections counted automatically, and of manually counted "overdense" reflections, as observed here at Kampenhout (BE) on the frequency of our VVS-beacon (49.99 MHz) during March 2021.

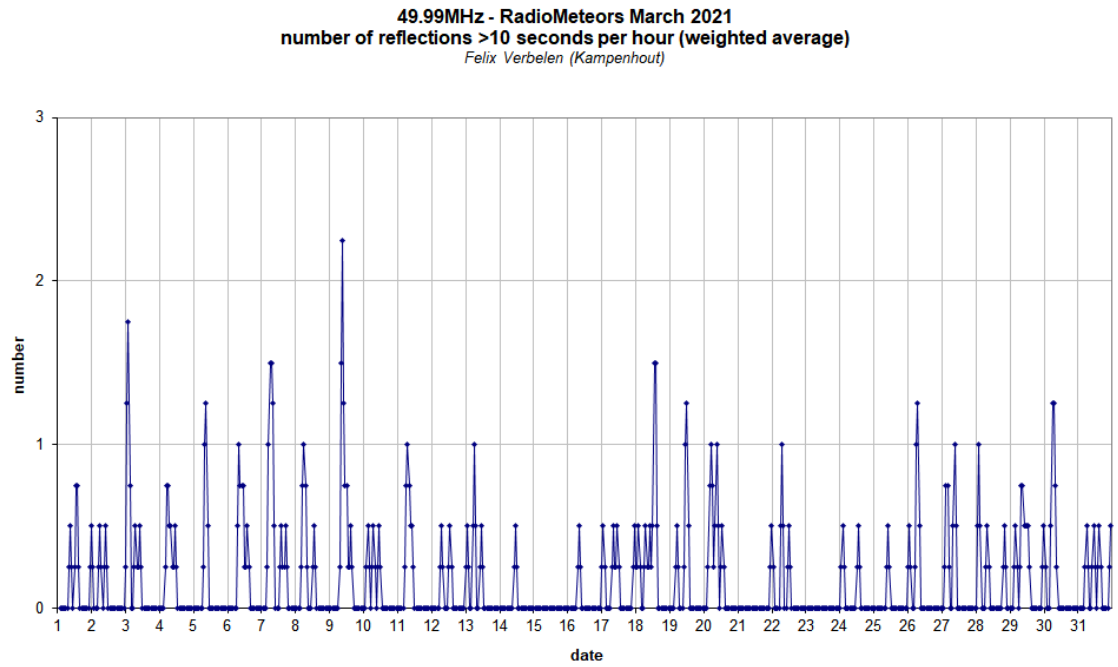

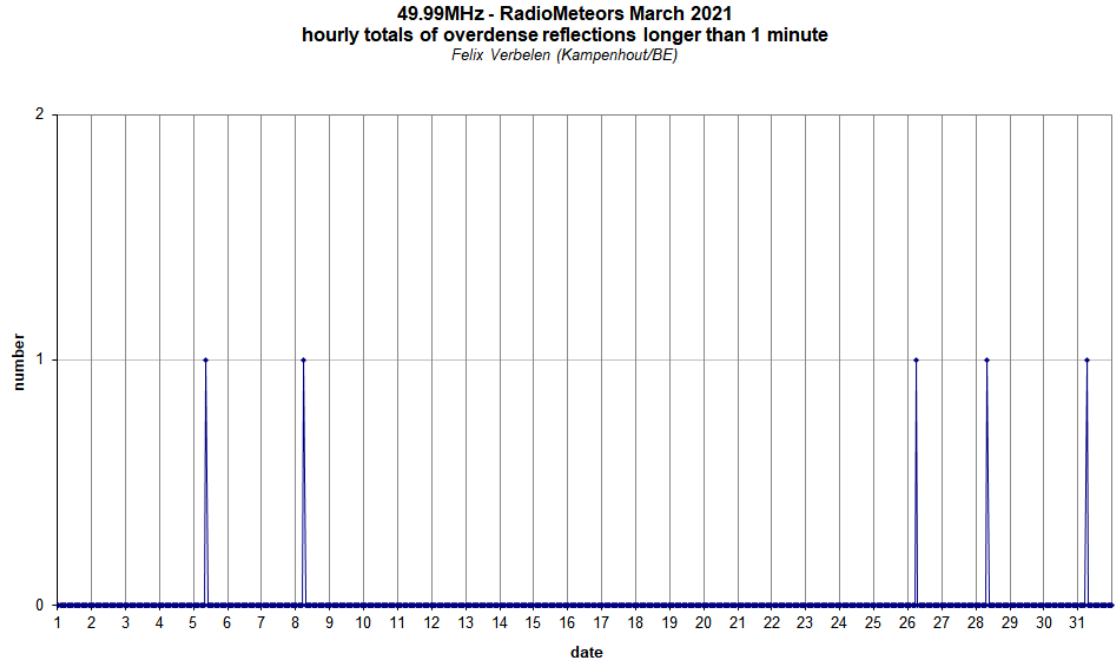

Figure 4 – The hourly numbers of overdense reflections longer than 10 seconds and longer than 1 minute, as observed here at Kampenhout (BE) on the frequency of our VVS-beacon (49.99 MHz) during March 2021.

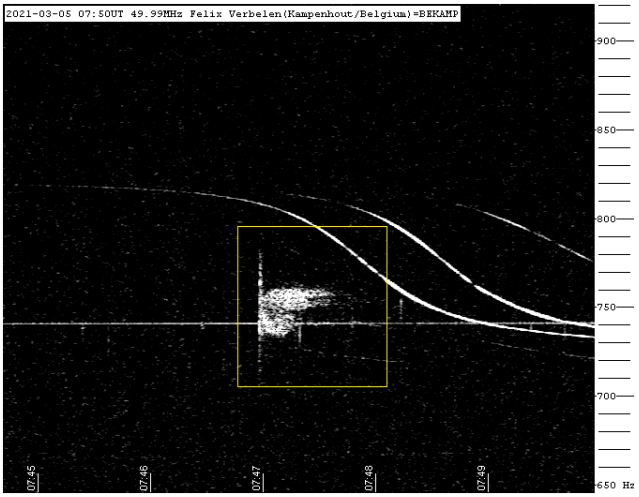

Figure 5 – Meteor reflection 5 March 2021, 07^h50^m UT.

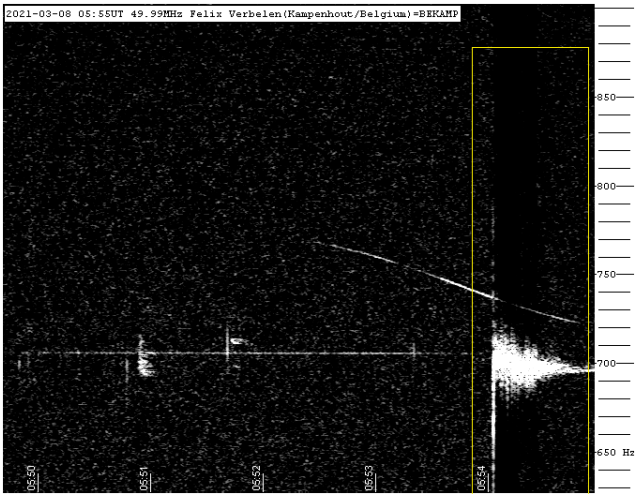

Figure 6 – Meteor reflection 8 March 2021, 05^h55^m UT.

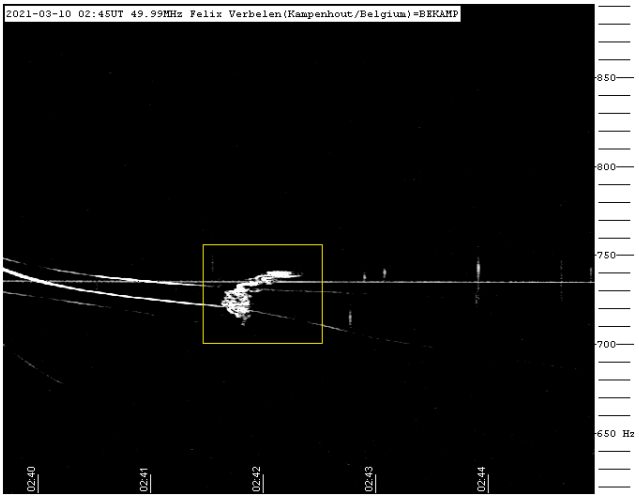

Figure 7 – Meteor reflection 10 March 2021, 02^h45^m UT.

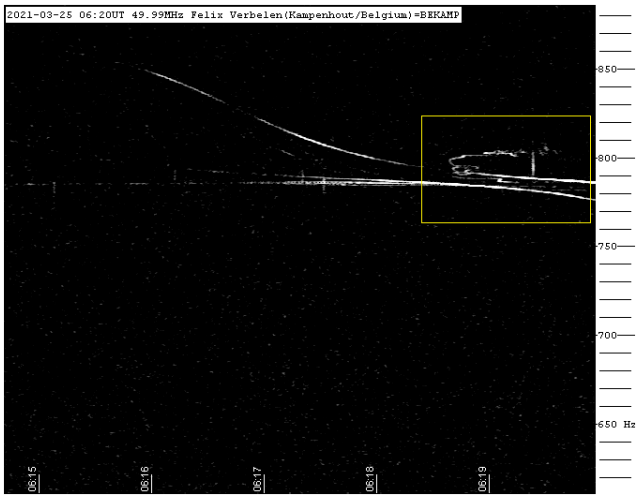

Figure 8 – Meteor reflection 25 March 2021, 06^h20^m UT.

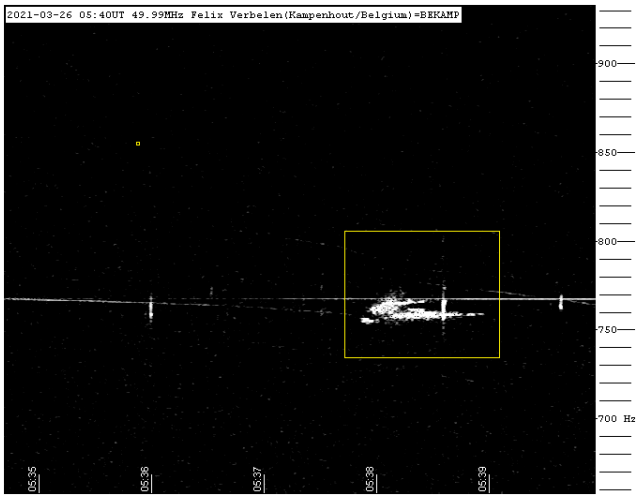

Figure 9 – Meteor reflection 26 March 2021, 05^h40^m UT.

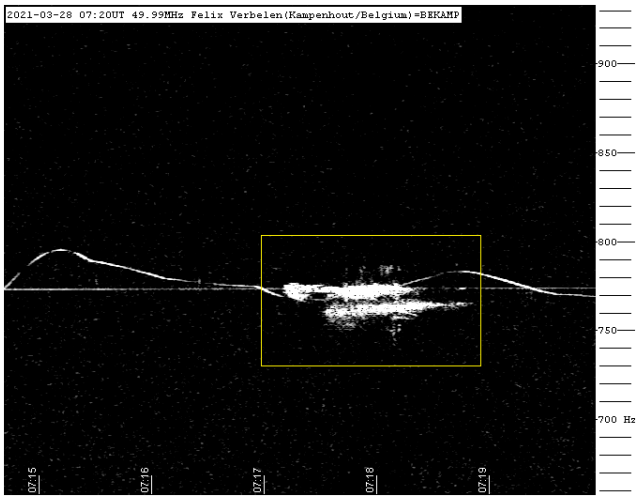

Figure 10 – Meteor reflection 28 March 2021, 07^h20^m UT.

Radio observations in February 2021

Ivan Sergei

Mira Str.40-2, 222307, Molodechno Belarus
seriv76@tut.by

This article presents the results of radio observations made in February 2021. The results of the radio observations are compared with the CAMS video network summaries.

1 Introduction

The observations were carried out at a private astronomical observatory near the town of Molodechno (Belarus) at the place of Polyani. A 5 element-antenna directed to the west was used, a car FM-receiver was connected to a laptop with as processor an Intel Atom CPU N2600 (1.6 GHz). The software to detect signals is Metan (author – Carol from Poland). Observations are made on the operating frequency 88.6 MHz (the FM radio station near Paris broadcasts on this frequency). "The "France Culture" radio broadcast transmitter (100 kW) I use is at about 1550 km from my observatory which has been renewed in 1997.

2 Automatic observations

There are no active visual showers in February. According to the IMO calendar (Rendtel, 2020), the Capricornids/Sagittariids (DCS #0115) peak as daytime shower activity on February 1, the χ-Capricornids (DXC #0114) are another daytime shower and peak on February 13. These are meteoroid streams with low activity, so they could not be registered. *Figure 1* shows the hourly numbers of meteors in February 2021 at 88.6 MHz.

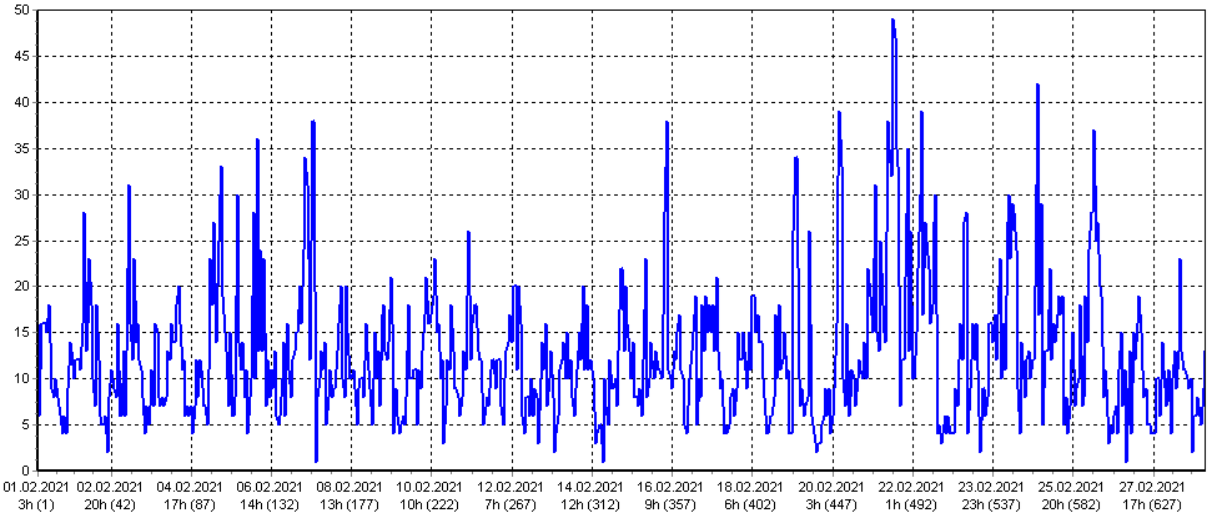

Figure 1 – Radio meteor echo counts at 88.6 MHz for February 2021.

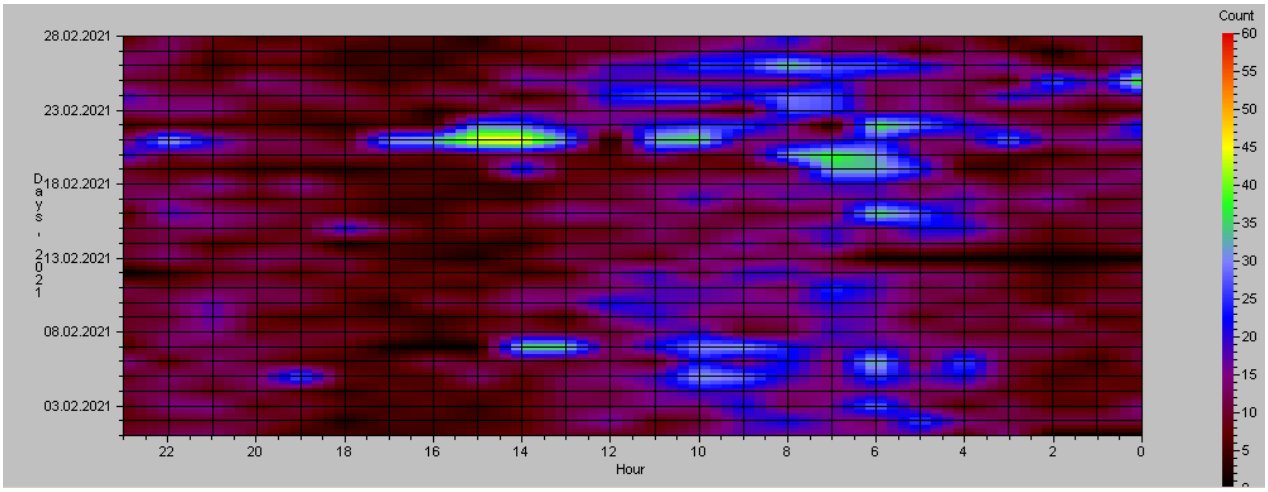

Figure 2 – Heatmap for radio meteor echo counts at 88.6 MHz for February 2021.

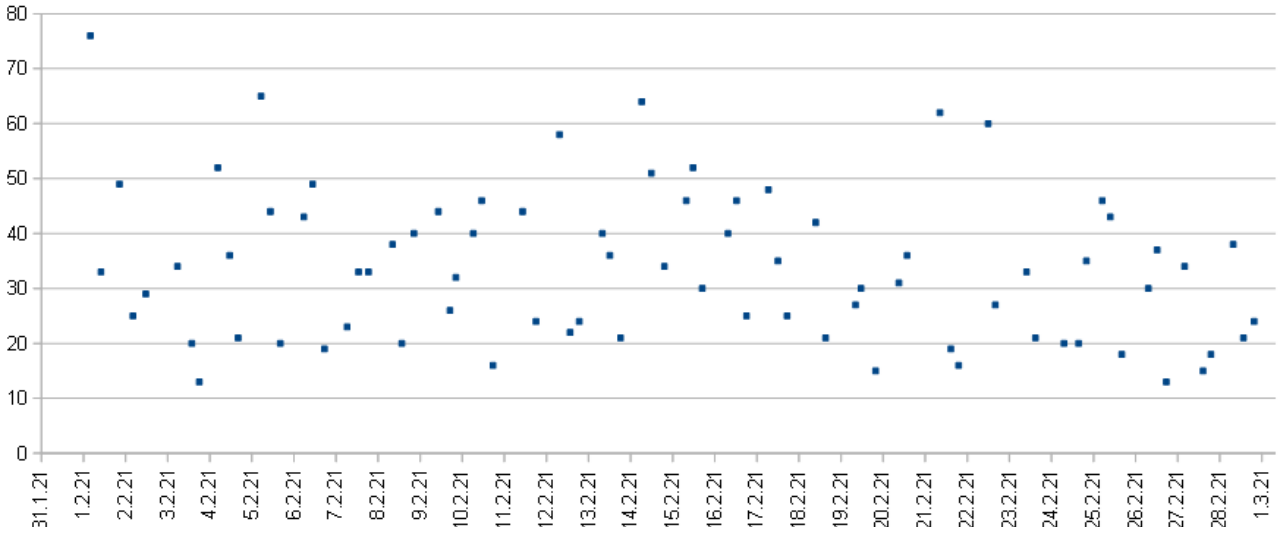

Figure 3 – The result with the calculated hourly numbers of meteor echoes by listening to the radio signals for February 2021.

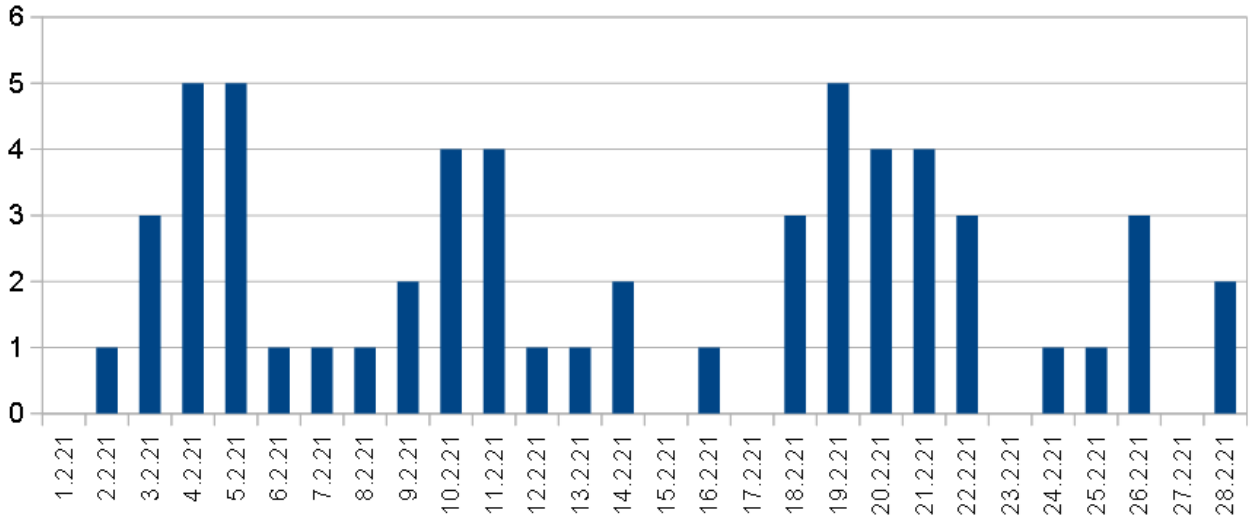

Figure 4 – Daily activity of radio fireballs in February 2021.

3 Listening to radio echoes on 88.6 MHz

Listening to the radio signals 1 to 3 times a day for one hour was done in order to control the level of the hourly activity, as well as to distinguish between periods of tropospheric passage and other natural radio interference. The total effective listening time was 78 hours. Some increase in meteor signal activity in the middle of the month can be explained by the registration of the maximum activity of the daytime meteoroid stream χ-Capricornids (#0114 DXC).

4 Fireballs

In order to quickly search for signals of the radio fireballs, the program SpectrumLab was running in parallel to the Metan program. Screenshots were saved every 10 minutes. The search for fireballs events was performed visually by viewing many thousands of screenshots obtained over a month. Then, we selected fireball events from the log files of the Metan program. For fireball activity statistics, I have selected signals from the log files with a peak power greater than 10000 as fireballs and with a signal duration greater than 10 seconds. *Figure 4* shows the daily activity of the fireball radio signals. During the month we can distinguish three peaks of bolide activity: February 4–5, February 10–11, February 19–21. Sharp fluctuations in the level of radio signals generated by larger meteoroids indicates a very uneven distribution of large meteoroids in space. *Figure 5* shows a typical 20.8-second radio fireball recorded by SpectrumLab on February 04 at 11^h28^m UT.

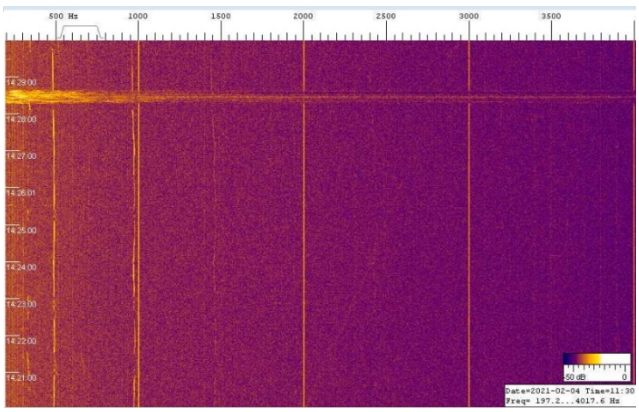

Figure 5 – Radio fireball recorded by SpectrumLab on February 04 at 11^h28^m UT.

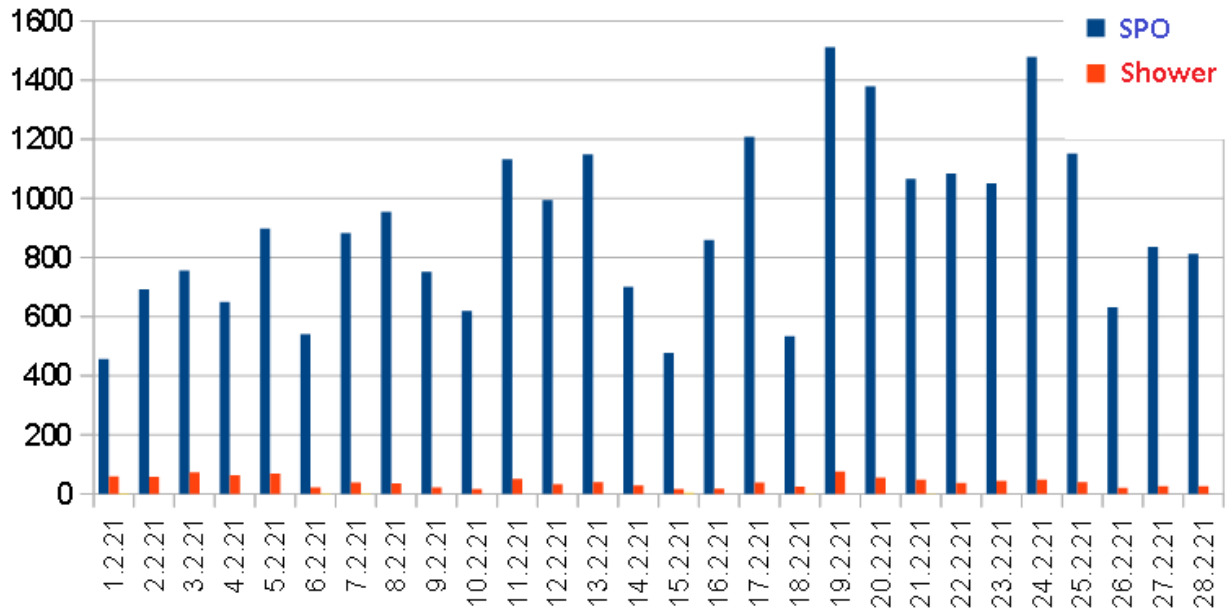

Figure 6 – Daily video meteor activity in February 2021 according to CAMS video networks.

5 CAMS Data

Figure 6 shows the total daily activity of meteors from the CAMS video network data (Jenniskens P., 2011). There is a noticeable correlation between the activity level of sporadic meteors and the activity level of shower meteors.

6 Conclusion

Automated observing data show a slight increase in activity in the period February 19–26. This agrees well with the slightly increased meteor activity from the CAMS video network, where the highest sporadic background activity for the entire month was from February 19–25. However, listening to the radio echoes showed some peak activity of the total number of signals in the middle of the month. The mismatch in the timing of peak activity can be explained by the fact that by listening to the radio fainter meteor signals can be recorded compared to the automatic observations. Theoretically, the data from CAMS video network and my automatic radio observations should agree with each other because they record phenomena with similar physical parameters (mass). Practical observations confirm this.

Acknowledgment

I would like to thank Sergey Dubrovsky for the software he developed for data analysis and processing of radio observations (software Rameda). I thank Carol from Poland for the Metan software. Thanks to Paul Roggemans for his help in the lay-out and the correction of this article.

References

Rendtel J. (2020). Meteor Shower Calendar 2021. IMO.

Jenniskens P., Gural P. S., Dynneson L., Grigsby B. J., Newman K. E., Borden M., Koop M., Holman D. (2011). “CAMS: Cameras for Allsky Meteor Surveillance to establish minor meteor showers”. *Icarus*, **216**, 40–61.

Radio observations in March 2021

Ivan Sergei

Mira Str.40-2, 222307, Molodechno Belarus
seriv76@tut.by

This article presents the results of radio observations made in March 2021. The results of the radio observations are compared with the CAMS video network summaries.

1 Introduction

The observations were carried out at a private astronomical observatory near the town of Molodechno (Belarus) at the place of Polyani. A 5 element-antenna directed to the west was used, a car FM-receiver was connected to a laptop with as processor an Intel Atom CPU N2600 (1.6 GHz). The software to detect signals is Metan (author – Carol from Poland). Observations are made on the operating frequency 88.6 MHz (the FM radio station near Paris broadcasts on this frequency). "The "France Culture" radio broadcast transmitter (100 kW) I use is at about 1550 km from my observatory which has been renewed in 1997.

2 Automatic observations

There are no active visual or daylight meteor showers in March (Rendtel, 2020). The average approximate background hourly signal activity is 3–20. *Figure 1* shows the hourly rates of radio meteors in March 2021 at 88.6 MHz. *Figure 2* shows the corresponding heat map.

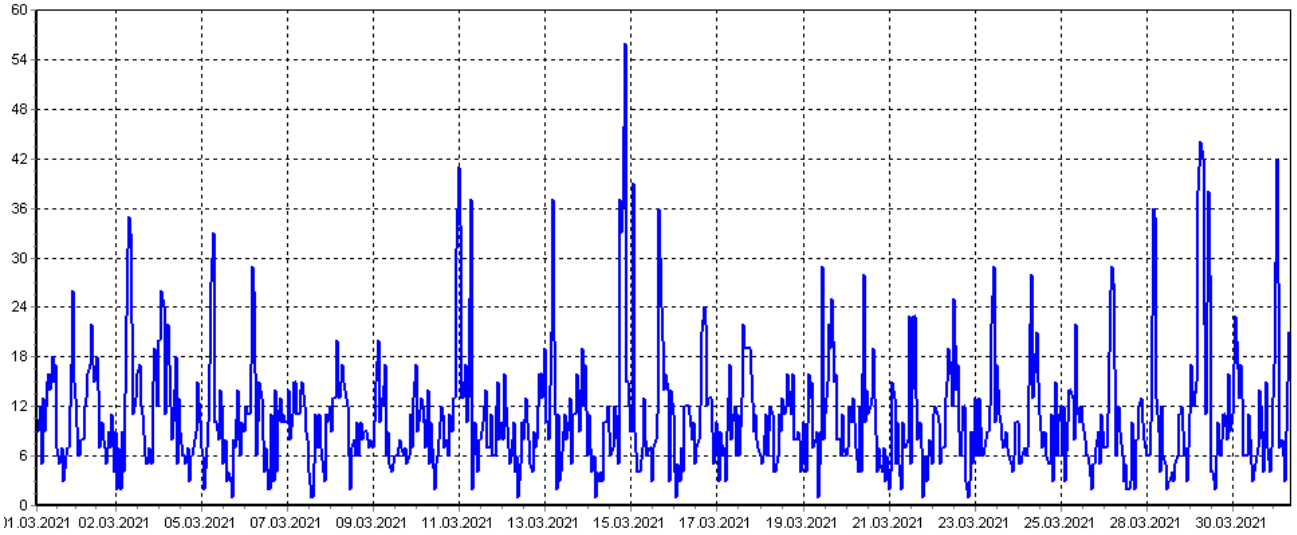

Figure 1 – Radio meteor echo counts at 88.6 MHz for March 2021.

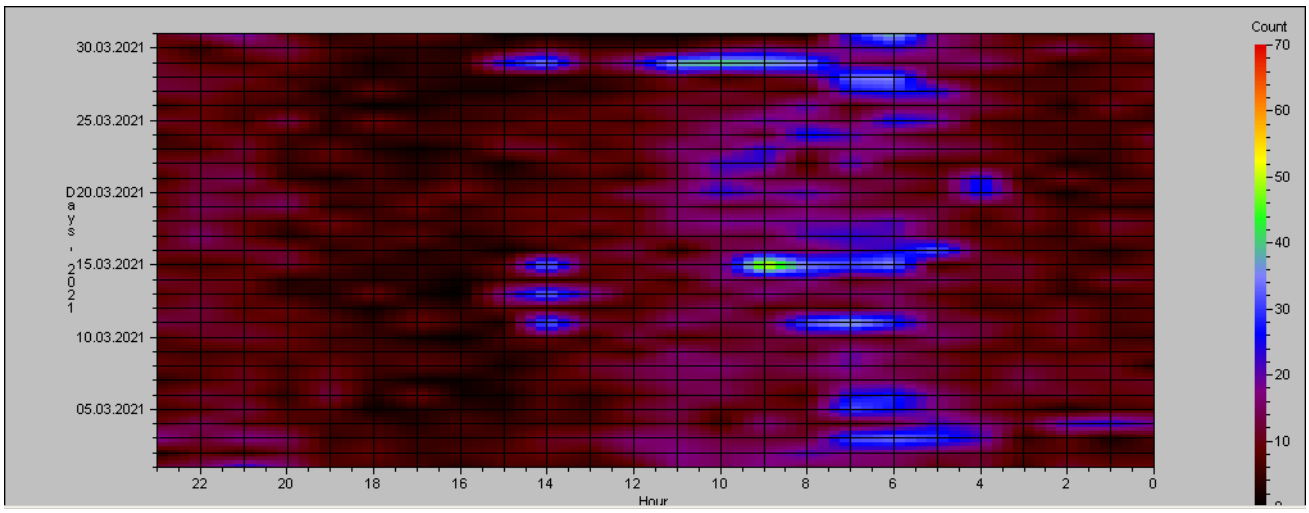

Figure 2 – Heatmap for radio meteor echo counts at 88.6 MHz for March 2021.

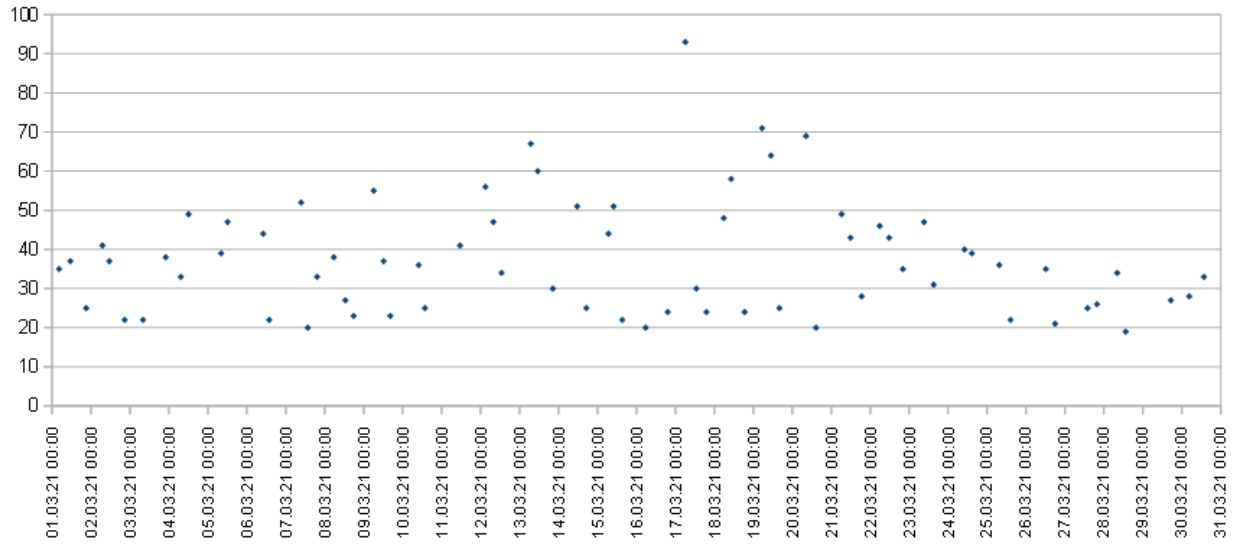

Figure 3 – The result with the calculated hourly numbers of meteor echoes by listening to the radio signals during March 2021.

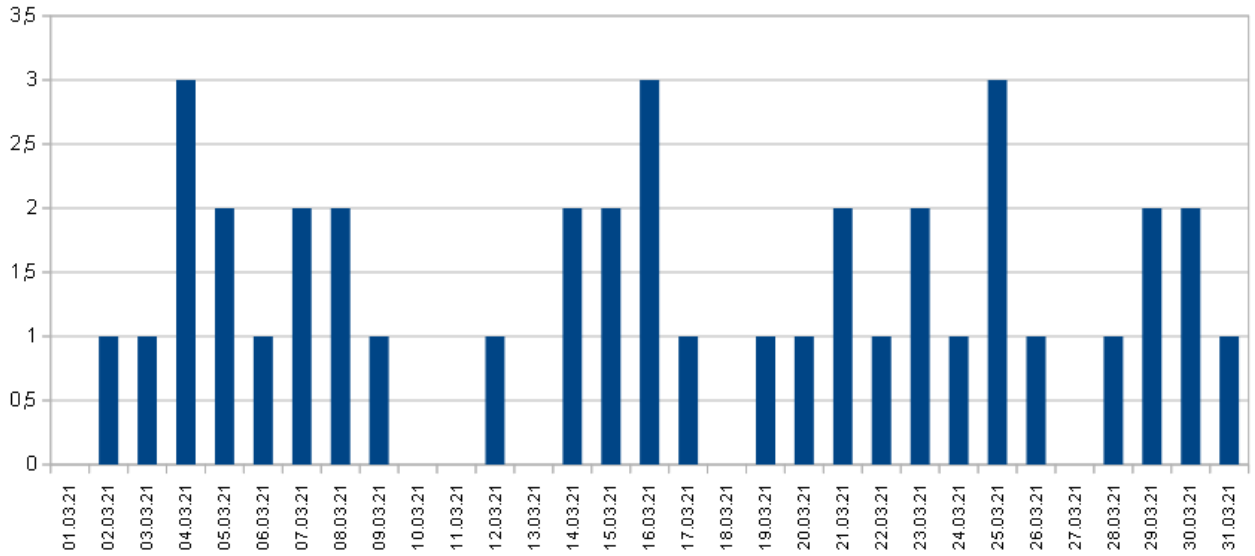

Figure 4 – Daily activity of radio fireballs during March 2021.

3 Listening to radio echoes on 88.6 MHz

Listening to the radio signals 1 to 3 times a day for one hour was done in order to control the level of the hourly rates, as well as to distinguish between periods of tropospheric passage and other natural radio interference. The total effective listening time was 72 hours. A slight increase in the level of activity is noticeable from about March 14 to 20.

The difference in activity levels between the listening method and the automatic observations can be explained by the fact that listening to the radio echoes allows to hear weaker meteor signals that remain too weak for recording by the software.

4 Fireballs

In order to quickly search for signals of the radio fireballs, the program SpectrumLab was running in parallel to the Metan program. Screenshots were saved every 10 minutes.

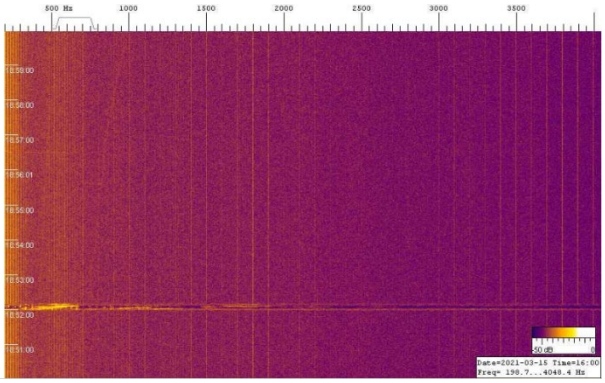

Figure 5 – Radio fireball recorded by SpectrumLab on March 15 at 15^h52^m UT.

The search for fireball events was performed visually by viewing many thousands of screenshots obtained over a month. Then, we selected fireball events from the log files of the Metan program. For fireball activity statistics, I have selected signals from the log files with a peak power greater

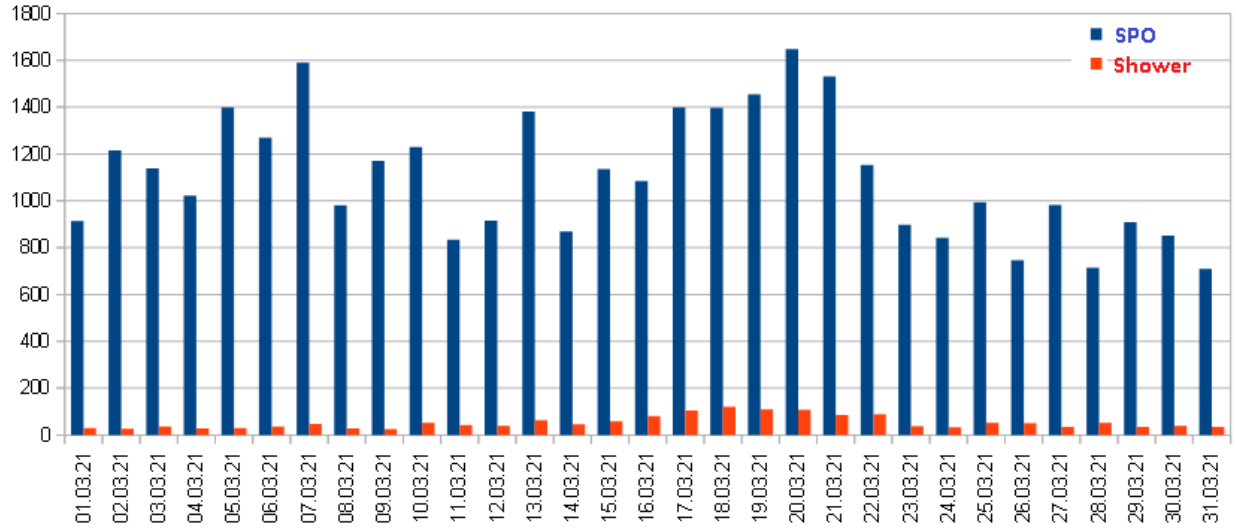

Figure 6 – Daily video meteor activity during March 2021 according to CAMS video networks.

than 10000 as fireballs and with a signal duration greater than 10 seconds. *Figure 4* shows the daily activity of the fireball radio signals.

Daily activity of fireballs did not exceed 3, indicating a "quiet" month in terms of activity. *Figure 5* displays one of the fireball radio echoes.

5 CAMS Data

Figure 6 shows the total daily activity of meteors from the CAMS video network data (Jenniskens et al., 2011). There is a noticeable correlation between the activity level of sporadic meteors and the activity level of shower meteors.

CAMS data show a weak increase in the activity level of the shower meteors in the period March 15–22, as well as an increase in the activity level of the sporadic background meteors.

6 Conclusion

The weak increase in radio meteor activity in the time interval March 12–22 is confirmed by CAMS data, which show a weak increase in shower and sporadic meteor activity during March 15–22. Automatic observations show a shorter time interval for a weak increase in signal activity from about March 11 to 15. This can be explained by the registration of larger meteoroids recorded automatically compared to the radio listening method. A joint analysis of the observations by different methods will show more reliable activity behavior by the meteors during this month.

Acknowledgment

I would like to thank Sergey Dubrovsky for the software he developed for data analysis and processing of radio observations (software Rameda). I thank Carol from Poland for the Metan software. Thanks to Paul Roggemans for his help in the lay-out and the correction of this article.

References

Rendtel J. (2020). "Meteor Shower Calendar 2021". IMO.

Jenniskens P., Gural P. S., Dynneson L., Grigsby B. J., Newman K. E., Borden M., Koop M., Holman D. (2011). "CAMS: Cameras for Allsky Meteor Surveillance to establish minor meteor showers". *Icarus*, **216**, 40–61.

Grazing meteor over Belarus

Igor Baluyk[1], Sergei Dubrovski[1], Yuri Goryachko[2], Konstantin Morozov[2] and Ivan Sergei[3]

[1] **Gomel astronomical club "Cirrus", Belarus**
balig@tut.by, toliman@tut.by

[2] **Astronominsk, Belarus**
astronominsk@gmail.com

[3] **Mira Str.40-2, 222307, Molodechno Belarus**
seriv76@tut.by

On 2021 April 11, the trajectory of a grazing meteor has been registered in the eastern part of Belarus.

1 Introduction

The object was recorded by six cameras at once: Daraganovo_12, Gomel_W, Gomel_NW, Daraganovo_10, MINSK_03 and MINSK_14. This allowed us to track it almost all the way. We watched the meteor for 24.7 sec (!). This is an absolute record for our meteor network! After that, the capture on the last camera MINSK_03 stopped, although the meteor still continued its path. According to my estimates, the time of visibility should not be less than 30 sec.

Figure 1 – The path of the grazing meteor registered by the camera of Sergei Dubrovski (Gomel).

Figure 2 – The path of the grazing meteor registered by the camera of Igor Balyuk (Gomel).

Figure 3 – The path of the grazing meteor registered by the camera of Konstantin Morozov (Minsk) in $19^h22^m58^s$ UT.

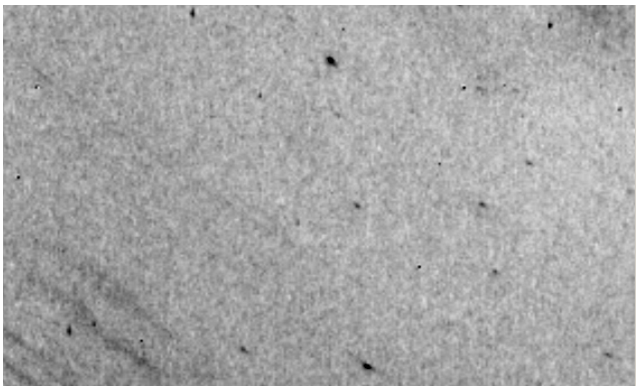

Figure 4 – Part of the flight of the grazer recorded by all-sky camera I.Sergey Polyani (cropped photo).

2 Trajectory and orbit

The Daraganovo_12 camera began to capture the meteor at an altitude of just over 94 km. In the middle of the trajectory the altitude was 88 km or slightly lower. The MINSK_03 camera lost the object at an altitude of 91 km. It can be seen that the meteor passed perihelion and began to move away from the Earth. Thus, we can state that we have observed a grazing meteoroid, which has travelled 430 km through the atmosphere (actually even more, because we did not see the end).

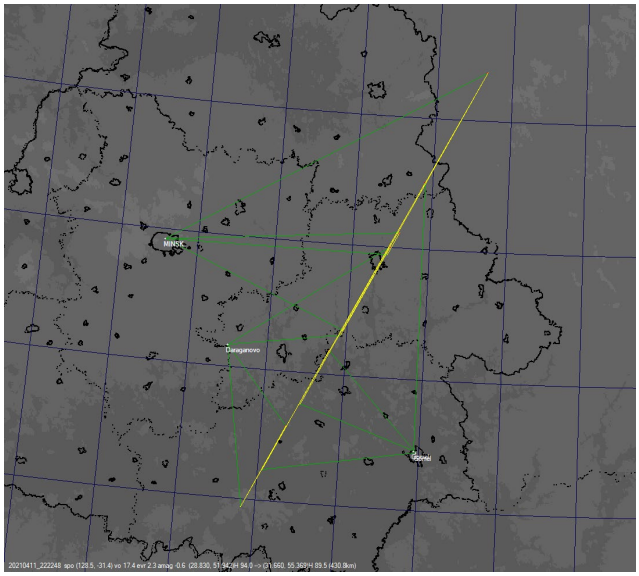

Figure 5 – The basic reconstruction of the grazing meteor trajectory by Belarusian cameras.

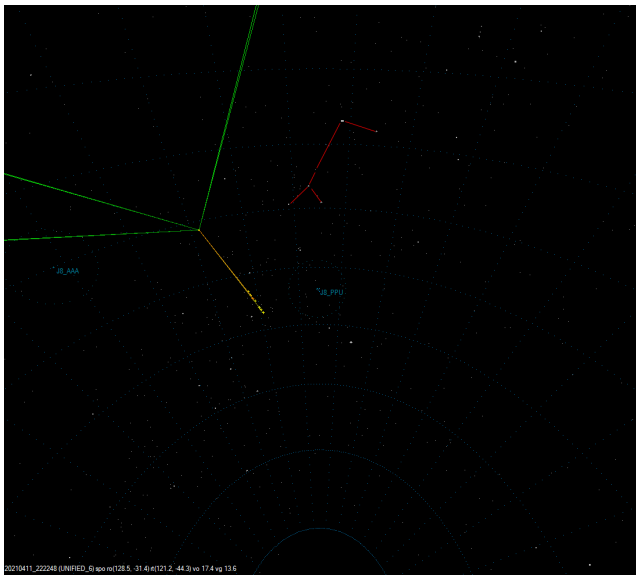

Figure 6 – Calculation of the radiant position obtained with the program UFO.

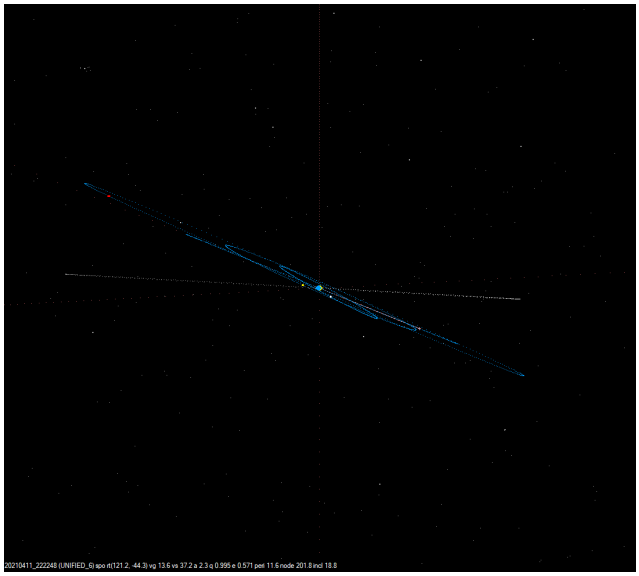

Figure 7 – Determination of the orbit of the meteor grazer in space computed by the UFO software.

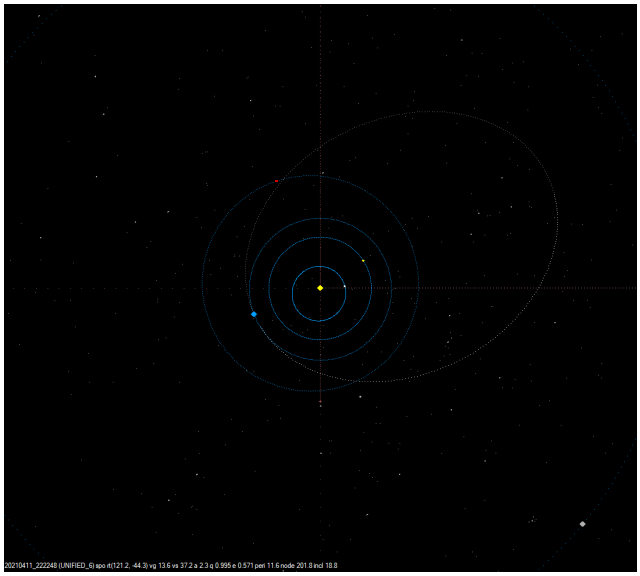

Figure 8 – Projection of the orbit of the meteor grazer in space in the ecliptic plane.

The radiant is located in the constellation Puppis (under Canis Major) very close to the radiant of the Pi Puppids (PPU). The mean geocentric velocity (slightly decreasing during the flight) is $v_g = 13.6$ km/s, close to that of the pi Puppids (15 km/s). This shower is active from April 8 to May 9. It is quite possible that our grazer is related to this meteor shower, although it did not come exactly from the radiant.

The object was also recorded by an all-sky camera near Molodechno in a place called Poliany.

Acknowledgment

The analysis of the video data of the Belarusian group was conducted by Yuri Goryachko. We thank Paul Roggemans for correcting this article.

The mission of MeteorNews is to offer fast meteor news to a global audience, a swift exchange of information in all fields of active amateur meteor work without editing constraints. MeteorNews is freely available without any fee. To receive a notification: https://www.meteornews.net/newsletter-signup/.

You are welcome to contribute to MeteorNews on a regular or casual basis, if you wish to. Anyone can become an author or editor, send an email to us. For more info read: https://meteornews.net/writing-content-for-emeteornews/

The running costs for website hosting are covered by a team of sponsors. We want to thank Anonymous (3x), Nigel Cunnington, Kai Frode Gaarder, Pierre Tioga Gulon, J Andreas Howell, Koen Miskotte, Paul Roggemans, Mark Upton, Lorenzo Barbieri, Peter Stewart, Carlos Adib and Joseph Lemaire for their financial contributions.

Webmaster & account administrator:
Richard Kacerek (United Kingdom): rickzkm@gmail.com

Contributing to this issue:

- ***J. Aceituno***
- ***I. Baluyk***
- ***A. Dal'Ava Jr.***
- ***E. de Guindos***
- ***L. de Sousa Trindade***
- ***S. Dubrovski***
- ***G. Gonçalves Silva***
- ***Y. Goryachko***
- ***J. Greaves***
- ***J. Izquierdo***
- ***C. Jacques Faria***
- ***P. Jenniskens***
- ***R. Kacerek***
- ***J.M. Madiedo***
- ***P. Mohan***
- ***K. Morozov***
- ***J.L. Ortiz***
- ***J. Palacián***
- ***P. Roggemans***
- ***P. Santos-Sanz***
- ***D. Šegon***
- ***I. Sergei***
- ***F. Verbelen***
- ***D. Vida***
- ***P. Yanguas***
- ***M. Zurita***

ISSN 2570-4745 Online publication https://meteornews.net

Listed and archived with ADS Abstract Service: https://ui.adsabs.harvard.edu/search/q=eMetN

MeteorNews Publisher:

Valašské Meziříčí Observatory, Vsetínská 78, 75701 Valašské Meziříčí, Czech Republic